Journal of Cardiovascular Magnetic Resonance®, 2(4), 279–314 (2000)

ABSTRACTS

Oral and Poster

1. Long-term prognosis of postsurgical aortic dissection: Magnetic resonance imaging evaluation

A Almeida, H M Gabriel, J Fançony, L Sargento, J Morais, C David, F Madeira, A Soares, L Beija, L C Guimarães, R Lima, M C Vagueiro.

Objectives: Patients (pts) operated for type A aortic dissection remain at high risk of late morbidity and mortality. The aim of this study was the detection of postsurgical complications and prognostic indexes during a long-term follow-up with magnetic resonance imaging (MRI).

Methods: Thirty-seven pts were studied (19 men, 18 women), 31–73 years old (54.4 ± 12.2), submitted to surgery for type A aortic dissection, with replacement of ascending aorta. All pts were followed with MRI yearly, since the surgery time until 39.3 ± 2.9 months to identify postsurgical complications in three aortic segments (arch, thoracic descending, abdominal)—aneurysm, false aneurysm, redissection, rupture, and death. Prognostic indexes analyzed were presence of residual aortic flap, false lumen patency, false lumen dimensions, initial aortic dimensions, and increase rate of aortic dimensions.

Results: One hundred eleven aortic segments were analyzed. Complications detected were that aneurysm occurred in 17/37 pts (23/111 segments, all in thoracic aorta); rupture of thoracic aorta and death occurred in 3 pts; and no redissection or false aneurysm was diagnosed. A residual flap was present in 65/110 segments, and 48 in thoracic aorta. Pts with aneurysms had significantly more often a residual flap ($p < 0.001$). False lumen was patent in 56/65 segments, thrombosis was present in 2, and patency was variable during follow-up in 6 segments. There was no association between patency and complications development. In all segments with flap, false lumen dimension was bigger than true lumen (ratio of 0.70–0.82%). This index had no influence on prognosis. The initial dimensions of the aortic segments with aneurysm were significantly ($p < 0.001$, for all levels of aorta) higher than the ones without aneurysm. An increase rate of aortic dimensions higher than 5 mm/year was associated significantly ($p < 0.001$) with aneurysm development in each segment of the three aorta levels.

Conclusion: Operated type A aortic dissection must be followed for timely detection of complications occurring on the residual aorta. The presence of a residual flap, increased initial aortic dimensions, and high increasing rate of aortic dimensions were indexes with prognostic influence. MRI was an excellent technique to monitor this situation at long-term evolution and evaluate those prognostic indexes.

2. Long-term follow-up of 82 patients with chronic disease of the thoracic aorta by magnetic resonance imaging

Matthias Schmidt,[1] P. Theissen,[1] G. Klempt,[1] H. J. Deutsch,[2] F. M. Baer,[2] M. Dietlein,[1] D. Moka,[1] E. Erdmann,[2] H. Schicha.[1] [1]*Klinik und Poliklinik für Nuklearmedizin und* [2]*Klinik III für Innere Medizin, University of Cologne, Germany*

Aims: To examine the clinical impact of magnetic resonance imaging in long-term follow-up of patients (pts) with chronic disease of the thoracic aorta such as coarctation of the aorta, chronic aortic dissection, and true aortic aneurysm.

Methods: Eighty-two pts with chronic disease of the thoracic aorta (31 pts with coarctation of the aorta [CoA], 29 pts with chronic aortic dissection, and 22 pts with true aneurysm) underwent repetitive magnetic resonance imaging for 6.5 ± 3.4 (mean ± SD) years. Diameters of the thoracic aorta were measured at predefined levels and morphological and functional parameters of special interest were analyzed in each patient group. Pts were classified as having constant or progressive disease and clinical end-points were defined as (re-)operation or death.

Results: Forty-three pts (52%) (CoA 15 pts, chronic dissection 16 pts, true aneurysm 12 pts) had constant findings. None of them underwent (re-)operation and seven patients (16%) died, two of them from their aortic disease. One patient died from an arrhythmogenic event, in the remaining 4 pts the cause of death could not be definitely established. Thirty-nine pts (48%) (CoA 16 pts, chronic dissection 13 pts, true aneurysm 10 pts) had progressive disease as demonstrated by repetitive magnetic resonance imaging. Of these 39 pts, 24 pts underwent (re-)operation; in 15 pts operation was postponed. Four pts died from their aortic disease.

Conclusion: Repetitive magnetic resonance imaging is a clinically feasible technique for long-term follow-up of pts with chronic disease of the thoracic aorta because it can detect progressive disease in a large subset of pts requiring elective surgery. The results of magnetic resonance imaging provided the rationale for either (re-)operation or conservative mangement, thus guiding patient management.

3. Carotid magnetic resonance angiography combined with duplexsonography is as valid to detect carotid stenosis as conventional angiography

C. Espinola-Klein,[1] T. Voigtländer,[1] K.-J. Kreitner,[2] K. Oberholzer,[2] M. Schmerer,[1] M. Thelen,[2] and J. Meyer.[1] [1]*2nd Medical Clinic, University Clinic, Mainz, Germany;* [2]*Institute of Radiology, University Clinic, Mainz, Germany*

With magnetic resonance angiography (MRA), it is possible to examine small vessel structures noninvasively. Conventional angiography is considered the gold standard to imagine carotid stenosis. The aim of the study was to compare the sensitivity and specificity of carotid MRA and duplexsonography with conventional angiography in patients with suspected carotid artery stenosis.

Methods: We included 25 patients (8 women, 32%) with 38 pathologic internal and 11 pathologic external carotid arteries. All patients were examined with MRA (Siemens; Vision 1.5 T TR/TE 3.0/1.2 and Harmony 1.0 T TR/TE 6.2/2.2) and duplexsonography. The results were compared with the results of a conventional angiography. All examinations were performed by different investigators in ignorance of the other results. For definition of a high-degree stenosis, the reference of each method was used.

Results: In the conventional angiography 30 stenosis were defined to be high degree (61%), 13 stenosis (27%) were defined to be moderate, and 6 vessels were occluded (12%). All occluded arteries could be detected in the three methods. In the MRA, 28 of the 33 high-degree carotid stenosis were identified, 2 high-degree stenosis were not seen in MRA, and 3 of the 13 moderate stenosis were overestimated. By duplexsonography all 13 moderate stenosis were detected exactly, but 7 of the 30 high-degree stenosis were underestimated to be moderate:

	MRA	Duplex	MRA + duplex
Sensitivity	93%	77%	100%
Specificity	77%	100%	100%
Negative predictive value	90%	100%	100%
Positive predictive value	83%	65%	100%

Conclusion: Using MRA, we achieved a 93% sensitivity in the detection of high-degree carotid stenosis, but the specificity was only 77%. With a combination of MRA and duplexsonography, we could exactly detect all carotid stenosis noninvasively and reached a 100% sensitivity and specificity.

4. Arterial Switch Operation in Patients with D-Transposition of the Great Arteries: Quantitative Evaluation of the Degree of Stenosis and Hemodynamic Changes with Magnetic Resonance Imaging

Matthias Gutberlet, MD, Thomas Boeckel, MD, Norbert Hosten, MD, Michael Vogel, MD, Christian Born, MD, Roland Hetzer, MD, Georg Bein, MD, Peter Lange, MD, and Roland Felix, MD.

Aims: To evaluate cine magnetic resonance imaging (MRI) and phase-shift velocity mapping for assessment of the hemodynamic relevance of stenotic segments or specific hemodynamic changes in the great vessels after an arterial switch procedure for correction of D-transposition of the great arteries.

Methods: Twenty consecutive patients (aged 2–17 years) with an acoustic window that was insufficient for Doppler transthoracic echocardiography were included in the study. Flow and diameter measurements of the pulmonary arterial trunk and its primary branches were performed with phase-shift velocity mapping (TR = 20 ms, TE = 2.4 ms, flip-angle = 30°, slice thickness = 3–6 mm, FOV = 150–300 mm, matrix = 96 × 128, retrospective gating) and cine MR imaging (TR = 14 ms, TE = 2.6 ms, flip-angle = 20°, slice thickness = 3–6 mm, FOV = 150–300 mm, matrix = 128 × 256, retrospective gating) on a 1.5-T scanner (ACS-NT Gyroscan, Philips, Best, Netherlands).

Results: There were good correlations between pressure gradients in the pulmonary arteries estimated with MRI and those measured with Doppler echocardiography ($r = 0.83$, $n = 15$) and cardiac catheterization ($r = 0.90$, $n = 13$). Cine MRI revealed that the diameters of the right and left pulmonary arteries decreased with the expansion of the aorta during systole, which increased the peak velocity. This temporary stenosis was more severe in the right than in the left pulmonary artery and was accompanied by a significantly ($p < 0.05$) lower volume flow in the right pulmonary artery.

Conclusion: The anatomic situation after arterial switch repair tended to produce temporary stenoses in the primary pulmonary arterial branches, with significant changes in hemodynamics. These changes may affect the long-term outcome and go undetected with other imaging modalities like cardiac catheterization in which usually no simultaneous visualization of the aorta and the pulmonary trunk is achieved.

5. Evaluation of congenital disease of the thoracic arteries with volume rendering of contrast enhanced MRA

R.J.M. van Geuns,[a] P.A. Wielopolski,[*] H.G. de Bruin,[*] P.M.A. van Ooijen,[a] M. Oudkerk,[*] P.J. de Feyter. [a]*Thorax-center and* [*]*Dept. of Radiology, Daniel den Hoed kliniek, University Hospital Rotterdam, The Netherlands*

Introduction: Congenital abnormalities of the aorta and pulmonary artery have a complex three-dimensional (3D) structure. MRI has proven to be of value to evaluate these structures although two-dimensional (2D) are difficult to interpret by clinicians. 3D contrast enhanced MRA (3D-MRA) (1,2) is a fast imaging modality which may be more suited to study complex congenital abnormalities of the pulmonary artery and thoracic aorta.

Table 1

MIP and VR were both of limited use for aortic root evaluation because of multiple overlapping structures

Aorta	Pulmonary artery
Recoarctation (2×)	Normal (2×)
Good postoperative results (3×)	Left pulmonary artery stenosis (1×)
Mirror arch (1×)	Aneurysm (1×)
Left arch, aberrant right subclavian artery (1×)	Pulmonary trunk stenosis (1×)
Right arch, aberrant left subclavian artery (1×)	
Cervical aortic arch (1×)	
Coarctation of the aorta (1×)	

Purpose: First, to evaluate the facilities and limitations of 3D-MRA in congenital disease of the thoracic aorta and pulmonary artery. Second, to investigate the possible significance of new 3D postprocessing techniques on these data

Methods: Fifteen patients (15–70 years) with suspected disease of the great arteries were included. Indications for MRI were suspected congenital aortic disease (3×), follow-up after surgery for aortic coarctation (5×), follow-up after pulmonary artery surgery (5×). After imaging with standard spin-echo (SE) and gradient-echo (GE) techniques, MRA was performed with a single breathhold contrast (Gadolinium) enhanced three-dimensional gradient echo technique. The field of view was 200 × 400 mm with a matrix of 165–195 × 512 and a slice thickness of 1.8 mm. TR and TE were 4.6 and 1.8 ms, respectively. A contrast dose of 19 ml of Gd-DTPA was delivered at a flow rate of 2 ml/sec intravenously with an MR compatible power injector. The time of arrival of contrast to the vessel of interest was adjusted depending on the circulation time. The circulation time was determined with 1-ml test dose of Gd-DTPA. Evaluation of the 3D-MRA study was performed with multiplanar reformatting (MPR), maximum intensity projection (MIP), and volume rendering (VR).

Results: MRA was successfully performed in all patients; in one study image quality was hampered by suboptimal contrast timing. All

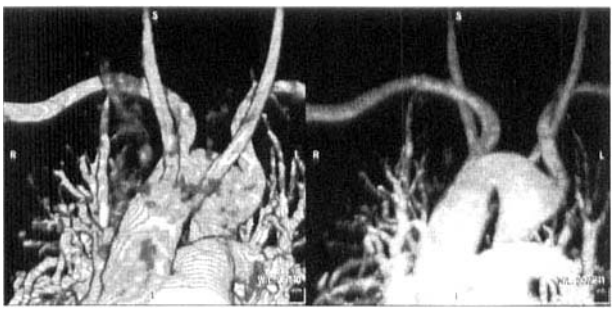

Figure 1. Patient with right aortic arch with a left subclavian artery (arrow) from the descending aorta (aberrant). The volume rendered image (left) provides more 3D information compared to the MIP image (right)

diagnoses from SE and GE imaging were visualized by 3D-MRA (Table 1). Preparation of MIP and VR images was completed within 10 minutes. Both MIP and VR were able to visualize the anomalies in three dimensions. Due to the limitations of MIP, confusion of the course of vessel anomalies was notified in three patients (Fig. 1).

Conclusion: 3D-MRA is a fast imaging technique for the evaluation of the great arteries. Post processing with VR provided the most information of complex 3D anomalies.

References

1. Prince MR, Narasimham DL, Stanley JC, Chenevert TL, Williams DM, Marx MV, Cho KJ. Breath-hold gadolinium-enhanced MR angiography of the abdominal aorta and its major branches. *Radiology* 1995; 197:785–92.

2. Krinsky GA, Reuss PM, Lee VS, Carbognin G, Rofsky NM. Thoracic aorta: comparison of single-dose breath-hold and double-dose non-breath-hold gadolinium-enhanced three-dimensional MR angiography. *AJR Am J Roentgenol* 1999;173:145–50.

6. Evaluation of Pulmonary Regurgitation and Biventricular Function in Response to Physical Exercise in Corrected Tetralogy of Fallot Patients with the Use of Ultra-fast Magnetic Resonance Imaging

Arno A.W. Roest,[1,2] Willem A. Helbing,[2] Patrik Kunz,[2] Albert de Roos,[1,2] Hildo J. Lamb,[2] Hubert W. Vliegen,[2] Ernst E. van der Wall.[1,2] [1]*Interuniversity Cardiology Institute of The Netherlands, Utrecht, The Netherlands;*[2] *Leiden University Medical Center, The Netherlands*

Background and Purpose: Pulmonary regurgitation (PR) is common after repair of tetralogy of Fallot. At rest the amount of PR correlates with right ventricular (RV) function (1), arrhythmias and sudden death. No quantitative data exist on the change of biventricular function and PR in response to supine physical exercise in these patients. PR and biventricular function can be quantified with MRI (2). The Aim of this study was to evaluate changes in PR and RV function in response to supine physical exercise in Fallot patients using an ultra-fast turbo field echo planar imaging (TFEPI) MRI technique.

Methods: Ventricular function at rest and immediately after exercise was studied in 15 corrected tetralogy of Fallot patients (4F) (mean age: 17.5 ± 2.5y) and 16 matched controls (mean age: 17.5 ± 2.3y) using a Philips Gyroscan ACS-NT15 (PowerTrak 6000 with cardiac software package: cpr 6). Exercise was performed in supine position on a MR-compatible bicycle ergometer (Lode B.V., The Netherlands). Prior to the MR examination, a maximal supine exercise test was performed with continuous measurement of heart rate and oxygen uptake. Exercise level during MRI examination was based on the workload corresponding to 60% of the maximal oxygen uptake.

At rest and during the exercise protocol (Fig. 1), 10 consecutive slices in the short-axis direction covering left ventricle (LV) and RV

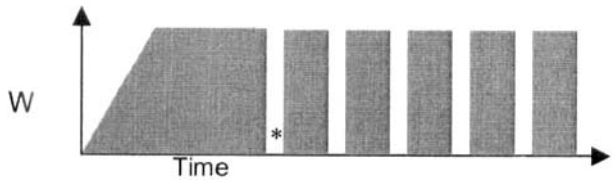

Figure 1. Exercise protocol: after reaching a steady state, five breath-holds (*) encompassing eight heartbeats are performed during which 10 short-axis slices are obtained. Each breath-hold is performed during cessation of exercise.

Table 1

Left and right ventricular parameters at rest and immediately after cessation of exercise of the healthy subjects (HS) and the change from rest to exercise (= p < 0.05 rest to exercise)*

Left Ventricle	Rest (HS)	Exercise (HS)	Change HS (%)
EDV (ml)	143 ± 29	138 ± 27	−3 ± 10
ESV (ml)	54 ± 17	36 ± 12*	−33 ± 11
SV (ml)	89 ± 14	100 ± 20*	+14 ± 8
EF (%)	63 ± 6	74 ± 6*	+19 ± 7
Right Ventricle	**Rest (HS)**	**Exercise (HS)**	**Change HS (%)**
EDV (ml)	146 ± 27	143 ± 24	−1 ± 5
ESV (ml)	58 ± 17	44 ± 12*	−25 ± 12
SV (ml)	88 ± 14	99 ± 16*	+15 ± 8
EF (%)	62 ± 6	71 ± 6*	+18 ± 7

were obtained during five breath-holds encompassing eight heartbeats each. An ultra-fast TFEPI MR sequence was used with the following parameters: flip angle 30°; TE 4.8 ms; TR 14 ms; FOV 420 × 210 mm; scanmatrix 128 × 40; EPI factor 5; turbofactor 2; shots 4. Ventricular parameters measured were end-diastolic volume (EDV in ml), end-systolic volume (ESV in ml), stroke volume (SV in ml = EDV-ESV), ejection fraction (EF in % = SV/EDV), PR volume (PRvol in ml = RVSV-LVSV), PR percentage (in % = (PRvol/RVSV) × 100) and Net RV output (in ml = RVSV-PRvol).

Results: Heart rate at peak exercise was lower in the patient group: 4F: 165 ± 16 vs. controls: 178 ± 11 bpm ($p < 0.05$). Maximal O_2 uptake per kg body weight was lower in the 4F patients (36 ± 5 ml/min/kg) as compared to the controls (39 ± 5 ml/min/kg). In the controls both ventricles showed a similar response to exercise (Table 1). Table 2 shows the change in ventricular parameters from rest to exercise

Table 2

Left and right ventricular parameters at rest and immediately after cessation of exercise of the Fallot patients (4F) and the change from rest to exercise (= p < 0.05 rest to exercise of 4F)*

Left Ventricle	Rest (4F)	Exercise (4F)	Change 4F (%)
EDV (ml)	141 ± 35	141 ± 35	−0.1 ± 6
ESV (ml)	67 ± 28	56 ± 28*	−21 ± 11
SV (ml)	74 ± 13	86 ± 15*	+13 ± 11
EF (%)	54 ± 7	62 ± 9*	+15 ± 7
Right Ventricle	**Rest (4F)**	**Exercise (4F)**	**Change 4F (%)**
EDV (ml)	224 ± 68	233 ± 63*	+3 ± 5
ESV (ml)	107 ± 47	110 ± 51	−3 ± 13
SV (ml)	117 ± 29	124 ± 29	+4 ± 7
EF (%)	54 ± 9	55 ± 10	+4 ± 8
PR vol (ml)	44 ± 29	38 ± 26*	−23 ± 30
Net RV output (ml)	74 ± 13	86 ± 15*	+13 ± 11
PR (%)	34 ± 20	28 ± 17*	−25 ± 29

in the corrected Fallot patients. As a result of the PR, RV-SV was significantly larger than the LV-SV, at rest. Due to this volume overload, RV-EDV and RV-ESV were increased (Table 2).

In the corrected Fallot patients, RV-EDV increased in response to exercise with no change in ESV. RV-SV increased and RV-EF remained unchanged. PR volume and PR percentage both decreased in response to exercise. LV response to exercise of the corrected Fallot patients was similar to the controls.

Discussion: MRI allows evaluation of PR and biventricular function in response to supine physical exercise in Fallot patients. Compared to the matched controls, LV response to exercise was similar in the corrected Fallot patients. Increase in RV-EDV, the lack of decrease of RV-ESV, and no increase of RV-EF in response to exercise in corrected Fallots suggests impaired RV function. Net RV output in these patients is increased by a combination of an increase in RV-SV and a decrease of PR volume.

References

1. Niezen RA, Helbing WA, van der Wall EE, et al. *Radiology* 1996; 201:135–40.
2. Rebergen SA, Chin JG, Ottenkamp J, et al. *Circulation* 1993;88: 2257–66.

7. Fast Spectroscopic Imaging of the Human Heart *In Vivo*

Thomas Wilhelm, Christian Wacker,* Wolfgang Bauer,* and Peter Bachert. *Dept. of Medical Physics and Biophysics, German Cancer Research Center (dkfz), D-69120 Heidelberg, Germany; *Department of Cardiology, University of Würzburg, D-97080 Würzburg, Germany*

Introduction: Besides the detection of high-energy phosphates in the human myocardium by ^{31}P-NMR (1–3), another focus of interest is the assessment of ^{1}H-NMR detectable metabolites, particularly of triacylglycerides, since a correlation was found between lipid signal and irreversibly damaged regions in the myocardium after infarction (4). Conventional chemical-shift-imaging (CSI) is less suitable for this examination because of long acquisition times. In contrast, echo-planar spectroscopic imaging (EPSI) (5) uses an oscillating readout gradient for simultaneous encoding of spatial and spectral information after a single excitation. The result is a shortening of acquisition time by a factor of 32 compared to CSI.

Materials and Methods: Healthy volunteers were examined on a 1.5-T whole-body scanner (Magnetom Vision; Siemens) equipped with a resonant actively shielded gradient system. The readout gradient of the EPSI sequence had sinusoidal shape and data acquisition was performed nonlinearly in time during gradient switching. The body coil was employed; geometric parameters were FOV = 160–200 mm, in-plane resolution = (5–6.25 mm^2), slice thickness = 15 mm. Slice-selective shimming was applied; breast and back tissue was presaturated. Water signal suppression, presaturation of breast and back tissue, and spin-echo excitation (2560-μs slice-selective 90° and 180° pulses, TE = 3 ms, ECG-triggering) were performed during systole, data sampling within 450 ms during diastole. The acquisition time was ca. 40 s for the whole measurement (depending on heart frequency).

Results: Resolved ^{1}H-NMR spectra of the human heart were obtained by EPSI showing different lipid peaks (Fig. 3a) in myo- and epicardium. Impairment of spectra (bad shim conditions, rapid suscepti-

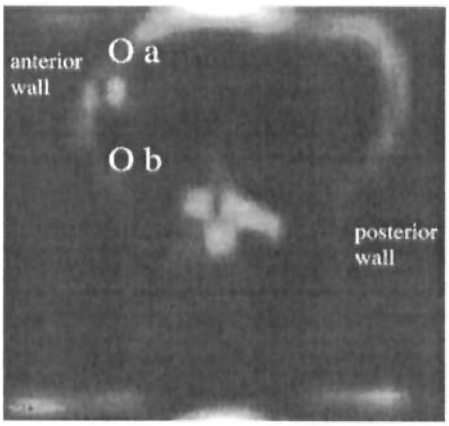

Figure 2. Metabolic image of the slice in Fig. 1: 2D plot of integrated intensity of chemical-shift range δ = 0–2.5 ppm of *in vivo* ^{1}H-EPSI spectra. Spatial resolution: 5 × 5 × 15 mm^3.

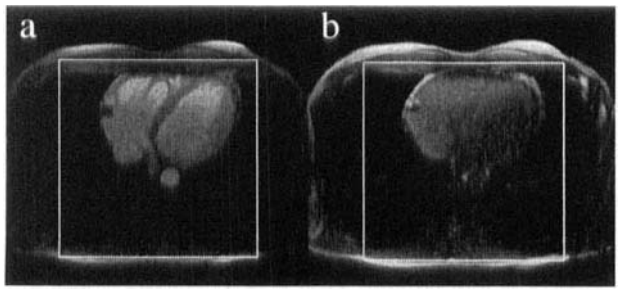

Figure 1. Transversal localizer image (segmented FLASH) of the heart region of a healthy volunteer obtained without (a) and with (b) water suppression.

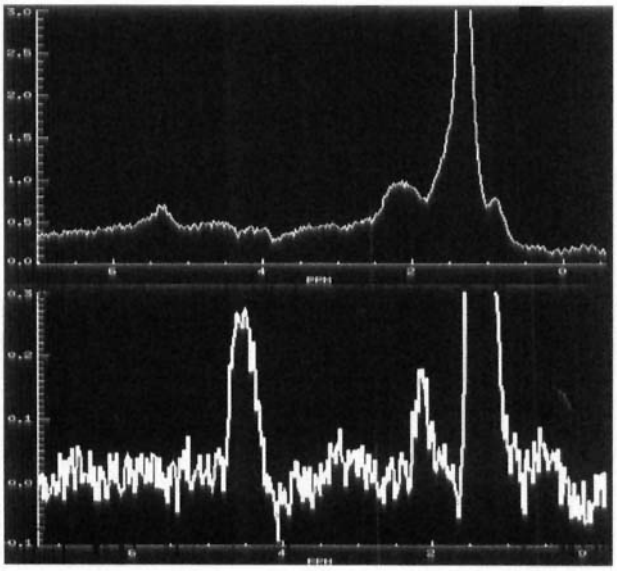

Figure 3. *In vivo* water-suppressed ^{1}H-NMR spectra extracted from EPSI data set (measurement time: 36 s) of the heart of a healthy volunteer. Resonances of triacylglycerides are resolved. The positions of the voxels are indicated in Fig. 2.

bility changes, partial volume effects) due to physiological motion was less than expected.

Conclusions: The data demonstrate that it is possible to obtain during a single breath-hold an array of resolved ^{1}H-NMR spectra of the human heart. The technique is sufficiently robust for patient studies. The detection of lipids in cardiac muscle is potentially important for the assessment of chronic ischamia (reduced β-oxidation of fatty acids), degenerative changes, and vitality.

References
1. Bottomley P et al. *Radiology* 191:593 (1994).
2. Neubauer S et al. *Mol. Cell. Biochem.* 184:439 (1998).
3. Löffler R et al. *J. Magn.-Reson.* 134:287 (1998).
4. Straeter-Knowlen IM et al. *Circulation* 93:1464 (1996).
5. Posse S et al. *Magn. Reson. Med.* 33:34 (1995).

8. High-energy phosphate metabolism in normal, hypertrophied, and failing myocardium in humans: absolute values of PCr and ATP determined by SLOOP ^{31}P-MRS

Meinrad Beer, M.D. *Institut für Röntgendiagnostik Würzburg, Germany*

Aims: Previously, ^{31}P-MR spectroscopy has allowed relative quantification of cardiac high-energy phosphates as the phosphocreatine/ATP ratio. This ratio has been found to be reduced in heart failure and correlates with the extent of mechanical dysfunction and with prognosis. We developed absolute quantification of high-energy phosphates and report on the first measurements in patients with left ventricular hypertrophy and heart failure.

Subjects/Methods: Ten patients with hypertensive heart disease (HHD), 10 patients with aortic valve stenosis (AVD), and 10 patients with dilated cardiomyopathy (DCM) were included in the study. Ten healthy age-matched volunteers served as control group (control). ^{31}P-MR spectroscopy with SLOOP (Spatial Localization with Optimal Pointspread Function) was used to measure absolute concentrations of phosphocreatine (PCr) and adenosine triphosphate (ATP). Functional data were determined by Cine MRI.

Results: Table 1 presents the functional data acquired using cine MR imaging. Table 2 presents the metabolic data acquired using SLOOP ^{31}P-MR spectroscopy.

Conclusion: PCr levels are reduced in AVD and DCM but not in HHD, whereas ATP levels are reduced in DCM only. The PCr/ATP ratio underestimates true changes of high-energy phosphate levels in heart failure.

9. Blood-oxygen-level-dependent MRI in patients with symptoms of coronary artery disease

M.G. Friedrich, T. Niendorf,* J. Schulz-Menger, O. Strohm, and R. Dietz. *Franz-Volhard-Klinik, University of Berlin, Germany; *GE Medical Systems, Leipzig, Germany*

Aims: Blood-oxygen-level-dependent (BOLD) MRI visualizes areas of reduced hemoglobin oxygenation (1) and is of proven value for functional brain imaging (2). BOLD MRI of the myocardium detects signal changes after pharmacological increase of blood supply (3,4). The purpose of this study was to assess the feasibility and clinical potential of BOLD MRI in patients with suspected CAD.

Methods: We applied T2*-sensitized gradient echo EPI (TE 17.4 ms) in a 1.5-T cardiovascular scanner (CV/i, GE Medical Systems, Milwaukee, WI) to 22 patients/132 segments with stress-inducible angina before, during, and after continuous infusion of adenosine (140g/kg/min) over 6 minutes. We compared the results to those of a subsequent (within 24 hours) thallium SPECT study using the same adenosine protocol.

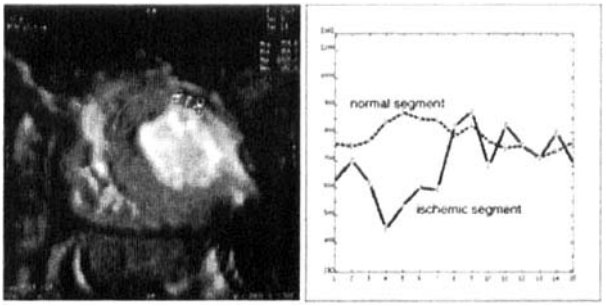

Figure 1. Time intensity curvse of the signal change during the protocol in a patient with a critical stenosis of a diagonal branch. Whereas the signal intensity increases in the septum (dotted line), there is a signal drop anteriorly.

Table 1

	Control (±)	HHD	AVD	DCM
LV EF (%)	69.3 ± 5.8	67.0 ± 6.0	57.7 ± 14.0*	18.4 ± 6.2**
LV M (g)	139.9 ± 23.8	217.1 ± 68.1*	230.0 ± 39.1**	234.7 ± 46.2**
LV EDV (ml)	102.3 ± 14.7	116.8 ± 27.2	123.9 ± 37.7	336.3 ± 76.4**
LV ESV (ml)	31.2 ± 9.9	38.5 ± 10.7	57.2 ± 38.2	274.5 ± 76.5**
LV SV (ml)	71.1 ± 7.4	78.3 ± 20.2	67.7 ± 15.0	68.0 ± 18.3

*$p < 0.05$ vs. vol.; **$p < 0.001$ vs. vol.

Table 2

	Control (±)	HHD	AVD	DCM
PCr (mmol/kg)	8.52 ± 1.54	8.24 ± 1.69	6.52 ± 1.79*	4.42 ± 1.32*
ATP (mmol/kg)	5.73 ± 1.66	5.56 ± 1.16	4.88 ± 0.93	3.58 ± 0.71**
PCr/ATP	1.69 ± 0.54	1.50 ± 0.30	1.34 ± 0.31*	1.26 ± 0.36*

*$p < 0.05$ vs. vol.; **$p < 0.001$ vs. vol.

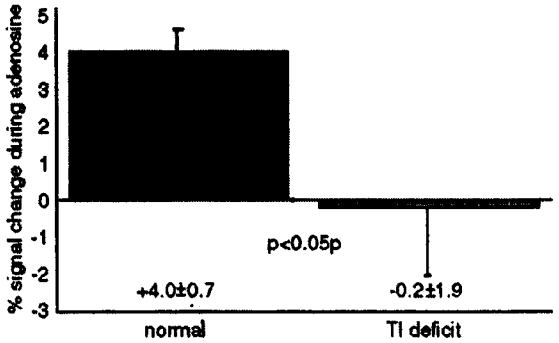

Figure 2. Mean signal change by adenosine infusion. In contrast to normal segments there is no signal increase in segments with a reduced T1 uptake.

Results: Sixty-nine segments showed a normal T1 uptake during and after adenosine, whereas 22 revealed a decreased signal counts with redistribution. Seven normal segments and two ischemic had to be excluded due to defined image quality criteria (ghosting, susceptibility artifacts). Ischemic areas as defined by the T1 uptake pattern revealed different signal intensity curves (Fig. 1).

Figure 2 shows the mean signal intensity change in the two groups of segments.

Using the lack of signal increase as a criterium, a T1 defined perfusion deficit was correctly detected in 51/62 segments (specificity 82%) and correctly excluded in 10/20 patients (sensitivity 50%).

The assessment of myocardial perfusion deficits by BOLD MRI using gradient echo EPI was feasible in patients with CAD. In our study areas of reduced perfusion could be detected with a good specificity but low sensitivity. The reason of the low sensitivity is unclear. Further studies need to address this.

References

1. Ogawa S, Lee TM, Kay AR, et al. *Proc Natl Acad Sci USA* 1990; 87:9868–72.
2. Niendorf T. *Magn Reson Med* 1999;41:1189–98.
3. Li D, Dhawale P, Rubin PJ, Haacke EM, et al. *Magn Reson Med* 1996;36:16–20.
4. Wacker CM, Bock M, Hartlep AW, et al. *Magn Reson Med* 1999; 41:686–95.

10. Screening for Coronary Artery Disease Using Magnetic Resonance Myocardial Perfusion Reserve Index

Eike Nagel, Nidal Al-Saadi, Susan Foerster, Ingo Paetsch, Simon Schalla, Christoph Klein, Uta Schneider, Bernhard Schnakenburg, Axel Bornstedt, Hans B. Lehmkuhl, Eckart Fleck. *Internal Medicine/ Cardiology, German Heart Institute & Charité, Campus Virchow, Berlin, Germany*

Introduction: With magnetic resonance imaging an index for myocardial perfusion, reserve can be determined from alterations of the signal intensity curves of the first pass of a gadolinium-DPTA (Gd) bolus before and after vasodilation (1,2). It has been shown that a linear fit of the upslope yields reproducible and valid results (3). In this study the value of MR perfusion measurements at rest and during vasodilation for the noninvasive detection of coronary artery disease in unselected patients with suspected coronary artery disease was assessed.

Figure 1. Breathing and injection scheme to acquire unenhanced images and first-pass perfusion images with minimal breathing motion.

Methods: One hundred and forty consecutive patients with suspected coronary artery disease referred for a primary diagnostic coronary angiography were examined with a 1.5-T MR tomograph (Philips ACS NT) using fast gradient systems (23 mT/m amplitude, 105 T/m/sec slew rate) and a dedicated five-element cardiac coil. To allow a small field of view, only the two anterior elements were used for imaging. Each heart beat five slices were acquired during the first pass of 0.025 mmol/kg Gd injected into the right cubital vein before and during adenosine (140 µg/kg body weight) vasodilation using a segmented k-space turbo-gradient-echo-EPI-hybrid sequence with a saturation prepulse (TE/TR/flip 3.3/12.5/30, acquisition time 104 ms, spatial resolution 1.7 × 1.9 × 8 mm)

Myocardial perfusion reserve index was determined from the alteration of the upslope of the myocardial signal intensity curves for six equiangular segments per slice using the MASS perfusion software (MEDIS. Leiden). A previously defined ischemic threshold was used to differentiate ischemic and nonischemic segments. Patients were defined as having significant coronary artery disease if any segment was below this threshold. A second analysis was performed using two segments as diagnostic criterion. Significant coronary artery disease was defined as an angiographic reduction of the luminal diameter of ≥75%. Contrast-to-noise ratio (enhanced versus unenhanced) was determined for the three coronary artery perfusion territories.

Results: Prevalence of coronary artery disease was 45%. Diagnostic signal intensity curves were achieved in 83% patients. The results for one respectively two segments below the ischemic threshold to define significant coronary artery disease are shown in the Table.

	1 Segment	2 Segments
Sensitivity	94%	90%
Specificity	68%	84%

Fourty-one false segments were found with the following distribution to vessel territories: LAD 24%, RCx 29%, RCA 46%. Contrast-to-noise ratio of the enhanced versus unenhanced images was LAD 8.3, RCx 6.9, RCA 4.8.

Conclusions: Magnetic resonance perfusion measurements allow a noninvasive diagnosis of significant coronary artery disease in an unselected prospective patient population with high diagnostic accuracy similar or superior to results reported from szintigraphic techniques. Most false-negative results can be found in the inferior wall, which is probably due to the lower contrast-to-noise ratio in these segments, related to the use of the anterior segments of the surface coil. MR perfusion measurements are a valid alternative for the examination of patients with known or suspected coronary artery disease.

References

1. Wilke N, Jerosch-Herold M, Stillman AE. *Magn Reson Q* 1994.
2. Wolff SD, Day RA, Santiago L. *Proc ISMRM* 1999.
3. Al-Saadi N, Nagel E, Klein C, et al. *Circulation* 2000 (in press).

11. Diagnostic Accuracy of Hybrid Echo-Planar Magnetic Resonance First Pass Perfusion Imaging in Patients with Suspected Coronary Artery Disease: A Comparison with Positron Emission Tomography and X-Ray Coronary Angiography

J. Schwitter, K. Bertschinger, D. Nanz, S. Kneifel, M. Buechi, F.W. Amann, T.F. Luescher, B. Marincek, G.K. von Schulthess.
University Hospital Zurich, Zurich, Switzerland

Purpose: To evaluate the diagnostic accuracy of a magnetic resonance (MR) first pass perfusion approach in comparison with positron emission tomography (PET) and conventional x-ray coronary angiography (x-CA) in patients with coronary artery disease (CAD).

Methods: In 8 healthy volunteers and 30 patients with suspected CAD, an MR first pass perfusion study (4–6 short-axis slices/2RR-intervals, echo-train length 4, 90 degree saturation pulse, delay time 120 ms) was performed. In the patients a PET study and x-CA were performed additionally. Patients with a history of myocardial infarction and/or hypo- or akinetic segments at rest (as assessed by MR) were excluded from the study. In all subjects extravascular GdDTPA (0.1 mmol/kg IV) was administered at 3 mL/sec during hyperemia (dipyridamole 0.56 mg/kg IV) and parametric maps of contrast medium (CM) wash-in were generated (pixelwise linear fits of signal intensity [SI] in the myocardium) after correction of the MR data set for gross cardiac motion, baseline SI, and input (parametric map divided by slope of SI increase in the left ventricular cavity). On these parametric maps, eight sectors/slice were analyzed beginning a the anterior junction of the right ventricle with the intraventricular septum (rotating clockwise). In all slices the sectors were assigned to the coronary arteries as follows: sector 1 and 8 to the left anterior descending coronary artery and branches, sector 3 to the circumflex coronary artery, and sectors 5 and 6 to the right coronary artery. In the same sectors of reformated short-axis dynamic ^{13}N-ammonia PET scans, resting and hyperemic myocardial blood flow and coronary flow reserve (CFR) were calculated. CAD was defined by MR (slope < mean-2SD of controls), by PET (CFR < mean-2SD of controls), and by quantitative x-CA (QCA: > 50% diameter stenosis).

Results: On the cine loops demonstrating CM first pass and on the corresponding parametric maps both, transmural and subendocardial zones of delayed CM wash-in were identified in myocardial territories subtended by stenosed coronary arteries. Sensitivity and specificity for the identification of individually diseased coronary arteries by MR were 82% and 70% vs. PET, respectively, and 79% and 66% vs. QCA, respectively. Sensitivity and specificity for detection of CAD by MR were 91% and 80% vs. QCA, respectively, and 95% and 82% vs. PET, respectively.

Conclusions: MR first pass perfusion imaging differentiates subendocardial from transmural perfusion defects in patients and MR-derived parametric perfusion maps are highly reliable in CAD detection.

12. Myocardial Perfusion Reserve Index Early After Successful Revascularization: Comparison of Stent and Balloon by Cardiac MR

N. Al-Saadi, E. Nagel, M. Gross, C. Klein, S. Schalla, *B. Schnakenburg, E. Fleck *Internal Medicine/Cardiology, Charité, Campus Virchow Clinic, Humboldt University, & German Heart Institute, Berlin and *Philips Medical Systems, Hamburg, Germany*

Since the reduction of myocardial perfusion is a sensitive sign of myocardial ischemia, the evaluation of myocardial perfusion is promising in the evaluation of patients with coronary artery disease. After angioplasty a residual early impairment of myocardial perfusion reserve has been reported in a variable fraction of patients, which has been mainly attributed to incomplete dilatation of the stenotic coronary artery and to a lesser extent to alterations of vascular (1). Further improvement of the initial morphological or functional degree of the success of a percutaneous transluminal angioplasty (PTCA) has been achieved by the use of intravascular stents (2). The aim of this study was to evaluate the changes of myocardial perfusion within 24 hours of successful PTCA or stenting in patients with coronary artery disease.

Methods: Thirty eight patients (29 male, 9 female, aged 58 ± 10 years) with significant single- or double-vessel coronary artery disease (≥75% area stenosis) referred for elective coronary intervention were prospectively included. All patients underwent quantitative biplane digital coronary angiography. Intervention was performed with or without stenting based on the decision of the physician performing the procedure.

Patients were studied with a 1.5-T whole body MR tomograph (ACS NT, Philips, Best, The Netherlands), using a five-element phased array cardiac surface coil. After two surveys, a short-axis view at the height of the origin of the papillary muscles was acquired using an ECG triggered T1-weighted inversion recovery single shot turbo-gradient echo sequence (inversion pulse, pre-pulse delay 360 ms, acquisition duration 360 ms, flip angle 15°, echo time 1.7 ms, repetition time 9 ms). Slice thickness was 8 mm with a spatial resolution of 1.7 × 1.9 mm. During an expiratory breathhold, a bolus of gadolinium-DTPA 0.025 mmol/kg body weight was injected via a central vein catheter. Dynamic images (one image per heart beat) were acquired during the first pass of the contrast agent before and after dipyridamole stress (0.56 mg/kg body weight for 4 minutes). The MR study was repeated within 24 hours after PTCA.

In all images the endo- and epicardial contours were traced. The myocardium was divided into six equiangular segments. Signal intensity was determined for all dynamics and segments. The upslope of the resulting signal intensity time curve was determined by the using a linear fit. The results were corrected for the input function by dividing the upslope of each myocardial segment by the upslope of the left ventricular signal intensity curve and perfusion reserve index (MPRI) was calculated. Using a previously defined ischemic threshold of 1.5 MPRI (3), segments were classified as ischemic or nonischemic.

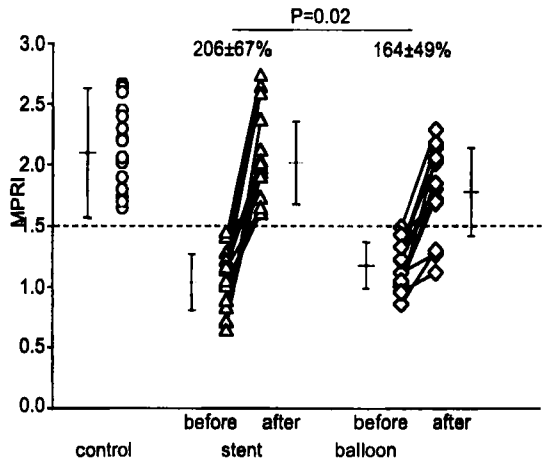

Results: Fifty-two coronary artery stenoses were found by angiography (LAD = 21, LCX = 15, RCA = 16). Two patients had triple-vessel disease and were referred for surgical revascularization. In all but two of the remaining patients, intervention was successfully performed (residual stenosis of <75%).

Before intervention MPRI was 1.13 ± 0.25 in segments supplied by a stenotic coronary artery and 2.18 ± 0.35 in control segments (p

< 0.001). Sensitivity and specificity for the detection of significant stenosis were 89% and 83%.

After intervention, MPRI increased significantly in segments supplied by successfully treated vessels (1.07 ± 0.24 before and 1.89 ± 0.39 after intervention; $p < 0.001$); however, it remained below the levels of the control segments ($p < 0.01$). Patients treated with stents ($n = 18$) showed a normalization of MPRI (1.99 ± 0.36 vs. 2.18 ± 0.35; n.s.), whereas those treated with balloon PTCA ($n = 13$) remained below the control group (1.72 ± 0.38, $p < 0.01$) and also below the patients treated with stents ($p < 0.05$).

The increase of MPRI was significantly higher in patients treated with stents (206 ± 67%) when compared with those without (164 ± 49%, $p = 0.02$).

Conclusions: Myocardial perfusion can be evaluated with cardiac MR by measuring MPRI. Significant coronary artery stenoses can be detected with high diagnostic accuracy. MPRI improved after coronary intervention and was more pronounced after stenting when compared with balloon PTCA. This technique may be used for the evaluation and follow-up of patients undergoing coronary intervention.

References

1. van Liebergen RA, Piek JJ, Koch KT, et al. *Circulation* 1998;98: 2133–40.
2. Kern MJ, Dupouy P, Drury JH et al. *J am Coll Cardiol* 1997;29: 1520–7.
3. Al-Saadi N, Nagel E, Gross M, et al. *Circulation* 2000 (in press).

13. Dobutamine Magnetic Resonance Myocardial Perfusion Reserve Index: a single stress test for an integrative examination

N. Al-Saadi, E. Nagel, M. Gross, *B. Schnackenburg, A. Bornstedt, E. Fleck *Internal Medicine/Cardiology, Charité, Campus Virchow Clinic, Humboldt University, & German Heart Institute, Berlin and *Philips Medical Systems, Hamburg, Germany*

Myocardial perfusion reserve has been determined in several studies to assess myocardial blood flow (1). This approach allows the evaluation of semiquantitative parameters rather than absolute quantification. In these studies dipyridamole or adenosine for vasodilation were used, which have been shown to yield valid results. Most perfusion studies preferred vasodilators such as dipyridamole or adenosine as they induce maximal vasodilation with minimal influence on hemodynamics. Whereas dobutamine is superior for the induction of wall motion abnormalities (2), it also increases myocardial perfusion by increasing coronary flow and cardiac work and may be used for the determination of perfusion reserve. The aim of the current study was to evaluate the value of dobutamine stress for the detection of significant coronary artery disease from the alterations of myocardial perfusion using magnetic resonance imaging.

Methods: To define normal values, 24 myocardial segments in five patients without angiographic coronary artery disease (3 male, 2 female, 53 ± 9 years) were studied. Then 25 patients (17 male, 8 female, 60 ± 8 years) with previously angiographically proven significant single- ($n = 14$) or double- ($n = 9$) vessel coronary artery disease were prospectively included. All patients underwent quantitative biplane, digital coronary angiography. Significant stenosis was determined as ≥75% area reduction. Patients were studied with a 1.5-T whole body MR tomograph (ACS NT, Philips, Best, The Netherlands), using a five-element phased array cardiac surface coil. After two rapid surveys, a short-axis slice at the height of the origin of the papillary muscles was acquired using an ECG triggered T1-weighted inversion recovery single shot turbo-gradient echo sequence (inversion pulse, pre-pulse delay 360 ms, acquisition duration 360 ms, flip angle 15°, echo time 1.7 ms, repetition time 9 ms). Slice thickness was 8 mm with a spatial resolution of 1.7 × 1.9 mm. During an expiratory breathhold, a bolus of gadolinium-DTPA 0.025 mmol/kg body weight (Magnevist, Schering AG, Berlin) was injected via a central vein catheter. Dynamic images (one image per heart beat) were acquired during the first pass of the contrast agent before and after dobutamine stress (5, 10, and 20μg/min/kg body weight for 3 minutes each).

In all images the endo- and epicardial contours were traced. The myocardium was divided into six equiangular segments. Images acquired after premature ventricular beats or insufficient cardiac triggering were excluded from the analysis to guarantee steady-state conditions. Signal intensity was determined for all dynamics and segments.

The upslope of the resulting signal intensity time curve was determined using a linear fit. The results were corrected for the input function by dividing the upslope of each myocardial segment by the upslope of the left ventricular signal intensity curve and perfusion reserve index was calculated.

Results: Median area reduction was 88%, and mean reference vessel diameter was 3.2 ± 7 mm. In patients with single coronary artery disease ($n = 14$), myocardial perfusion reserve index in ischemic segments was significantly lower than the contralateral segments (0.90 ± 0.18 versus 1.73 ± 0.32, $p < 0.0001$) or segments of the patients without coronary artery disease (2.0 ± 0.39, $p < 0.0001$). Myocardial perfusion reserve index in ischemic segments of all patients was (0.95 ± 0.22, $p < 0.0001$ vs. controls) (Figure).

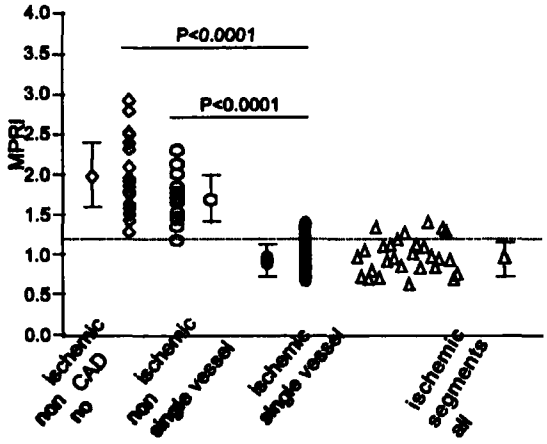

An ischemic threshold of 1.22 was defined from segments of patients without coronary artery disease (mean-2SD). The sensitivity, specificity, and diagnostic accuracy of this cut off value for the prospective detection of significant stenosis were 82%, 74% and 78% (Table).

	Stenosis ≥75%	Stenosis <75%
MPR ≤ 1.22	23	9
MPR > 1.22	5	26
	sensitivity = 82%	specificity = 74%

Conclusion: Dobutamine allows the assessment of myocardial perfusion reserve index using cardiac MR and yields a high diagnostic accuracy in the detection of coronary artery stenosis. Dobutamine can be used for an integrative cardiac examination combining the detection of wall motion abnormalities and the assessment of myocardial perfusion—the one step shop.

References
1. Al-Saadi N, Nagel E, Gross M, et al. *Circulation* (in press)
2. Nagel E, Lehmkuhl H, Bocksch W, et al. *Circulation* 1999;99:763–70.

14. ^{23}Na-Magnetic Resonance Imaging after myocardial infarction in human—preliminary results

J. Sandstede, T. Pabst, M. Beer, W. Kenn, K. Bäuerle, C. Lipke, D. Hahn, S. Neubauer[1] *Institut für Röntgendiagnostik & Medizinische Klinik[1], University of Wuerzburg, Germany*

Aim: ^{23}Na-MRI has previously been shown to have the potential to measure infarct size and to assess myocardial viability in an animal model. ^{23}Na images of the human heart have been acquired in volunteers. The aim of this study was to demonstrate the feasibility of ^{23}Na-MRI to assess myocardial infarction in patients.

Methods: Five healthy volunteers and four patients (5–190 days and 18 years after myocardial infarction, respectively) were examined in prone position using a ^{23}Na surface coil at 1.5 T. Double angulated short-axis images of the heart were imaged with an ECG-triggered 3d-FLASH-sequence. A field of view of 450 mm and a matrix of 64 × 128 resulted in an in-plane resolution of 3.5 × 7 mm^2; slice thickness was 16 mm. Therefore, six slices at average covered the entire heart. For the reduction of respiratory artifacts, 32 acquisitions were averaged. In the patients, conventional cine-MRI was used for the detection of wall motion abnormalities.

Results: With all examinations diagnostic image quality was acquired. The volunteers showed a higher ^{23}Na signal intensity in the anteroseptal wall and a lower signal intensity in the posterolateral wall according to the surface coil's profile without differences from base to apex. All patients showed an area of elevated ^{23}Na signal intensity in the anteroseptal or the posterolateral wall, respectively. These areas correlated well with the areas of wall motion abnormalities detected by cine-MRI.

Conclusion: Elevated ^{23}Na-MR image signal intensity has the potential to demonstrate subacute and chronic myocardial infarction in human. Further study is necessary to evaluate the relationship of ^{23}Na image signal intensity and myocardial viability.

15P. Quantitation of wall shear stress and subpixel lumen area in the coronary arteries using MRI phase contrast and the 3DP method

Sten Oyre, Sebastian Kozerke,* Peter Bosiger* & Erik Morre Pedersen *Department of Cardiothoracic & Vascular Surgery T, MR Research Center, Inst. for Exp. Clin. Research, Aarhus University Hospital, Denmark *Institute of biomedical Engineering and Medical Informatics, University of Zürich and Swiss Federal Institute of Technology, Zürich, Switzerland.*

Purpose: The purpose of this study is to quantify wall shear stress (WSS) and accurate subpixel lumen area in the right coronary artery using advanced postprocessing (1,2) of high resolution MRI velocity data combined with dedicated navigators.

Methods: The right coronary artery (RCA) was studied in eight healthy volunteers 1–3 cm after the origin from the aorta diastole (Philips NT 1.5 T MR scanner). Respiration control was obtained by using real-time, prospective navigator motion adapted gating (MAG, 3), and slice correction (correction factor between diaphragm and heart 0.6). Initial visualization of the RCA was obtained using an ECG gated 3D turbo field echo—echo planar imaging (TFEEPI) sequence gated to mid-diastole. Flow velocity were measured in a single time frame in mid-diastole using a standard ECG gated velocity encoded gradient echo sequence with 128 × 128 matrix, FOV 64 mm, 3 NSA, 6.00-mm slice thickness, V_{max} = 20 cm/s, flip angle 45°, and an 11 cm diameter circular RF receiver coil. Based on the initial manual segmentation of the RCA, the velocity data within 0.3–1.3 mm from the arterial wall in each of 12 circumferentially equidistantly located sectors (360 degree wide) were fitted using the 3DP method (1).

Results: In two subjects the data quality was insufficient for data analysis. In Table 1, the mean results from the six analyzed volunteers can be seen. In Fig. 1, an example of the raw data and corresponding edge detection is illustrated. Note the subpixel 95% limits for the edge points.

Table 1

Mean in vivo *results and fit statistics*

	Mean (SD)	Range
Area, mm^2	11.92 (5.97)	6.24–29.16
Diameter, mm	3.79 (0.99)	2.82–5.07
WSS, N/m^2	0.52 (0.17)	0.37–0.84
WSS SE, N/m^2	0.034 (0.012)	0.023–0.052
Pixels, n	27 (8)	19–39
3DP fit SD, cm/s	1.0 (0.3)	0.5–1.4
Adjusted R^2,	0.86 (0.05)	0.80–0.94
Edge point SE, μm	65 (15)	37–79

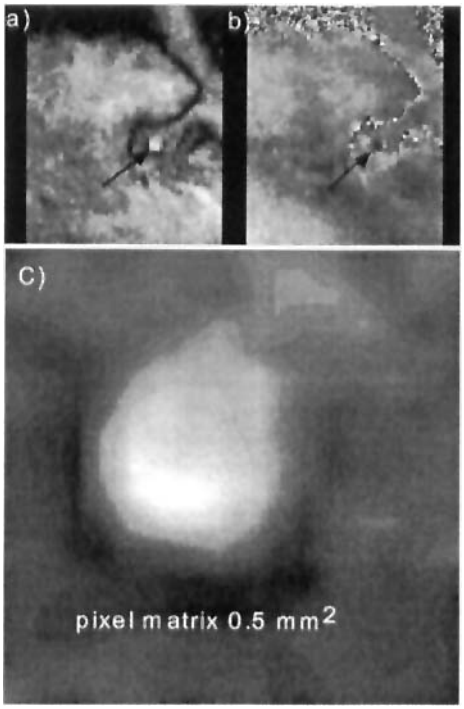

Figure 1. The (a) modulus and (b) velocity image of the cross-section of the right coronary artery (arrow) in mid-diastole at 540 ms after the QRS complex. (c) Magnified modulus image with the edge points radial × 95% limits (O) was determined.

Discussion: This study reports the first MRI-based measurements of subpixel lumen area and WSS in the coronary. The study has some limitations. First, the measured velocity is not quantitatively correct, unless corrected for through-plane heart motion. Second, correct perpendicular angulation is difficult, since in-plane/out-plane motion in the RCA is large (4). Finally, the correction factor of 0.6 for the heart motions relation to the diaphragm is an average and will be quite wrong for some individuals (5). Recently, the use of individually adjusted navigators has been suggested (5). This optimization or the navigator placed distal to the RCA directly on the heart would most likely improve the results of the present study and make it more robust.

When the present limitations are overcome in addition to further hardware and software improvements, it should be possible in the near future to use a more advanced version (2) of the present study method (1) for determination of e.g., endothelial function in the coronary arteries.

References

1. Oyre S et al. *JACC*, 32:128, 1998.
2. Oyre S et al. *MRM*, 40:645, 1998.
3. Weiger M, et al. *MRM*, 38:322, 1997.
4. Hofman MB et al. *JMRI*, 8:568, 1998.
5. Nagel E et al. *MRM*, 42:408, 1999.

16P. Diagnostic value of 2- and 3-dimensional image reconstruction techniques for detection of coronary artery stenoses using contrast-enhanced magnetic resonance coronary angiography

Matthias Regenfus, Dieter Ropers, Stephan Achenbach, Winfried Kessler, Werner G. Daniel, Gerhard Laub,* Werner Moshage
*Department of Cardiology, University of Erlangen-Nürnberg, Germany; *Siemens Medical Engineering Group, Erlangen, Germany*

Aims: Contrast-enhanced magnetic resonance (MR) coronary angiography allows visualization of coronary arteries and detection of coronary artery stenoses. Postprocessing may be performed by various 2- and 3-dimensional techniques. We compared three techniques of image reconstruction in respect to their accuracy to detect coronary artery stenoses.

Methods: MR imaging was performed in 61 patients on a 1.5-T scanner (VISION, Siemens) within one breath-hold using an ultrafast contrast-enhanced 3D gradient-echo sequence (TR/TE 4.2/1.6, spatial resolution 1.4 × 1.25 × 1.5 mm^2). In two successive studies, the imaging volume was positioned in oblique planes along the course of right (RCA) and left circumflex (LCX) and along left main (LM) and left anterior descending (LAD) coronary arteries, respectively. During each measurement, 20 ml gadolinium-DPTA (MAGNEVIST, Schering) was injected intravenously. Besides original source images, cine-loop image displays and maximum intensity projections (MIP) were independently evaluated. Results were compared to conventional coronary angiography in a blinded manner.

Results: Four hundred twenty seven coronary artery segments (LM and proximal and mid segments of LAD, LCX, and RCA) were assessed. In the assessable segments, source images showed highest accuracy; joint evaluation yielded 85.5% sensitivity and 89.3% specificity: Evaluation of unprocessed source images showed highest accuracy in detecting coronary artery stenoses by contrast-enhanced MR coronary angiography. MIP postprocessing is compromised by a higher number of unevaluable images due to overlap of coronary arteries with adjacent cardiac structures in this technique with oblique imaging planes.

	Assessable	Sensitivity	Specificity
Source images	76.8% (328/427)	85.3% (58/68)	90.4% (235/260)
Cine loop	75.6% (323/427)	83.6% (56/67)	89.5% (229/256)
MIP	73.8% (315/427)	84.4% (54/64)	87.3% (219/251)
Joint evaluation	77.9% (330/427	85.5% (59/69)	89.9% (233/261)

17P. Methods and clinical importance of magnetic resonance imaging in the evaluation of coronary bypass grafts

Th. Wittlinger,[1] T. Voigtlnder,[1] K.F. Kreitner,[2] S. Petersen,[1] P. Kalden,[2] M. Thelen,[2] J. Meyerl.[1] *2nd Medical Clinic[1] and Department of Radiology,[2] University Hospital Mainz, Germany*

Aim: The aim of the study was to evaluate the reliability of magnetic resonance imaging (MRI) in the assessment of coronary bypass grafts.

Methods: We investigated 110 patients with a total of 325 bypass grafts (235 saphenous venous grafts, 90 internal mammarian grafts). MRI (1.5-T Vision, Siemens AG) was performed using a multislice, ECG-gated, breath-hold turbo spin echo sequence (HASTE) and 3D-contrast media enhanced angiography sequence (FISP). The HASTE-sequences served as a fast orientation of the vessel course and as basis for planning flow quantitative measurements. The FISP-sequence is characterized by short repetition and echo times. This sequence allows at an investigation time of 25–30 seconds the imaging of the proximal anastomosis and of the vessels course.

Results:

Sequence	Sensitivity	Specificity	Distal anastomosis
HASTE	94%	97%	80%
FISP	92%	94%	68%

Conclusions: These results show that coronary bypass grafts can reliably be detected using MRI. A total imaging of the vessel is possible by combining different imaging techniques. The distal anastomosis can be detected in 80% of the cases with the HASTE-Sequence; the best results of the maximal bypass parts will be achieved the FISP-3D-sequence.

18P. Reliability of magnetic resonance flow measurement in coronary grafts is more influenced by velocity encoding than by field of view or temporal resolution

S. Petersen

Background: MR flow measurement in coronary grafts is challenging due to a pulsatile flow character with low velocities and small vessel

diameters. In vitro we studied the influence of velocity encoding (VENC), field of view (FOV), and nonsegmented and segmented sequences on the reliability of the results.

Methods: A dicrotic pulsatile flow pattern (peaks 1 and 2) typical for a vein graft to the right coronary artery was generated by a computer-controlled pump. The pump was connected with a tube system (inner diameter 4.5 mm). At the tube site of MR flow measurements (1.5 T, Siemens) a transit time flow meter (TTF) was used as reference. We calculated the relative errors of MR to the TTF results for mean flow, peak 1, and peak 2. In a first step we investigated the influence of varying VENCs (75 and 150 cm/sec) and FOVs (150 and 200 mm) on the reliability using a segmented sequence. Then we compared the results of a segmented and nonsegmented sequence in a FoV of 150 mm and a VENC of 75 cm/sec.

Results: Relative errors of MR measurements compared to TTF are summarized. A significant loss of reliability of the MR measurements occurred when using a VENC of 150 cm/sec for all three parameters (mean flow, peaks 1 and 2; $p < 0.001$). An increased FOV (i.e., decreased in-plane resolution) did not change the relative error for mean flow. Peaks 1 and 2 were also less reliable with a diminished spatial resolution. The temporal resolution showed no significant influence on reliability comparing segmented and nonsegmented sequences.

Conclusions: Optimized adaptation of VENC is crucial for reliable MR flow measurement in coronary grafts. Mean flow measurement was not significantly influenced by decreased temporal or spatial resolution.

19P. Improved MRI Assessment of Coronary Artery Flow: Prospective Real-Time Correction for Through-Plane Motion

P. Kunz,[1] H.J. Lamb,[1] S. Kozerke,[2] P. Boesiger,[2] J. Doornbos,[1] A. de Roos.[1] [1] *Department of Radiology, Leiden University Medical Center, Leiden, The Netherlands;* [2] *Institute of Biomedical Engineering and Medical Informatics, University and ETH Zurich, Switzerland*

Introduction: Several investigators have recently reported methods for measuring velocity and flow in coronary arteries with a high temporal and spatial resolution using MRI. However, the vigorous motion of the coronary arteries throughout the cardiac cycle might hamper the accuracy of flow measurements. To accurately assess flowthrough heart valves a method has been proposed that adapts the imaging slice position for each heart phase according to the trajectory of the heart valve throughout the cardiac cycle (1). The aim of the present study was to assess coronary artery flow prospectively corrected for through-plane motion.

Methods: Flow in the left anterior descending artery (LAD) of 10 healthy subjects was assessed using a Philips ACS/NT 1.5-T system. Multiple survey scans were accomplished to obtain a slice where the proximal part of the LAD is in plane. Perpendicular to the LAD a subtractive labeling technique (90° slice selective followed by ±90° nonselective pulse; acquisition during a breath-hold in expiration) allows marking and subsequent following of a single line on the myocardial muscle during the cardiac cycle. With image analysis software labeled points were extracted automatically that resulted in the trajectory of the LAD during the cardiac cycle. Slice angulation, off-center, and through-plane velocity of the successive phase contrast flow measurement were individually calculated for each heart phase.

The imaging slice for phase contrast imaging was positioned perpendicular to the LAD. Slice angulation and off-center of each cine-frame of the phase contrast scan were individually adapted according to the previously assessed trajectory. Parameters of the phase contrast scan were as follows: FOV 256 × 180 mm^2, matrix size 256 × 180, slice thickness 5 mm, velocity encoding range 40 cm/s, TE = 4.1 ms, temporal resolution 30 ms. Respiratory motion was compensated by using prospective navigator gating.

Results: Assessment of LAD flow was possible in all subjects. Maximum systolic through-plane velocity of the LAD was 8.0 ± 0.9 cm/s, whereas a maximum through-plane velocity of 7.9 ± 0.8 cm/s was found during diastole. Peak through-plane motion of the LAD was 11.4 ± 1.7 mm. Without correction a mean diastolic LAD flow velocity of 9.9 ± 2.1 cm/s was assessed, whereas an increased diastolic mean flow velocity of 13.2 ± 2.2 cm/s was calculated after correction of the through-plane velocity (mean systolic LAD flow velocity: uncorrected 5.3 ± 1.0 cm/s; corrected 1.2 ± 1.4 cm/s).

Discussion: Accurate assessment of coronary artery flow by MRI requires correction for through-plane motion of the vessel of interest. The currently presented heart motion adapted scan method provides a simple and accurate method to prospectively correct for through-plane velocity by tracing the actual trajectory of the vessel. Application of heart motion adapted scanning enables reliable quantification of diastolic-systolic flow ratios that may be an absolute measure of stenosis severity in patients.

Reference

1. Kozerke S, et al. *MRM* 42:970–978 (1999).

20P. Mortality after Myocardial Infarction is Increased in Rats after Severe Phosphocreatine Depletion with β-Guanidinopropionate

Michael Horn, Helga Remkes, Mark de Groot, Kai Hu, Stefan Neubauer *Medizinische Universitätsklinik Würzburg, Germany*

Introduction: In residual intact myocardium after acute myocardial infarction, phosphocreatine (PCr) and total creatine (Cr) contents are reduced by ~35%. Energy reserve via creatine kinase in these hearts is reduced by ~50%. To test whether loss of PCr contributes to chronic contractile dysfunction (remodeling), we depleted phosphocreatine and creatine by feeding the creatine analogue β-guanidinopropionate (GP). Chronic feeding causes a ~90% decrease of phosphocreatine and creatine in control rats.

Methods: Male Wistar rats were subjected to sham operation or coronary artery ligation (MI). Four groups were studied: normal diet (no GP feeding, $n = 6$); fed with GP for 56 days after MI ($n = 7$), fed with GP 14 days before MI ($n = 43$), fed with GP 28 days before MI ($n = 45$). Fifty-six days after MI, hearts were isolated and perfused isovolumically.

High-energy phosphates were determined by ^{31}P-NMR spectroscopy at 7 T. One hundred fifty two FIDs were averaged over 5 min, using a 45° pulse and a TR of 1.53 sec. Spectra were phased individually and integrated (NMR1, Tripos) and values obtained were corrected for partial saturation. Creatine levels were determined with HPLC.

Results: When rats were fed GP post-MI, hearts adapted by increasing LV mass. When rats were pre-fed with GP (groups 3 and 4), **mortality** of MI rats within 2 months was **100%** and only shams survived. See table and graphs on following page.

Conclusions: Rats with approximately 90% depletion of phosphocreatine and creatine **cannot survive** an acute MI. Depletion of phosphocreatine and creatine after MI increases heart weight, suggesting increased LV hypertrophy.

Data for rats fed after MI

	Sham	MI	Sham + GP	MI + GP
Heart rate, min^{-1}	259 ± 8	234 ± 16	267 ± 5	255 ± 11
LVDP, mm Hg	87 ± 17	59 ± 9*	58 ± 7#	51 ± 7
HW, g	1.80 ± 0.06	+2.14 ± 0.10*	1.80 ± 0.08	2.54 ± 0.22*
HW/BW, g/kg	3.62 ± 0.25	3.85 ± 0.13*	3.48 ± 0.14	5.37 ± 0.43*#
PCr, mM	13.6 ± 1.1	11.8 ± 1.0*	3.4 ± 0.1	2.2 ± 0.3*#

*$p < 0.05$ Sham vs. MI, #$p < 0.05$ GP vs. no GP.
HW = heart weight, BW = body weight, LVDP = left ventricular developed pressure, PCr = phosphocreatine

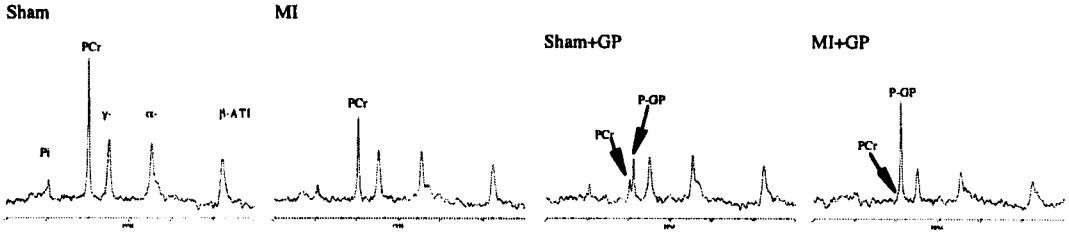

21P. A clinical qualitative approach to perfusion MRI for the detection of coronary artery disease

P.R. Sensky,[1] C. Reek,[2] N.J. Samani,[1] G.R. Cherryman[2] *Departments of Cardiology[1] and Radiology,[2] Glenfield Hospital, Leicester, United Kingdom.*

Aim: To establish the value of qualitative reporting of myocardial perfusion images for the detection of significant CAD (50% angiographic cross-sectional area reduction).

Methods: Thirty patients with known CAD underwent PMRI (Siemens Vision, 1.5-T scanner), using a dynamic inversion recovery snapshot-FLASH sequence; TR 4.5ms, TI 300ms, TE 2ms, FOV 300 × 300mm, slice thickness 9mm, 96 × 128 matrix, 25 measures. Basal, midpapillary, and apical short-axis planes were acquired after a bolus of 0.025 mmol/kg Gd-DTPA was injected at rest and during adenosine infusion (140 mg/kg/min for 6 minutes). The myocardium was divided into eight radial regions of interest (ROIs). Each ROI was assigned to a coronary artery territory (CAT) according to coronary artery (CA) anatomy described by the Green Lane reporting system. Stress and rest scans were assessed for abnormal regional perfusion (hypoenhancement). For each CAT, PMRI was reported as abnormal if one or more ROIs within that territory showed a perfusion deficit. Eighty-six CATs were assessed. (In four patients, the right CA failed to reach the left ventricle).

Results: All patients completed the protocol. Imaging time was 20–25 minutes. Image quality was sufficient to allow qualitative reporting in all patients. Only 15/720 ROIs (2%) could not be evaluated because of artifact. PMRI scans were abnormal in all patients. The number of CATs supplied by an angiographically diseased vessel that were detected on PMRI is shown in Table 1.

Table 1

Detection of significant CA stenosis (CA+) by PMRI

	CA+	CA−
PMRI+	66	6
PMRI−	5	9

For the individual CATs, the overall sensitivity for the detection of a significant CA stenosis was 93% with a specificity of 60%. Overall diagnostic accuracy was 87%.

Conclusion: Qualitative assessment of perfusion with MRI has a high accuracy for the detection of significant CAD. This approach also meets the need for rapid reporting required by physicians in the clinical workplace.

22P. Semiquantitative Perfusion Analysis with Cardiac Magnetic Resonance: Comparison of Peripheral and Central Gadolinium-DTPA Injection

N. Al-Saadi, E. Nagel, M. Gross, *B. Schnackenburg, A. Bornstedt, E. Fleck. *Internal Medicine/Cardiology, Charité, Campus Virchow Clinic, Humboldt University, & German Heart Institute, Berlin and *Philips Medical Systems, Hamburg, Germany*

Introduction: Previous magnetic resonance imaging (MR) studies of first pass myocardial perfusion used a gamma variate fit for (semi-) quantitative analysis of the signal intensity curves of a gadolinium-DPTA (Gd) bolus (1). This approach requires a central venous injection of a very compact contrast agent bolus (2). We have recently shown that a linear fit of the upslope of a central veneously injected contrast Gd bolus yields reproducible and valid results in patients with suspected coronary artery disease (3). In this study we evaluated differences between central and peripheral injection of a contrast agent bolus, if a linear fit of the upslope is used for (semi-) quantification.

Methods: In 20 patients MR perfusion measurements were performed with a 1.5-T MR tomograph (Philips ACS NT). Each heart beat 1 short-axis view was acquired during the first pass of 0.025 mmol/kg Gd using an ECG-triggered T1-weighted inversion recovery single shot turbo-gradient echo sequence (inversion pulse, pre-pulse delay 360 ms, acquisition duration 360 ms, flip angle 15°, echo time 1.7 ms, repetition time 9 ms, spatial resolution 1.7 × 1.9 × 8 mm). During an expiratory breath hold, a bolus of Gd 0.025 mmol/kg body weight was injected into the superior vena cava via a central venous catheter. Dynamic images (one image per heart beat) were acquired during the first pass of the contrast agent. Twenty minutes later to allow clearance of the contrast agent, measurements were repeated with contrast agent injection into the right antecubital vein. In four patients perfusion reserve after

vasodilation with dipyridamole (0.56 mg/kg body weight for 4 minutes) was calculated for both central and peripheral injection. Using the MASS perfusion software (MEDIS) the endo- and epicardial contours were traced in all images. The myocardium was divided into six equiangular segments. Signal intensity was determined for all dynamics and segments. The upslope of the resulting signal intensity time curve was determined by the use of a linear fit. The results were corrected for the input function by dividing the upslope of each myocardial segment by the upslope of the left ventricular signal intensity curve (relative upslope) and perfusion reserve index (MPRI) was calculated.

Intraobserver variability of the linear fit after central and after peripheral injection of Gd were determined in 100 segments each. Linear regression and relative error were calculated for repeated injections and repeated measurements.

Results: Intraobserver variability for the linear fit yielded excellent correlation for central (r = 0.98) and peripheral (r = 0.96) injection. Relative differences were 4.7 ± 5.4% and 11.3 ± 12.4% (Fig. 1). Central and peripheral Gd injection showed a close correlation for the relative upslope (n = 84 segments, r = 0.91, $p < 0.0001$) and for MPRI (n = 24 segments; r = 0.88; $p < 0.05$) (Fig. 2). However, both relative upslope and MPRI were lower after peripheral injection due to the slower arrival and, thus, larger dispersion of Gd during the passage through peripheral veins. MPRI in myocardial segments supplied by a stenotic coronary artery was significantly lower than in segments supplied by a nonstenotic coronary artery both in the central and peripheral group ($p < 0.001$).

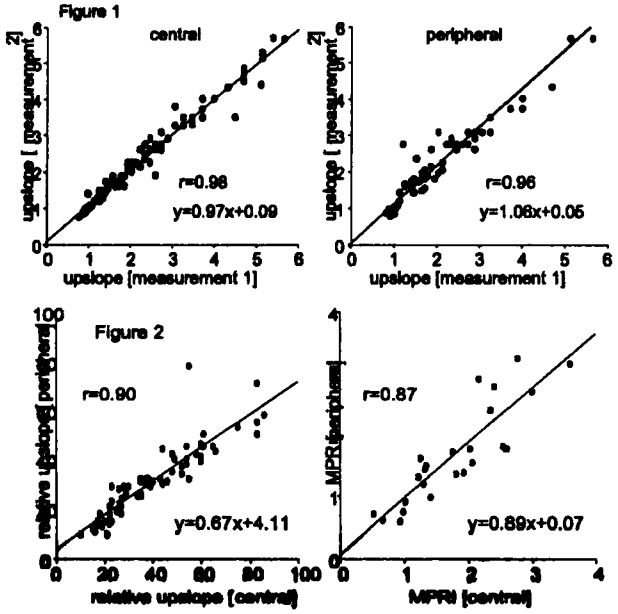

Conclusions: Using the linear upslope of the signal intensity curves, peripheral injection yields reproducible results with minimal differences to central injection. This is in contrast to previous (semi-) quantification from a gamma-variate fit, which requires a central venous injection. This simple approach will facilitate perfusion measurements for clinical use as a noninvasive procedure.

References

1. Wilke N, Juronch Harold M, Wang Y, et al. *Radiology* 1997;204: 373–84.
2. Keijer JT, van Rossum AC, Eenige MJ, et al. *Am Heart J* 1995;130: 893–901.
3. Al-Saadi N, Nagel E, Klein C, et al. *Circulation* (in press).

23P. Observer-independent and time-efficient analysis of magnetic resonance first-pass perfusion data

Daniel Nanz, Katrin Bertschinger, Thomas F. Luescher, Borut Marincek, Gustav K. von Schulthess, Juerg Schwitter. *University Hospital Zurich, Switzerland*

Purpose: Magnetic resonance first-pass perfusion imaging during hyperemic conditions has been shown to accurately delineate hypoperfused myocardium in patients with coronary artery disease (CAD). To date, the evaluation of such dynamic data sets is either observer dependent and/or very time consuming. Segmentation of left ventricular (LV) myocardium at the blood pool–myocardial interface is crucial, since subendocardial layers are most sensitive to ischemic insults. An evaluation software is presented that automatically identifies the blood pool–myocardial interface based on a pixelwise time-series correlation analysis.

Methods: In six healthy volunteers and six patients with known CAD, and MR first-pass perfusion study (4–6 slices/2RR-intervals, 90 degree preparation pulse, delay time 120ms) was performed. During data acquisition extravascular GdDTPA (0.1 mmol/kg IV) was administered at 3 mL/sec during hyperemia (dipyridamole 0.56 mg/kg IV). Translational image registration was performed in case the subject was not able to hold his breath long enough. The LV epicardial border was then traced manually on a combination image with maximum contrast between right ventricular blood pool and myocardium for best identification of the septal borderline portion. The LV blood pool–myocardial interface was traced manually on a combination image with maximum contrast at the LV blood pool–myocardium interface and obtained automatically from a threshold-free correlation analysis using the LV time-intensity curve. After a mouse click on the anterior junction between the right ventricle and the intraventricular septum, contrast medium induced maximum relative signal-intensity increases in eight sectors per slice were automatically evaluated as a measure of perfusion.

Results: The automatic algorithm detected the LV blood pool–myocardial interface in all hearts (48 slices; 384 sectors). The total analysis time for one study was approximately 5 minutes. Correlation of manually and automatically obtained slope values was excellent (slope = 0.97, r = 0.98, $p < 0.0001$). Bland Altman analysis indicated a slight overestimation of the slope values in the automatic approach by 1.7 ± 5.6%. The 95% confidence interval for the two techniques was ±11.0%.

Conclusions: Time-series correlation analysis automatically detects the blood pool–myocardial interface in dynamic first-pass MR perfusion data sets and time efficiently provides an observer-independent quantification as a complement to subjective visual assessment of MR first-pass perfusion data.

24P. Time Resolved Sodium Imaging of the Human Heart at 1.5 T

Renate Jere_i_,[1] Michael Bock,[1] Christian Wacker,[2] Wolfgang Bauer,[2] Lothar R. Schad.[1] [1]*Dept. of Biophysik und Medizinische Strahlenphysik, Deutsches Krebsforschungszentrum (DKFZ), Heidelberg, Germany* [2]*Dept. of Cardiology, University of Würzburg, Würzburg, Germany*

Introduction: A number of noninvasive ^{1}H-MR imaging methods exist to study myocardial viability (1). In nonviable tissue the ^{23}Na gradient between intra- and extracelluar space cannot be maintained. Therefore, ^{23}Na-MRI has the potential to differentiate viable from ischemic myocardium noninvasively (2–4). Due to the reduced MR sensitivity of the sodium nucleus and the lower spin density, long acquisition times are used in ^{23}Na-MRI. In ^{23}Na cardiac imaging often no ECG-triggering is used to reduce the scan time. This results in a diastolic weighting of the sodium MR images. In this study ECG-triggered sodium imaging of the human heart is implemented. With fast gradient echo pulse se-

quences and shared echo reconstruction methods, a total scan time of less than 19 min is achieved.

Materials and Methods: An ECG-triggered, segmented, 2D-FLASH sequence was implemented on a 1.5-T whole body scanner (VISION, Siemens, Germany) for the acquisition of time resolved sodium images. Within a single heart cycle nine k-space lines per image were acquired. The central portion of k-space was updated every 60 ms, whereas outer k-space information (four lines) was shared between subsequent phases. Eleven images could be acquired per cardiac cycle. By acquiring an asymmetric echo in frequency encoding direction (asymmetry: 1/4) and by using a short (2000 μs) slice selective sinc-pulse a short echo time TE of 4.4 ms was achieved.

Other imaging parameters were as follows: matrix 36 × 64, FOV 350 mm, slice thickness (SL) 25 mm, NEX 250, readout bandwidth 156 Hz/pixel, acquisition time TA 18 min 34 s.

Before acquisition of the sodium images, ^{1}H imaging was performed for shimming, slice positioning, and anatomical localization of the ^{23}Na images. For comparison, a pulse sequence with the same sequence timing (SL 20 mm, NEX 1, TA 15 s) was used for proton imaging of the heart. All sodium images were then acquired with a rectangular linear polarized ^{23}Na surface coil (Rapid, Würzburg). To avoid patient repositioning, ^{1}H images were obtained with the standard body coil and the disconnected sodium coil left in place.

Results: Figure 1 shows for three selected heart phases a comparison between the sodium and the corresponding proton images. Both right and left ventricles and the myocardium are clearly visible. The signal-to-noise ratios (SNR) were 7.4 for the ventricle, 5.5 in the septum, and 10.3 in rib cartilage (SNR was calculated as mean signal intensity in the object/mean signal intensity in the background). In cine mode the contraction of the ventricles can be clearly seen in the sodium images. ^{23}Na images were interpolated to a 128 × 128 matrix.

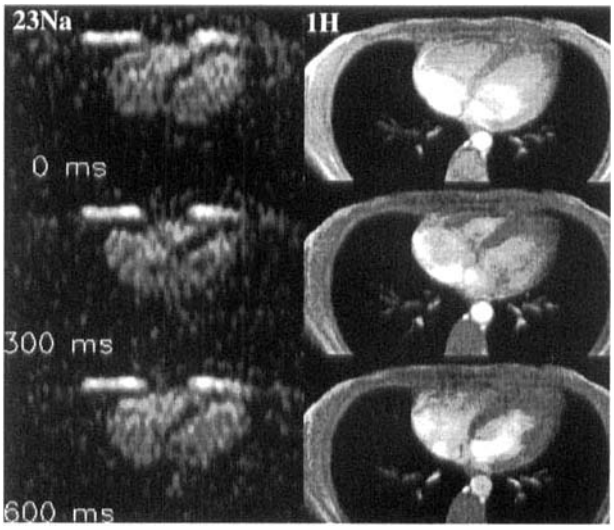

Figure 1. Three selected sodium (left) and proton (right) images of a healthy volunteer from a time series of 11 heart phases. In the transverse slice through the heart, the right and left ventricles are visualized together with the myocardium. The time denotes the difference between the R-wave of the ECG and the acquisition of the central k-space line of the image.

Discussion and Conclusion: As we have shown, it is possible to acquire time-resolved sodium images of the human heart in a clinically feasible scan time (18 min 34 s). A good correlation between ^{23}Na and ^{1}H imaging is seen. The slice positions agree well, as the proton images are acquired during free breathing like the sodium images, even though the slice thickness is not exactly the same.

At a TE of 4.4 ms the ^{23}Na signal predominantly reflects extracelluar sodium that reflects mainly the long T2. As it takes about 400 ms for the sodium gradient between intra and extracelluar ^{23}Na to return to baseline, the temporal resolution of the presented method should be sufficient to detect signal changes in the myocardium during one heart cycle. Future work aims at the differentiation of intra and extracelluar sodium, by applying a double-echo sequence with a short and long TE.

References

1. Wacker CW, et al. *Magn. Reson. Med* 41, 686–695, 1999.
2. Kim RJ, et al. *Circulation* 95, 1877, 1997.
3. Bottomly PA, et al., *Proc. ISMRM*, 892, 1998.
4. Constantinides C, et al. *Proc. ISMRM*, 221, 1999.

25P. Blood-oxygen-level-dependent (BOLD) MRI in healthy volunteers and patients with peripheral occlusive arterial disease (PAOD)

T. Poetsch, T. Niendorf,* R. Dietz, and M.G. Friedrich. *Franz-Volhard-Klinik, Humboldt-University of Berlin, Germany; *GE Medical Systems, Leipzig, Germany*

Background: The BOLD effect on the T_2^* relaxation of MRI signals has been extensively studied. Brain studies comprise most of the published data.[1] In a recent report Lebon et al.[2] observed the temporal relationship between intensity changes in MRI images and tissue oxygen content, measured by myoglobin proton NMR spectroscopy in the skeletal muscle. The purpose of this work is to demonstrate the impact of improved perfusion on the oxygenation as visualized by signal intensity changes in T_2^*-weighted images of skeletal muscle during ischemic stress test imposed on healthy volunteers and PAOD patients.

Methods: MRI was carried out on a whole body 55-cm free bore 1.5-T MR scanner system (CV/i, GE Medical System, Milwaukee, WI). T2*-sensitized gradient echo EPI (TE < 50 ms) has been applied in 13 healthy volunteers and 34 patients with PAOD Fontaine stage I–IV *(6 pat.), IIa (10 pat.), IIb (21 pat.), III (3 pat.), and IV (5 pat.)*. The subjects were placed in a supine position with extended legs and a large cuff placed above the knee and the investigated calf below was centered in a birdcage coil. For each patient 250 images were obtained with a temporal solution of 1.7 s during an ischemic protocol *consisting of three sections: 60 s resting condition, 240 s leg ischemia (cuff pressure 30–50 mm Hg above systemic blood pressure), 120 s postischemic recovery*. Off-line evaluation included a computer-based calculation of time-signal-intensity curves with resulting parametric images (negative and positive enhancement images).

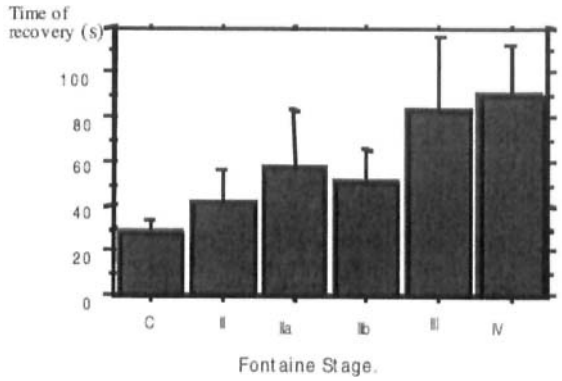

Figure 1. Histogram of healthy volunteers (C) and patients with PAOD (Fontaine stages I–IV). There is a delayed postichemic recovery after intermittent ischemia as induced by cuff inflation.

Results: In all cases the image quality was sufficient for analysis. In all subjects signal intensity decreased immediately after cuff inflation. Upon reperfusion, signal intensity revealed an overshoot in all healthy volunteers but not in patients with severe PAOD. In patients with advanced disease, the time of signal recovery to baseline values was significantly longer (Fig. 1).

Conclusion: BOLD-MRI using gradient echo EPI detects changes in the skeletal muscle during ischemia. Patients with advanced PAOD may reveal specific patterns of signal intensity curves. *Further studies need to address sensitivity and specificity.*

References

1. Haacke EM, Lai S, et al. *Human Brain Mapping* 5:341–346; 1997
2. Lebon V, Brillault-Salvat C, et al. *MRM* 40:551–558

26. Cardiac MRI Diagnosis of Ventricular Abnormalities associated with Arrhythmias of Right Ventricular Origin

T Bloomer, S Plein, JP Ridgway, DJ Beacock, UM Sivanathan. *MRI Unit Leeds General Infirmary, Leeds, United Kingdom.*

Aims: Right ventricular (RV) arrhythmias are a significant cause of cardiac mortality. The differential diagnosis of RV tachycardia includes arrhythmogenic right ventricular cardiomyopathy (ARVC) and right ventricular outflow tachcardia (RVOT). Cardiac MRI enables visualization of the RV free wall structure and function. RV abnormalities by MRI have been reported in ARVC and more recently in RVOT. We have scanned over 80 patients referred with arrhythmias of RV origin. The purpose of this study is to review the cardiac MRI abnormalities with respect to the clinical diagnosis based on the clinical history and electrophysiological studies.

Methods: We have retrospectively reviewed cardiac MRI scans from 41 patients with possible RV arrhythmias who underwent the Leeds protocol on a Philips 1.5-T MR system with a cardiac surface coil.

The Leeds protocol comprises

Supine scans

1. Breathhold axial gradient echo cines from diaphragm to pulmonary bifurcation,
2. Tagged gradient echo through the RV free wall and outflow tract (tags AP),
3. Tricuspid inflow velocity encoded flow map.

Prone scans

4. Axial spin echo images (optimised sequence, TD 50–100 ms, R-R interval window 50–60%, ascending slice order),
5. Axial spin echo with fat supression,
6. Axial T2 weighted breathhold multishot turbo spin echo ("black blood").

Images were evaluated for intramyocardial fat, RV thinning, RV outpouching or dilation, and RV wall dyskinesia. Reviewers were blinded to the clinical information.

Results: The cohort includes patients with ARVC, RVOT, RV ectopy, and undiagnosed ventricular tachycardia. The ARVC group (five patients) all showed RV abnormalities with fat infiltration (2), thinning of the RV wall (4), localized outpouching and dilation (4), or dyskinesia (2). Four patients with ARVC had three or more different abnormalities. The RVOT tachycardia group (four patients) also all demonstrated RV abnormalities with fat infiltration (1), thinning of the RV (3), outpouching of the outflow tract (1), and RV dyskinesia (2) (1 in RV outflow). In the RV ectopy cohort (nine patients), two patients had normal MRI. The rest all showed RV thinning (7), outpouching (2), or RV outflow dilation (1). No patients with left ventricular origin arrhythmias (4 patients) demonstrated RV abnormalities on cardiac MRI.

Conclusion: Cardiac MRI demonstrated RV abnormalities in patients with arrhythmias of RV origin. More abnormalities were found in ARVC than in other groups. Cardiac MRI abnormalities overlap between ARVC, RVOT, and RV ectopy. Increasing experience will allow the diagnostic accuracy of the different MRI criteria to be defined for the cause of RV origin arrhythmias.

27. Magnetic Resonance Imaging to Assess Atrial Transport Function as a Marker of Procedural Success after Maze Operation

A. John, T. Dill, Z.A. Szalay,° W. Ricken, G. Bachmann,* R. Brandt, E.P. Bauer, C.W. Hamm. *Departments of Cardiology, Radiology* and Cardiothoracic Surgery°, Kerckhoff Clinic, Bad Nauheim, Germany*

Objective: Maze operations are being performed on patients with atrial fibrillation refractory to medical treatment. Our aim was to investigate whether magnetic resonance imaging (MRI) can provide valid hemodynamic information about the recovery of atrial transport function after this operation.

Methods: Twenty-four patients (15 male, mean age 66 years, range 43–84) were included. All underwent 6 months of follow-up imaging consisting of MRI and transthoracic echocardiography, and 14 have had 12 months follow-up imaging yet. MR examinations were performed on a 1.5-T Magnetom Vision (Siemens, Erlangen, Germany) using 10-mm ECG-gated flash 2d-cine slices (TE 3.6 ms, TR 80 ms) in short axis orientation encompassing the entire atrial cavity. For postprocessing, images were transferred into the Argus program (Siemens) for volumetric assessment. Transmitral flow was estimated via through-plane flash 2d flow measurement (TE 5 ms, TR 24 ms, slice thickness 8 mm, pixel size 1.15 × 1.15 mm) to facilitate a second approach of assessing atrial function. Recovery of atrial transport function was defined as an A-wave in the mitral flow curve and an ejection fraction on atrial volumetry.

Results: At 6 months follow-up, 22 of 24 patients were in sinus rhythm. On MRI 18 of 22 patients (82%), had on echo 17 of 22 (77%) had an atrial transport function. Six patients (seven on echo, respectively) did not show any signs of atrial contraction. All patients who underwent 12 months follow-up were in sinus rhythm. MRI showed an atrial transport function in 10 of 14 (71%) and echo in 11 of 14 (79%).

Conclusions: This study demonstrates that the Maze operation restores atrial transport function in patients with refractory atrial fibrillation. Both MRI and echo showed comparable results and provide hemodynamic information on procedural success after Maze procedure. MRI results may therefore be used to assess the need for further anticoagulation.

28. Long-term follow-up of patients with acute myocarditis by magnetic resonance imaging

A. Wagner, J. Schulz-Menger, O. Strohm, R. Dietz, and M.G. Friedrich. *Franz-Volhard-Klinik, Charité, Humboldt University of Berlin, Germany.*

Background: The long-term course of acute myocarditis is not well understood. Whereas in many (if not most) cases it may not even really be noticed by the patient, the disease may be fatal for others. In a prospective study we included 19 patients with acute myocarditis into a clinical and magnetic resonance imaging (MRI) protocol (1).

Methods: We observed the clinical status and the MRI findings from 19 patients during 36 months after acute viral myocarditis. MRI studies

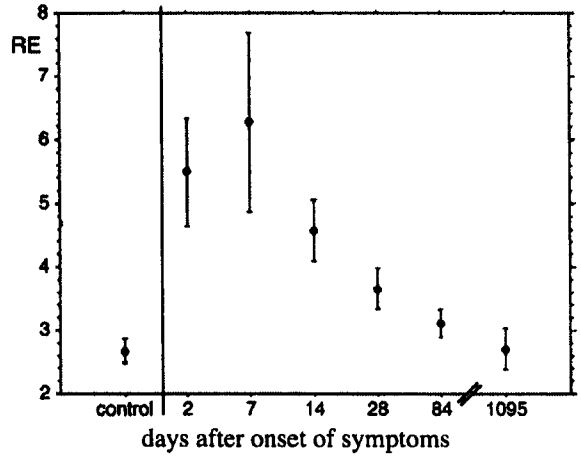

Figure 1. Course of the relative myocardial contrast enhancement (RE) in the 16 surviving patients in acute viral myocarditis. The mean value in normal subjects is indicated as "0" (2.5 ± 0.2).

were performed on a standard clinical system (Siemens Impact 1.0 T, Siemens AG, Erlangen, Germany). Contrast-enhanced, T1-weighted, fast spin echo images were obtained to characterize myocardial tissue enhancement. The myocardial signal increase after Gd-DTPA administration was compared with that of the skeletal muscle (relative enhancement, RE). Left ventricular ejection fraction (EF) was measured with breathhold gradient echo cine sequences in contiguous short-axis planes (TE 6.1 ms, TR 90ms, slice thickness 10 mm). The 3 months' data have already been published (2).

Results: From the 19 patients, nobody was lost to follow-up. One patient commited suicide due to other reasons. Of the remaining 18 patients, 11 (61%) recovered uneventfully. Two patients (10.5%) died due to congestive heart failure. Of the remaining 16 patients, 5 patients (31%) were still symptomatic, 3 of them reported a significant impairment of their quality of life.

The RE was increased in the early course of the disease and normalized after 4 weeks (Fig. 1). There was an inverse development for the EF (Fig. 2). RE correlated very well with the symptoms as defined by a symptom score. The RE on day 2 correlated to the symptom persistence and to the ejection fraction 36 month after onset of disease ($p < 0.01$). The initial findings in contrast-enhanced MRI correlate with long-term clinical outcome of viral myocarditis.

Conclusion: The full recovery of acute myocarditis seems to be a delayed process, which is completed between than 3 months and 3 years after its onset. The findings in contrast-enhanced MRI correlate with the clinical activity of viral myocarditis. The initial extent of the myocardial injury seems to have a strong impact of the long-term clinical and functional outcome.

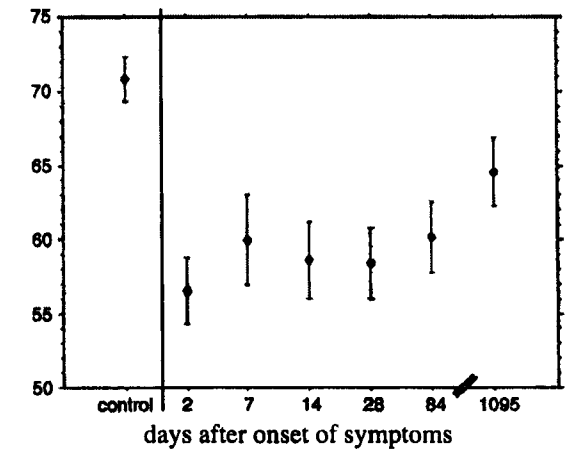

Figure 2. Course of the left ventricular ejection fraction (EF) in the 16 surviving patients after acute viral myocarditis. There is a delayed recovery of LV function correlating to the course of the contrast enhancement as shown in Fig. 1.

Reference

1. Friedrich MG, Strohm O, Schulz Menger J, et al. *Circulation* 1998; 97:1802–9.

29. Cardiac Magnetic Resonance Imaging (MRI) vs. biopsy in β-thalassemia.

S.I. Mavrogeni, L. Kaklamanis, D. Tsiapras, I. Paraskevaidis, D.V. Cokkinos, L. Vlahos[1] and D.T. Kremastinos. *Onassis Cardiac Surgery Center and [1]Areteion University Hospital, Athens, Greece.*

Serum ferritin levels are considered a valuable index of iron tissue deposition, although they may be affected by factors such as fever or inflammation. On the other hand, biopsy is the only way to detect iron deposition in individual organs. The aim of this study was to apply MRI, a noninvasive technique, in the assessment of myocardial iron deposition and compare the results with cardiac biopsy data and serum ferritin levels.

Twenty patients, aged 22 ± 8 yrs, were studied. ECG-gated spin echo images were obtained from all patients using a 0.5-T superconducting system. Heart T2 relaxation time was calculated using TR = HR and TE = 17 msec in seven symmetrically repeatable echoes (17–119 msec). Biopsy was performed in all patients within 5 days of the MRI scan. Serum ferritin levels were calculated from the average values of the last 5 years.

All study patients were in heart failure (NYHA II–III). According to biopsy, heart iron deposition was graded as mild in 4 and severe in 16 patients. Agreement between biopsy and MRI was found in 15/16 patients with high iron deposition and in 3/4 patients with low iron deposition. Heart T2 relaxation time correlated negatively with serum ferritin ($r = -0.88$, $p < .001$) and cardiac biopsy results (Spearman's test, rho = -0.47, $p < 0.04$). Ferritin also correlated with biopsy results (rho = -0.50, $p < 0.03$)

According to our results, heart T2 relaxation time measured noninvasively by MRI appears in agreement with ferritin and cardiac biopsy data. Although the correlation between biopsy and MRI is very strong, further studies are needed in milder cases.

30. MRI in the assessment of subclinical anthracycline cardiotoxicity

M.G. Friedrich, R. Waβmuth,* A. Wagner, J. Schulz-Menger, O. Strohm, and R. Dietz, *Franz-Volhard-Klinik, University of Berlin, Germany; *NHLBI, NIH, Bethesda, MA, USA.*

Background: Anthracyclines used in antineoplastic therapy may lead to cardiotoxic long-term effects in a considerable number of patients. So far no reliable markers to detect early cardiac damage have been found. We tested the ability of magnetic resonance imaging (MRI) to

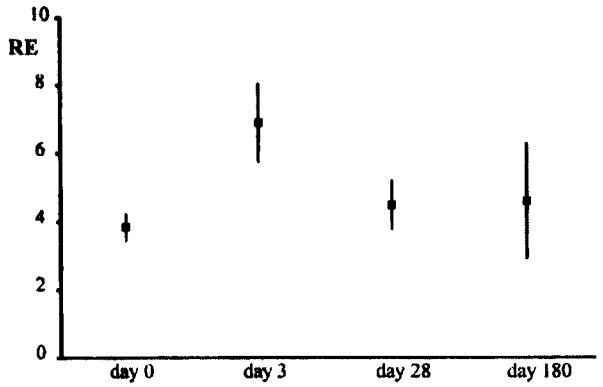

Figure 1. Relative myocardial contrast enhancement (RE) after the onset of anthracycline therapy. There is a significant increase on day 3 with a normalization in most of the patients during the later course.

show early changes in myocardial signal and cardiac function after anthracycline therapy.

Methods: In this study 22 patients without preexisting heart disease were investigated before, 3 days after, 28 days after, and 180 days after anthracycline therapy using a standard clinical scanner (Siemens Impact 1.0 T, Siemens AG, Erlangen, Germany). Contrast-enhanced, T1 weighted, fast spin echo images were obtained to characterize myocardial tissue enhancement. The myocardial signal increase after Gd-DTPA administration was compared with that of the skeletal muscle (relative enhancement). Left ventricular ejection fraction (LVEF) was measured with breathhold gradient echo cine sequences in contiguous short axis planes (TE 6.1 ms, TR 90 ms, slice thickness 10 mm).

Results: There was no clinical evidence for acute cardiotoxic injury in any patient. The relative myocardial signal enhancement increased from 3.83 ± 0.37 to 6.91 ± 1.13 ($p < 0.01$, see Fig. 1). LVEF decreased from 67.8 ± 1.4% to 61.9 ± 1.7% after 180 days ($p < 0.05$, see fig. 2). There was a trend toward correlation between the increase of the relative enhancement on day 3 and the LVEF loss at 180 days.

Conclusion: MRI detects a subtle loss of left ventricular contractility in asymptomatic patients after anthracycline therapy. Early changes of myocardial contrast accumulation may be a useful early marker of a cardiotoxic myocardial injury.

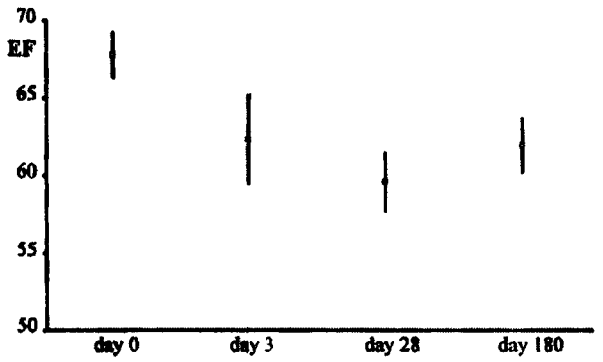

Figure 2. Left ventricular ejection fraction (EF) after anthracycline therapy. There is a small loss early after onset of therapy within the normal range but remained significantly decreased.

31. Three-year follow-up with MRI after septal artery embolization in patients with HOCM

J. Schulz-Menger, O. Strohm, F. Uhlich, R. Dietz, M.G. Friedrich.
Franz-Volhard-Klinik, Charité, Humboldt-Universität, Berlin

Aims: The morphological changes after septal artery embolization (TASH) in hypertrophic obstructive cardiomyopathy (HOCM) are not well understood. MRI reproducibly depicts cardiac anatomy. We assessed the ventricular changes during a 3 year follow-up.

Methods: We investigated 11 patients with HOCM in a conventional MRI scanner (Siemens-Expert 1.0 T resp. GE Signa 1.5 T) during 6 months to 3 years after TASH and compared the results with patients without intervention. Furthermore, we investigated the observer variability. Using gradient echo sequences, we directly measured minimal orifice area of the left ventricular outflow tract (LVOT) during maximal blood flow in systole as a parameter to quantify obstruction of the LVOT. Furthermore, we estimated left ventricular diameter, ejection fraction (EF), and mass.

Results: There was an increase of the LVOT area during 3 years after TASH by 123 ± 27%. The increase correlated with the improvement of the clinical outcome ($r = 0.9$). There was a significant difference to a control group of patients without HOCM (2.5 ± 0.2 vs. 5.0 ± 0.2 cm^2, $p < 0.03$), whereas there was no difference as compared with 17 patients with HOCM without or only mild symptoms (2.6 ± 0.4 cm^2, Fig. 1).

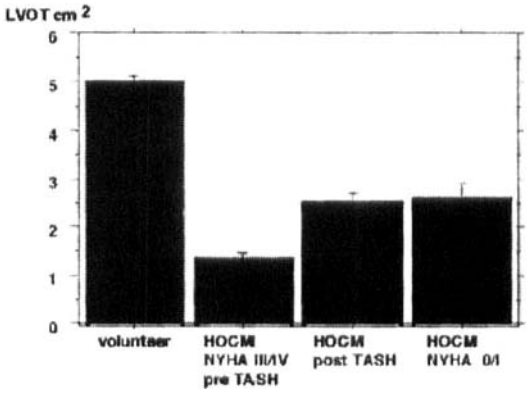

Figure 1. Comparison of LVOT area.

In the interventional group there was no significant reduction of the posterior wall thickness (from 15.1 ± 2.1 to 13.7 ± 1.8 mm). EF did not change (66 ± 3 vs. 67 ± 3%). MRI studies are very well suitable for follow-up studies in patients after TASH. The increase of the LVOT area as measured by planimetry correlates to the clinical outcome, without a complete normalization of the LVOT. The long-term result after intervention corresponds to the LVOT area of patients with HOCM without or mild symptoms.

32. Serial assessment of cardiac remodeling by MRI after myocardial infarction in rats

M. Nahrendorf,[1] K.-H. Hiller,[1] F. Wiesmann,[2] K. Hu,[2] C. Waller,[2] J. Ruff,[1] A. Haase,[1] G. Ertl,[2] W.R. Bauer[2] [1]*Physicalisches Institut (EP5), Universität Würzburg,* [2]*Medizinische Universitätsklinik Würzburg, Germany*

Background: The rat model of myocardial infarction (MI) has proven important parallels to the process of cardiac remodeling and develop-

Results

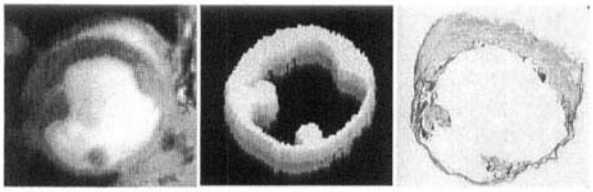

Short axis view | result of segmentation | histology

Figure 1.

ment of heart failure in the human heart. It was involved in the introduction of ACE inhibitors into therapy of heart failure (1). We therefore tested the application of cine FLASH MRI to this model, compared it with invasive techniques (2–4), and did serial MRI investigations.

Methods: MRI scans were done 4, 8, 12, and 16 weeks after left coronary artery ligation in a 7-T scanner using an ECG-triggered cine-FLASH sequence: 16 short-axis slices, slice thickness 1 mm, echo-time 1.2 ms, resolution 230 μm. MI size, left ventricular (LV) mass, LV volumes, cardiac index (CI), ejection fraction (EF), end-diastolic wall (EDW), and scar thickness (SCT) were determined in 11 Wistar rats. In four controls, ligature was not closed.

After MRI hemodynamic measurements were done for determination of the same parameters by electromagnetic flowmeter (2) and postmortal pressure-volume curves (simultaneous infusion at 0.76 ml/min and pressure recording, EDV is infused volume at in vivo measured end-diastolic pressure) (3). LVs were weighted. In an additional set of experiments of 26 infarcted rats, MRI-acquired and histological MI size (picric red dye after formalin fixation) (2) was compared.

Results: MRI and invasive methods were in good agreement (MI size $r = 0.97$ with significant difference of 5%, LV mass $r = 0.97$, EDV $r = 0.97$ with significant difference of 9%, CO $r = 0.8$).

Conclusion: The study showed good agreement of MRI-acquired data with established methods. A significant weight gain of the infarcted LV and increased wall thickness of the surviving myocardium demonstrate that hypertrophy took place from 4 to 16 weeks after MI accompanied by dilation of the LV. This remodeling of the LV did not lead to a further decline of the slightly depressed resting cardiac output. This technique is well suited to assess future therapeutic options for heart failure.

Table 1

Results of serial MR investigations

	4 weeks	16 weeks after MI
LV mass (mg)	531.8 ± 19.3	863.3 ± 34.4*
EDV (μl)	591.3 ± 40.8	711.3 ± 65.7*
EDW (mm)	1.28 ± 0.06	1.9 ± 0.05*
SCT (mm)	0.97 ± 0.05	0.47 ± 0.05*
EF (%)	36.5 ± 2.8	34.2 ± 2.2
CI (ml/kg · min)	225 ± 7.9	227.9 ± 16.3

Mean ± SEM, *$p < 0.05$ vs. 4 weeks. Resulting MI size was 30.2 ± 3.1%. Eight and 12 weeks not shown.

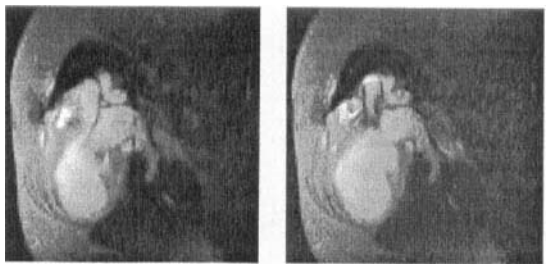

diastolic long axis | sytolic long axis view

16 weeks after myocardial infarction

Figure 2.

References

1. Pfeffer JA, Pfeffer MA, Fletcher PJ, Braunwald E. Influence of chronic captopril therapy on the infarcted left ventricle of the rat. *Circ Res* 1985;57:84–95.
2. Pfeffer MA, Pfeffer JM, Fishbein MC, Fletcher J, Spadaro J, Kloner RA, Braunwald E. Myocardial infarct size and ventricular function in rats. *Circ Res* 1979;44:503–512.
3. Pfeffer MA, Frohlich ED. Electromagnetic flowmetry in anesthetized rats. *J Appl Physiol* 1972;33:137–140.
4. Fletcher PJ, Pfeffer MJ, Pfeffer MA, Braunwald E. Left ventricular diastolic pressure-volume relations in rats with healed myocardial infarction. *Circ Res* 1981;49:618–626.

33. Low-dose ramiprilate treatment improves wall thickening after myocardial ischemia and reperfusion

S.E. Petersen, G. Horstick, D. Becker, T. Voigtländer, W. Schreiber,[1] H. Ruetten,[2] M. Thelen,[1] O. Kempski,[3] J. Meyer. *2nd Medical Clinic, [1]Department of Radiology, [3]Institute for Neurosurgical Pathophysiology, University Hospital Mainz, Germany; [2]Aventis Pharma Frankfurt a.M., Germany*

Background: Reperfusion of a previously ischemic area results in an inflammatory response leading to additional damage of myocytes that are still viable at the end of the ischemic period. There is evidence in the literature that the local renin-angiotensin-aldosterone-system (RAAS) is activated by reperfusion. To prove the concept of local RAAS activation, we examined the effect of low-dose ramiprilate administration (preventing ACE-inhibitor-dependent afterload reduction) on infarct size and regional myocardial function.

Methods: After anesthesia with chloralhydrate, intubation, and mechanical ventilation, left lateral thoracotomy was performed. The left coronary artery (LCA) was occluded for 30 minutes. Five minutes prior to reperfusion an arterial blood gas was drawn and either ramiprilate (10 mcg/kg, n = 6) or NaCl 0.9% (n = 6) was infused into the left atrium under normoxic conditions and six-lead ECG control. Rats were extubated after reperfusion and reintubated 24 hours later for final examinations. Evans-Blue was injected after reclusion of the LCA to determine the area at risk (AR) followed by a vital staining with TTC. The left ventricle (LV), the area at risk (AR) and the zone of myocardial infarction (MI) were determined by planimetry.

Examinations of myocardial wall motion were performed on a conventional 1.5 T Siemens Vision system using a small eye coil. The ECG-triggered spin-echo sequences (TR/TE = 600 ms/14 ms, FOV 85 mm, MA = 192 × 256, slice thickness 2 mm) had an in-plane resolution of 0.3 × 0.3 mm. Images were recorded at 20 ms increments following the R-wave of the ECG acquiring a basal and an apical slice. Maximum diastolic relaxation and systolic contraction were used for off-line analysis of regional wall thickening.

Results: The area at risk was similar in both groups (ramiprilate: 44 ± 5% vs. NaCl 0.9%: 41 ± 6%). Areas of MI/AR were not different between both groups (ramiprilate: 45 ± 11.7% vs NaCl 0.9%: 35 ± 15%). Concerning regional wall motion analysis, apical slices demonstrated significantly improved wall thickening of the reperfused lateral wall after treatment with ramiprilate.

Conclusion: The study clearly demonstrated improved regional wall thickening after ischemia and reperfusion with low-dose ramiprilate treatment despite equivalent infarct sizes in both groups. We conclude that low-dose ACE-inhibitor administration might reduce myocardial stunning after a brief period of ischemia.

34. Detection of myocardial edema by black blood breath-hold STIR MRI in the diagnosis of subacute myocardial infarction

A.M. Beek, M.J.W. Götte, J.T. Marcus, A.C. v. Rossum, C.A. Visser *University Hospital Vrije Universiteit, Amsterdam, The Netherlands*

Background: In acute prolonged coronary occlusion, increased capillary permeability, loss of cellular integrity, and compression of lymph vessels results in edema formation in the interstitial space. The increased water content leads to prolongation of myocardial relaxation times T1 and especially T2, which can be detected by magnetic resonance imaging (MRI). The modified short τ inversion recovery (STIR) is a turbo spin-echo sequence characterized by dark blood preparation, fat suppression, diastolic image acquisition, and predominant T2 weighting. It is presumed to be sensitive to changes in tissue composition after myocardial infarction. This study evaluates STIR in the detection and localization of infarct-related edema in a prospective group of patients with first myocardial infarction.

Patients and Methods: Thirty-eight patients (aged 59 ± 9 years) were studied 5 days (4–14) after admission. Myocardial infarction was confirmed by a more than twofold rise in CK. Infarct site according to ECG was anterior in 23 patients and inferior-posterolateral in 15 patients. Thirty-three patients received revascularization therapy (17 thrombolysis, 16 primary PTCA). Mean peak CK was 1530 ± 1052. All images were acquired on a 1.5-T scanner with the use of a cardiac body array coil. The imaging protocol included breath-hold cine imaging and breath-hold STIR at identical short-axis and long-axis positions in the left ventricle. Regional wall motion and STIR signal intensity (SI) were assessed in three short-axis slices (basal, mid, and distal) or in three long-axis slices (two-, three-, and four-chamber view). Short-axis slices were divided in six equiangular segments, starting at the posterior insertion of the right ventricle. Each segment was scored for the presence of wall motion abnormalities (WMA) (hypo-, a-, or dyskinesia) and abnormal high SI. STIR defined infarct location was presumed correct if there was a minimal overlap of two segments with the area of WMA. See Figure 1 below.

Results: In 32 patients (84%) STIR correctly identified infarct location. In four (11%), STIR images either showed indiscriminate SI distribution or were of poor quality due to respiratory artifacts, making analysis unreliable. A gradual decrease in SI was noted in most patients from anteroseptal to posterolateral region and from basal to distal slice position due to differences in distance to the body array coil. This was generally easily differentiated from the regional and more circumscript high SI seen at infarct sites but may have led to the misdiagnosis of two patients (5%) with posterolateral infarcts. Infarct area per slice was smaller by STIR than by WMA (mean number of segments 6.13 ± 2.55 vs. 7.54 ± 2.95, $p < 0.0001$). A total of 539 segments in 31 patients were further analyzed. In 152 of 228 segments with abnormal wall motion, STIR showed high SI compatible with edema (sensitivity 67%). In 273 of 311 segments without WMA, STIR did not show abnormal SI (specificity 88%).

Conclusion: Edema can be demonstrated by unenhanced STIR MRI in most patients in the subacute phase of MI. The area of edema by STIR was smaller than the area of WMA by cine MRI, which might be explained by the fact that edema is not found in regions with myocardial stunning but only at regions that have become necrotic.

35. Visualization of infarct-related acute myocardial edema and necrosis in patients by MRI

J. Schulz-Menger, O. Strohm, F. Uhlich, R. Dietz, M. G. Friedrich. *Franz-Volhard-Klinik, Charité, Humboldt-Universität Berlin*

Aims: The very early myocardial changes in acute myocardial infarction are not thoroughly investigated. On the basis of a defined myocardial infarction, performed as a therapeutical option in patients with hypertrophic obstructive cardiomyopathy, we applied MRI techniques to visualize myocardial features early after infarction and in a short-term follow-up.

Methods: We investigated 11 patients on days 1, 3, 7, 14, and 28, with a subgroup of 5 patients within 45 min after embolization with a MRI scanner (Siemens-Expert 1.0 T resp. GE Signa 1.5 T). The visualization of the myocardial infarction and the associated edema was performed using T2-weighted spin echo sequences (STIR, TE 64 ms) and T1-weighted spin echo sequences before and after application of 0.1 mmol/kg Gd-DTPA (Magnevist®, Schering AG; Berlin).

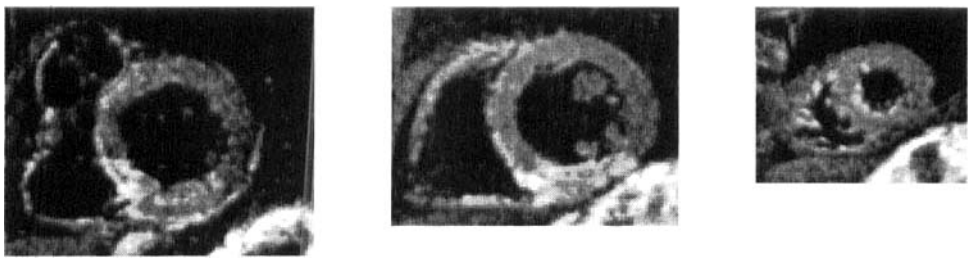

basal *mid* *distal*

Figure 1. Example of basal, mid, and distal short-axis STIR in a patient with inferior myocardial infarction, showing circumscript regions of high signal intensity in the basal and midventricular slice (inferoseptal-inferior segments and inferior-posterolateral segments, respectively). In all slices, a gradual decrease in SI is visible from anteroseptal to posterolateral region.

Results: Within the first 45 min after the myocardial infarction there was no edema. The visualization was possible between days 3 and 14. In the T1-images a strong signal enhancement in the uninfarcted region could be visualized 20 min after contrast media application. The intensity and the extent of the localized enhancement showed large differences. It is noticeable, that the borders to the normal myocardium are sharper in the induced infarction than in the classic myocardial infarction.

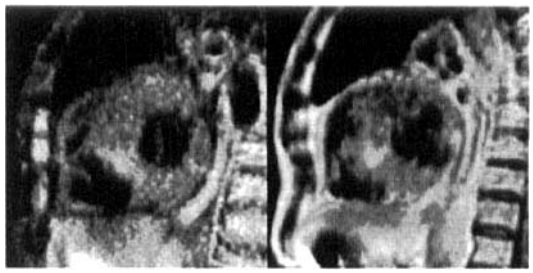

Figure 1. Imaging of acute myocardial infarction 7 days after septal artery ablation. Left panel: Localized edema in T2-weighted imaging. Right panel: Necrosis visualization by contrast-enhanced T1-weighted imaging.

Conclusion: The development of myocardial edema after induced myocardial infarction is delayed. The prognostic value of the variable contrast enhancement has to be investigated in further studies.

36. Extent and severity of acute myocardial infarction can be determined with delayed contrast-enhanced MRI

S.E. Petersen

Background: Hyperintense areas in contrast-enhanced magnetic resonance imaging (ceMRI) reflect nonviable tissue in acute reperfused myocardial infarction as shown in an animal model with TTC staining (Kim et al. *Circulation* 1999). The aim of our study was to show the reliability of ceMRI to show the extent and the severity of acute myocardial infarction in humans.

Methods: We investigated 10 patients with acute myocardial infarction using a 1.5-T scanner (Siemens Magnetom Vision). Prior to ceMRI the global myocardial function was analyzed with a standard cine MR sequence with 5–7 slices. Corresponding slices were acquired using the delayed enhancement sequence 5–10 minutes after the application of the contrast agent (TurboFLASH, TR/TE 2350/3.4 ms; TI 150–200 ms, FoV 350 × 350 mm). As contrast medium we used gadolinium-DTPA in a concentration of 0.2 mmol/kg as a bolus via a venflon positioned in a cubital vein. The area of hyperenhancement and the area of the left ventricle was determined for each slice by planimetry. The percentage of hyperenhancement in relation to the area of the left ventricle (LV) was then calculated for the entire heart. Maximal concentrations of creatine kinase (CKmax) were determined.

Results: All 10 MR investigations were of excellent image quality, and demarcation of hyperenhanced areas was easy. No reliable CKmax was available in one patient. The area of hyperenhancement in relation to the left ventricle correlated very well with CKmax (%hyperenhancement/LV = 0.008 × CKmax + 3.4; $r = 0.86$, $p < 0.001$). The area of hyperenhancement was also correlated to ESVI (%hyperenhancement/LV = 0.9 × ESVI − 1.86; $r = 0.68$, $p < 0.05$).

Conclusions: The area of hyperenhancement in acute myocardial infarction is significantly correlated to an in vivo marker of cell damage (CKmax). This supports the hypothesis of prolonged contrast agent accumulation in damaged myocardial areas caused by a change in the distribution volume due to damaged cellular membranes. The size of the myocardial lesion predicts the global myocardial function.

37. Comparison of delayed contrast-enhanced MRI and dobutamine cine-MRI in the identification of regional left ventricular (LV) recovery following coronary artery bypass grafting (CABG) in patients with poor ejection fraction.

P.R. Sensky,[1] R. Keal,[2] N.J. Samani,[1] G.R. Cherryman.[2] *Departments of Cardiology[1] and Radiology,[2] Glenfield Hospital, Leicester, United Kingdom*

Aim: To compare the sensitivity and specificity of contrast-enhanced MRI (CE-MRI) with dobutamine (Db) cine-MRI in the prediction of post-CABG regional LV functional recovery in patients with established coronary artery disease (CAD) and preoperative low ejection fraction (EF).

Methods: Nine patients undergoing CABG with EF < 35% were studied. Regional systolic function and preoperative contractile reserve (CR) were assessed using breath-hold gradient echo cine-MRI (3 short-axis slices base, mid-papillary, apical, each divided into 8 radial regions of interest [ROIs]; horizontal and vertical long-axis planes, each divided into 7 ROIs), at rest and during low dose dobutamine (10μg/kg/min). Systolic thickening (SWT) in each ROI was assessed qualitatively as normal, mild, moderately or severely* impaired, akinetic,* or dyskinetic*. A contractile reserve, predictive of LV recovery, was defined as improvement in SWT with dobutamine. CE-MRI in 8 patients (short axes as for cine-MRI) was acquired 15 minutes after 0.025mmol/kg gadodiamide bolus using an inversion recovery snapshot-FLASH sequence. Hyperenhancement was reported in each ROI as absent or patchy (predictive of LV recovery) or transmural. LV recovery predictions for each modality were compared with postoperative recovery (cine-MRI) assessed at 6 months, defined as SWT improvement from preoperative resting state.

Results: Severe systolic dysfunction(*) was observed in 52 ROIs evaluated by CE-MRI and in 65 ROIs assessed by Db cine-MRI. The prediction of regional post-operative LV recovery compared with reported recovery is shown in table 1.

Table 1

Number of ROIs predicted to recover (+) or not (−) by CE MRI and Db MRI compared with postoperative recovery (R+) or no recovery (R−)

	CE MRI	CE MRI	Db MRI	Db MRI
Prediction	R+	R−	R+	R−
+	12	6	22	10
−	4	30	7	26

The sensitivity, specificity, and overall accuracy for CE-MRI was 75%, 83%, and 81% (SE 5%) and for Db cine-MRI 75%, 72%, and 74% (SE 5%), respectively.

Conclusion: In patients with low EF, our study shows CE-MRI to have a significantly greater predictive value for the recovery of regional LV function post-CABG than Db-cine MRI. This is a consequence of the greater specificity of CE-MRI.

38. Comparison of dobutamine-MRI and dipyridamole-scintigraphy for the detection of myocardial ischemia in patients not suitable for stress-echocardiography

Matthias Scmidt,[1] M. Jochims,[2] P. Theissen,[1] E. Voth,[1] F.M. Baer,[2] E. Erdmann,[2] H. Schicha[2] [1]*Klinik und Poliklinik für Nuklearmedizin und* [2]*Klinik III für Innere Medizin, University of Cologne, Germany*

Aims: Stress-echocardiography (stress-echo) has become an established method for detection of myocardial ischaemia in patients (pts) with coronary artery disease (CAD). However, stress-echo may be limited in pts with a poor acoustic window. It was the aim to compare the clinical value of dobutamine magnetic resonance imaging (Dobu-MRI) with dipyridamole myocardial scintigraphy (Dipy-SZ) in pts who could not be evaluated by stress-echo.

Methods: Thirty pts in whom two or more segments according to the model of the American Society of Echocardiography could not be evaluated underwent Dobu-MRI and Dipy-SZ. For Dobu-MRI dobutamine was given intravenously with increasing doses from 10 to 40 µg/kg x min. Long- and short-axis breath-hold tomograms were acquired on each level. For Dipy-SZ 0.75 mg dipyridamole/kg was given and stress-redistribution tomograms were acquired after thallium-201 injection. Dobutamin-induced wall motion abnormalities and redistribution of thallium-201 were criteria for ischemia, respectively. Myocardial segments were assigned to the perfusion territories of the coronary arteries and the results were compared with the results of coronary angiography (stenosis ≥50%).

Results: Twenty-nine of 30 Dobu-MRI and 30/30 Dipy-SZ could be evaluated. In comparison to coronary angiography Dobu-MRI had a sensitivity of 79%, a specificity of 80%, a positive predictive value of 88%, and a negative predictive value of 67%. For Dipy-SZ values of 90%, 70%, 85%, and 78% were calculated, respectively.

Conclusion: In pts with a poor acoustic window who cannot be evaluated by stress-echo, Dobu-MRI and Dipy-SZ are both valuable techniques for detection of myocardial ischaemia. Dipy-SZ had a higher sensitivity and a lower specificity in comparison to Dobu-MRI. The decision for either of both methods depends on the pts and on the observer's experience.

39. Real-time High-dose Dobutamine Stress Magnetic Resonance Imaging for the Detection of Left Ventricular Wall Motion Abnormalities in Patients with Coronary Artery Disease

S. Schalla, E. Nagel, C. Klein, I. Paetsch, A. Bornstedt, *B. Schnackenburg, H. Lehmkuhl, E. Fleck *Internal Medicine-Cardiology, Charité Campus Virchow, Humboldt University & German Heart Institute Berlin, Germany; *Philips Medical Systems, Hamburg, Germany*

Background: Magnetic resonance (MR) has been shown to be superior to dobutamine stress echocardiography for the detection of left ventricular wall motion abnormalities (WMA). A shortcoming in comparison with echocardiography is the need to acquire images during several cardiac cycles which prohibits the assessment of new onset of WMA in real-time. In this study real-time imaging was compared with standard echo planar imaging for the detection of WMA.

Methods: In 22 patients with coronary artery disease, left ventricular wall motion was examined with multiphase echo-planar imaging (EPI) (TE 5.6 ms; TR 1 heartbeat; flip angle 30°; spatial resolution 1.3_2.6 mm; temporal resolution 30 ms) and a new real-time imaging technique (RT) (TE 6.8 ms; TR 16.5 ms; flip angle 20°; spatial resolution 2.2_4.4 mm; temporal resolution 60 ms) at rest and maximum dobutamine stress (up to 40µg/kg +atropine) using a 1.5-T whole body MR tomograph (Philips ACS-NT PT 6000). Three short-axis views were divided into 16 segments and assigned to perfusion territories of coronary arteries according to the suggestions of the American Society of Echocardiography.

Results: The numbers of perfusion territories with WMA at rest detected with EPI and RT are shown at the top of Table 1 and the numbers of ischemic perfusion territories (new onset or aggrevation of WMA) at dobutamine stress at the bottom.

Table 1

	EPI+	EPI−
RT+	26	1
RT−	—	39

	EPI+	EPI−
RT+	10	—
RT−	1	55

This results in a sensitivity of 100% and a specificity of 98% for the diagnosis of WMA at rest and a sensitivity of 91% and a specificity of 100% for the detection of new or worsening WMA at dobutamine stress for RT in comparison with EPI.

Conclusions: Real-time imaging of left ventricular wall motion is possible under stress conditions. WMA can be detected with similar accuracy as current standard techniques. In combination with improvements in real-time reconstruction and image display, this technique can be used for an on-line analysis of wall motion at pharmacological stress. Scan time can be reduced and safety of patients improved.

40. Evaluation of hemodynamic data in patients with aortic regurgitation by MRI and correlation with the left ventricular function

Th. Wittlinger,[1] T. Voigtländer,[1] K.F. Kreitner,[2] S. Petersen,[1] P. Kalden,[2] H. Brinkmann,[1] W. Schreiber,[2] M. Thelen,[2] J. Meyer[1] *2nd Medical Clinic[1] and Department of Radiology[2], University Hospital, Mainz, Germany*

One major problem in the management of patients with aortic regurgitation (AR) is the assessment of the severity of the disease, especially in patients with reduced left ventricular ejection fraction. It was the purpose of the study to evaluate the hemodynamic data of patients with AR and to show the correlation between magnetic resonance imaging (MRI) and aortic root angiography.

Methods: We investigated 50 patients (35 male, 15 female, aged 58.5 y) with a clinical manifested AR Iϕ–IIIϕ. MR cineventriculography was performed (Magnetom Vision, 1.5 T, Siemens AG, Erlangen) using an ECG-gated, breathhold, multislice, FLASH 2D sequence with a slice thickness of 8 mm. The quantification of the aortic flow was performed with a FLASH-2D sequence (TR 110 ms, TE 5 ms, velocity encoding 250 cm/s). In all patients the AR was verified by aortic root angiography within 1 week. The patients were divided in a group with normal (EDVI < 100 ml/m²) and reduced (EDVI > 100 ml/m²) left ventricular function.

Results:

AR	Iϕ	IIϕ	IIIϕ
RF MRI	12%	22%	39%
EDVI > 100 ml/m²	(5–18%)	(15–30%)	(28–57%)
RF Angio	15%	26%	43%
EDVI > 100 ml/m²	(6–30%)	(12–38%)	(17–60%)
RF MRI	14%	23%	40%
EDVI < 100 ml/m²	(13–17%)	(20–27%)	(25–43%)
RF Angio	12%	22%	39%
EDVI < 100 ml/m²	(5–18%)	(15–30%)	(20–57%)

Conclusions: The accuracy in quantification of the aortic valvular flow was demonstrated by a significant correlation between MRI and the RF.

There is no correlation between the RF and the angiographic classification in patients with reduced left ventricular function, because the RF will be underestimated. Especially in patients with reduced left ventricular function, MRI is superior to the aortic angiography, because the determination of the aortic regurgitation is independent of the left ventricular function. Further studies have to show, whether MRI can became the gold standard in the management of patients with aortic regurgitation.

41. Aortic valve stenosis: Dynamic valve area assessment using cine gradient echo sequences

A. John, T. Dill, R. Brandt, M. Rau, C. Müller, W. Ricken, G. Bachmann, C.W. Hamm *Kerckhoff Clinic, Bad Nauheim, Germany*

Background: Invasive or semiinvasive techniques such as cardiac catheterization (CC) and transesophageal echocardiography (TEE) are frequently used to assess the severity of aortic valve stenosis. The aim of this pilot study was to show that noninvasive estimation of the aortic valve area (AVA) by magnetic resonance imaging (MRI) is feasible and correlates well with TEE and CC results.

Methods: Thirty patients (18 male) underwent CC, TEE, and MRI for aortic stenosis. MRI studies were performed on a 1.5-T Magnetom Vision (Siemens Medical Systems, Erlangen, Germany) using a flash 2d ECG-gated cine gradient echo sequence, TR 60–80 ms, TE 3 ms, flip angle 20, slice thickness 4 mm, pixel size 1.24–2.91 × 1.17–1.56 mm. Imaging planes were chosen perpendicular to the stenosis jet as deducted from the poststenotic signal void at valvular level. Aortic valve planimetry was performed by two independent observers blinded to CC and TEE results. The dynamic AVA was averaged over the duration of systole in three different imaging planes. Intraobserver variability was determined by repeat measurements after 2 months.

Results: Mean AVA was 0.78 ± 0.16 qcm for MRI, 0.95 ± 0.26 qcm and 0.7 ± 0.26 for CC. MRI results correlated well with TEE and CC ($p < 0.008$ and $p < 0.001$, respectively). Interobserver variability was 0.054 ± 0.058; intraobserver variability was 0.055 ± 0.042.

Conclusion: Evaluation of aortic valve stenosis by MRI is safe, feasible, and of excellent reproducibility. It is a promising alternative to current invasive and semiinvasive techniques. It provides information on valve morphology and valve movement and change of AVA over the duration of the cardiac cycle.

42. Subendocardial Perfusion in patients with Aortic Valve Stenosis and Left Ventricular Hypertrophy

K. Rajappan, O. Rimoldi, D.J. Sheridan,[2] P.G. Camici,[1] D.J. Pennell. *Cardiovascular MR Unit, Royal Brompton Hospital;* [1]*MRC Clinical Sciences Centre;* [2]*Academic Cardiology Unit, NHLI, ICSM, London, UK*

Aims: Patients with left ventricular hypertrophy (LVH) secondary to aortic stenosis (AS) show electrocardiographic signs of subendocardial ischemia despite normal coronary arteries. To ascertain if the coronary vasodilator reserve (CVR) is more severely blunted in the inner LV layers, we measured the transmural distribution of myocardial blood flow (MBF) using positron emission tomography (PET). Furthermore, we investigated how the severity of the transvalvular gradient affects CVR in these patients.

Methods: Eight patients (aged 72 ± 6 years) with severe AS and angiographically normal coronaries were enrolled. Peak pressure gradient across the stenosed valve at rest was measured echocardiographically with continuous-wave Doppler (peak gradient 94 ± 16 mm Hg). To assess LV mass subjects were imaged on a Picker Edge 1.5-T scanner (Picker, Cleveland, OH), using the body coil and electrocardiographic (ECG) triggering. The cardiac short axis was determined from three scout images, and a segmented FLASH breath-hold cine was used for acquisition of contiguous 10-mm short-axis slices. End-diastolic epicardial and endocardial borders were traced manually for each slice. From the area within the contours and the slice thickness, the epicardial and endocardial volumes were calculated, the difference representing myocardial volume. LV mass (g) was derived from this volume multiplied by the specific density of myocardium (1.05 g/cm^3), and this was then divided by the body surface area (g/m^2). Using a high-sensitivity PET scanner (EXACT 3D, 4.5-mm resolution Full-Width Half-Maximum) and Oxygen-15 labeled water, we measured noninvasively subendocardial (Endo), subepicardial (Epi), and transmural (Tm) MBF at rest and during i.v. dipyridamole (Dip, 0.56mg/kg). CVR was calculated as Dip/rest-MBF after correcting the latter for rest rate-pressure product (RPP).

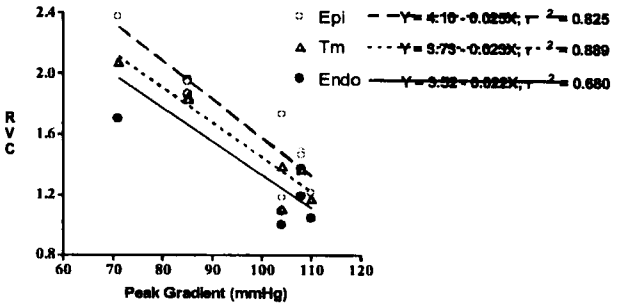

Figure 1.

Results: LV mass was 146 ± 32 g/m^2. The results of MBF measurements using PET are shown in the table below:

	Rest	Dip	CVR
Heart rate (beats/min)	63 ± 10.7	76.3 ± 7.0*	
RPP	7908 ± 1005	9069 ± 1110*	
Tm MBF (ml/min/g)	0.95 ± 0.22	1.80 ± 0.46*	1.52 ± 0.35
Endo MBF (ml/min/g)	1.02 ± 0.25	1.74 ± 0.39*	1.40 ± 0.39
Epi MBF (ml/min/g)	0.88 ± 0.21	1.82 ± 0.55*	1.66 ± 0.40†
Endo/Epi ratio	1.18 ± 0.21	0.99 ± 0.12*	

Mean ± SD
*$p < 0.05$ vs. Rest
†$p < 0.05$ vs. Endo MBF

The reduction of Tm, Endo, and Epi CVR was inversely related to the gradient across the valve in resting conditions. There was no relationship between reduction in mean arterial pressure during Dip and CVR.

Conclusion: The preliminary results of the present study indicate that in these patients with LVH assessed by MR, CVR is more severely blunted in the subendocardium and that the reduction in CVR is inversely related to the severity of the gradient. Endo CVR seems to be affected to a greater extent by LV cavity pressure overload.

43. Stress-Strain Relation of the Left Ventricle: Noninvasive Measurement of Contractility

F.E. Rademakers, J. Bogaert *University Hospital Gasthuisberg, Leuven, Belgium*

Intrinsic contractility of the left ventricle is hard to quantify, even using invasive techniques. Like the pressure-volume relation, the stress-strain relation is a possibility to analyze intrinsic contractile function, but this normally warrants several loading conditions to construct a meaningful relation. We hypothesized that left ventricular contractility could be analyzed using regional stress-strain relations at one loading level; the regional inhomogeneity in stress and strain would allow to construct such a linear relationship.

To test this hypothesis, we analyzed a group of normal individuals (normal clinical exam, echocardiogram and stress test; $n = 86$) and patients with idiopathic dilated cardiomyopathy (IDC) with MR tagging. By combining short- and long-axis images, regional strains at 32 regions in a local cardiac coordinate system were obtained: thickening (RR), circumferential shortening (CC), and longitudinal shortening (LL). Local radii of curvature in the short and long axis and the regional ejection fraction (REF) could also be obtained. These data were measured both at the epicardium and the endocardium. Local stresses were approximated using the formula systolic blood pressure × radius of curvature/wall thickness. Circumferential stress-strain relations were evaluated using the circumferential radii of curvature, longitudinal ones using the longitudinal radii of curvature; thickening was evaluated against both circumferential and longitudinal measures. The most tight regression was obtained using the REF and endocardial CC versus the endocardial circumferential stress ($R = 0.9$; $p < 0.0001$). Less tight but still significant relations could be found for the epicardial and longitudinal stress-strain relations. IDC patients differed from normals by showing smaller strains but comparably larger stresses, resulting in very similar stress-strain relations.

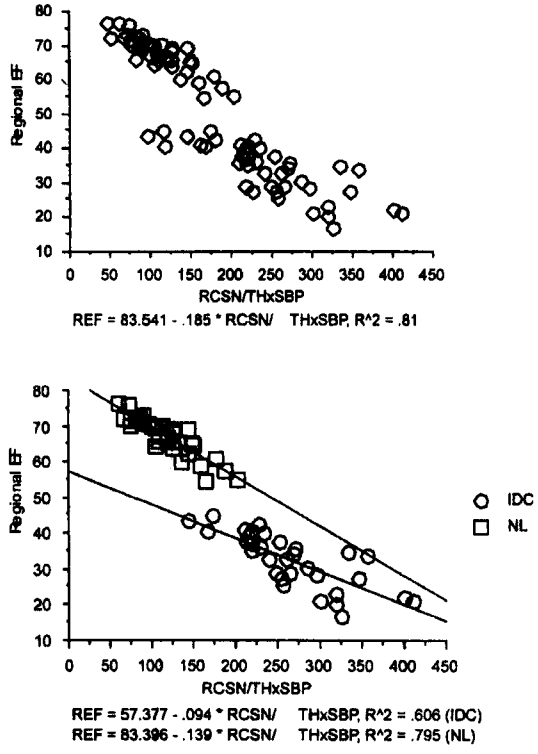

Figure 1.

Using MR tagging, stress-strain relations can be obtained, showing very high correlations, also in individual patients. The relations in normals and IDC patients were very similar; although the stress definition in IDC could differ from the one in normals, these results would suggest that the poor function in IDC is to a large extent explained by the larger stresses, with only a slightly different stress-strain relation or contractility.

44. Left Ventricular Mass Measured by Magnetic Resonance Imaging: Effect of Endocardial Trabeculae on the Observed Wall Thickness

J.T. Marcus,[1] J.P.A. Kuijer,[1] M.J.W. Götte,[2] R.M. Heethaar,[1] A.C. Van Rossum[2] [1]*Dept of Clinical Physics & Informatics,* [2]*Dept of Cardiology, ICaR-VU, Vrije Universiteit, Amsterdam, The Netherlands*

Introduction: The aim of this study is to quantify the left ventricular (LV) mass contributions provided by the most basal LV slice (which shows the LV wall only in diastole), the papillary muscles, and the endocardial trabeculae.

Methods: Healthy subjects ($n = 40$, 11 female), aged 19–69 years, were imaged on a Siemens whole body magnetic resonance imaging (MRI) system. A stack of parallel short-axis image slices was acquired, fully covering the LV from the very base to the apex, as planned in diastole. LV mass was calculated by slice summation. End-diastolic mass, denoted as EDM, was measured without the most basal image slice and papillary muscles (PM). EDM+base is the EDM with most basal slice included. EDM+base+pm includes the PM in addition. ESM is the end-systolic mass, always including the PM.

Results: Results are given below as mean ± SD. The contribution of the basal slice to LV mass is 18 ± 4 g; the PM contribute 6 ± 5 g. Most striking is the value of ESM, which is larger than the EDM+base+pm (paired-samples t-testing: $p = 0.002$), by the amount of 5 ± 9 g.

EDM	= 131 ± 25 g
EDM + base	= 148 ± 27 g
EDM + base + pm	= 154 ± 29 g
ESM	= 159 ± 30 g

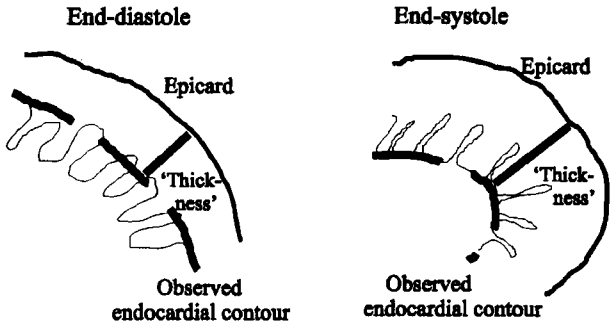

Figure 1.

Discussion: The observed ESM is *larger* than EDM + base + pm, although in the ESM calculation at least one image slice *less* contributes (the basal slice). At *end-diastole* many individual trabeculae are difficult to trace due to their small size, and the trabecular zone is thus largely *excluded* by an observer who traces the endocardial border. Figure 1, left panel, shows the observed endocardial contour (dashed line) at end-diastole. During *systole*, however, the individual trabeculae will join to form a more compact compartment, clearly different from the

blood pool. Thus, at end-systole (right panel), the observed contour will now *include* the trabeculae, and the apparent thickness is enlarged in part by these joined trabeculae. These included trabeculae explain the increased mass at end-systole. As the observed wall thickening is partly due to the confluence of trabeculae, the true radial strain can only be assessed by myocardial tagging with marker points inside the myocardium.

Conclusion: For a proper comparison of LV mass measures in multicenter trials, we propose guidelines to include the most basal LV slice and the PM to the total LV mass. Also, the difference between the observed end-diastolic and end-systolic mass implies that the cardiac phase of LV mass measurement should be specified. The end-systolic mass measure has the advantage of more consistent inclusion of the trabecular part of the myocardium.

45. Robust automatic detection of right and left ventricular contours in short-axis cardiac MR images using active appearance models

B.P.F. Lelieveldt,[a] S.C. Mitchell,[b] R.J. van der Geest,[a] M. Sonka,[b] J.H.C. Reiber[a] *[a]Division of Image Processing, Dept. of Radiology, Leiden University Medical Center, Leiden, the Netherlands, [b]Dept. of Electrical and Computer Engineering, The University of Iowa, Iowa City*

Background: To quantitatively evaluate global and regional left ventricular (LV) and right ventricular (RV) function from short-axis cardiac MR images, the contours of the LV endocard (ENDO), LV epicard (EPI), and Right ventricle need to be traced in the images. In clinical studies typically consisting of 200–300 images, this is mainly performed manually, which is time consuming and sensitive to inter- and intraobserver variations.

Aim: To develop and validate a robust automated contour detection technique for tracing the ENDO, EPI, and RV contours in short-axis cardiac MR images.

Methods: Previous experience has shown that a robust contour detection method requires a mathematical description of prior knowledge about typical organ shape, typical organ appearance, and anatomical or pathological shape variations. In this work, a trainable statistical model named "active appearance model" (AAM) is applied, which consists of two components: a statistical model of the *shape* of the heart, which is combined with a statistical model of the *image appearance* of the heart in a set of example cardiac MR images. The combined model is trained to learn the shape and image structure of the LV and RV from a representative set of cardiac MR images from 11 patients and 23 normal subjects. The AAM can be automatically matched to a new study image, yielding the locations of the ENDO, EPI, and RV contours. The AAM technique has been evaluated on 60 end-diastolic mid-ventricular cardiac MR images from 9 patients and 11 normal subjects.

Results: The results of the current evaluation study demonstrated

1. An excellent correspondence between the automatically and manually derived area measures such as LV cavity area ($r = 0.96$, $N = 56$), and RV cavity area ($r = 0.94$, $N = 56$). The average paired difference between the automatic/manual measurement pairs was $0.9 \pm 6\%$ for the LV cavity area and $2 \pm 7\%$ for the RV cavity area, which is comparable to inter- and intraobserver variabilities in manual measurements.
2. A high degree of robustness of the AAM contour detection with respect to noise and image artifacts, even in low- fidelity, routinely acquired cardiac MR images from sometimes severely deformed patient hearts (in 56/60 images, the automated method delivered visually correct ENDO, EPI, and RV contours).
3. The ability of the AAM method to generate LV contours, which exclude papillary muscles and epicardial fat.

Conclusions: Active appearance models have demonstrated to be a highly robust contour detection method for RV, ENDO, and EPI contours and may potentially reduce analysis time for cardiac MR examinations to a minimum.

46. Single Breath-Hold Ejection Fraction Determination by 3D Cine Imaging after Injection of a New Blood Pool Contrast Agent CLARISCAN™

MBM Hofman,[1] PA Wielopolski,[2] W.G. van Dockum,[1] A. Lehning,[3] M. Oudkerk,[2] AC van Rossum[1] *[1]University Hospital Vrije Universiteit, Amsterdam and [2]University Hospital Rotterdam, The Netherlands, [3]Nycomed Amersham Imaging, Munich, Germany*

Background: Current 3D MR imaging of the whole heart is hampered by the low signal of blood due to the limited inflow within a thick slab. The use of a blood pool agent could overcome this limitation. CLARISCAN™ (NC100150, Nycomed Amersham Imaging, Oslo, Norway) is such a new agent. It allows fast 3D imaging with still sufficient MR signal in the left ventricle. We tried a 3D cine technique to cover the whole left ventricle in a single breath-hold as a tool for fast ejection fraction determination.

Methods: Administration of CLARISCAN™ results in a strong reduction of blood T1: 100 or 50 ms at a dose of 2 or 5 mg Fe/kg BW, respectively. As the agent remains intravascular, the contrast in T1 of blood to myocardium is high and does not rely on inflow anymore. These characteristics make 3D cine imaging of the left ventricle feasible.

The 3D cine technique used was a multiphase segmented k-space gradient echo pulse-sequence (TR 2.8 ms, TE 1.3 ms, readout bandwidth 780 Hz/pixel). Partial Fourier encoding was applied to reduce the acquisition time to 20 heartbeats. The temporal resolution was 58 ms with a spatial resolution of $2.0 \times 2.4 \times 13$ mm^3 and an FOV of $26 \times 20 \times 13$ cm^3. The excitation angle was set to 20° or 26° (depending on the agent dose), which was calculated to produce the optimum contrast of blood to myocardium.

Within a phase II clinical trial, six patients were imaged using this new 3D cine technique. MR imaging was performed on a 1.5 -T whole body scanner (Magnetom Vision, Siemens, Germany) using a body phased-array receiver coil. CLARISCAN™ was administered intravenously at a dose of 2 or 5 mg Fe/kg body weight.

For comparison, prior to injection short-axis 2D GE cine imaging was performed (with a higher spatial resolution), the current standard technique for MR ejection fraction determination. After contrast administration the ejection fraction was also determined in each subject by a full coverage of the left ventricle using multiple 2D GE cine acquisitions, each obtained in a single breath-hold.

Data analysis consisted of the determination of signal-to-noise ratio (SNR) of blood and contrast-to-noise ratio (CNR) of blood to myocardium. The ejection fractions were determined using the software package MASS (Leiden University Medical Center, NL).

Results: In all cases a clear delineation of the left ventricle could be observed with the 3D-cine technique. Figure 1 shows images at a mid-ventricular level from a 3D cine dataset. High signal of blood is obtained and a good contrast to myocardium is found. The SNR of blood was not significantly different from the standard technique: 58 ± 14 and 66 ± 15 for the 3D cine postcontrast and the 2D cine precontrast, respectively. Also the CNR of blood to myocardium was similar for both techniques: 52 ± 12 and 42 ± 13 for the 3D cine and 2D cine, respectively. The ejection fractions are still under analysis.

Conclusion: Using the blood pool contrast agent CLARISCAN™, a 3D cine BH technique is feasible for determination of left ventricular ejection fraction within a single breath-hold. Compared to the standard technique of multiple 2D cine acquisitions, this technique is faster and

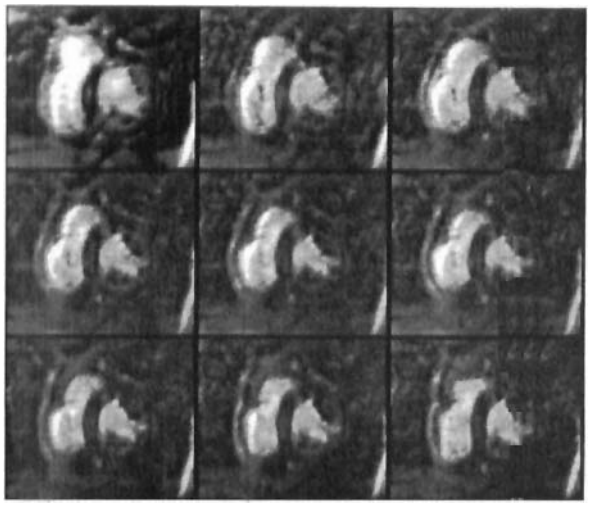

Figure 1. Images of the 3D cine technique at mid-ventricular level at different phases of the cardiac cycle, obtained at a contrast dose of 2mg Fe/kg body weight.

not subjective to slice misregistration due to variations in breath-hold position at the cost of a lower resolution and image quality.

47P. Hyperoxic reperfusion increases myocardial infarction and impairs myocardial function

G. Horstick, W. Schreiber,# D. Becker, S. Petersen, A. Heimann,* O. Kempski,* T. Voigtländer, M. Thelen,# & J. Meyer *2nd Medical Clinic, Institute for Neurosurgical Pathophysiology,* und Clinic for Radiology#, University Clinic, Mainz*

Hyperoxic reperfusion is suspected of oxygen free radical increase. It is unclear whether reperfusion under hyperoxic conditions of a previously ischemic area aggravates resulting myocardial infarction and affects myocardial function. Therefore, we examined the results of normoxic and hyperoxic reperfusion upon myocardial function in rats with proximal ligation of the left coronary artery (LCA) with MRI.

Methods: After anesthesia with chloralhydrate, intubation, and mechanical ventilation, a left lateral thoracotomy was performed. The LCA was occluded for 30 min and reperfused under normoxic (n = 10, paO2 = 91 ± 6 mm Hg) or hyperoxic ventilation (n = 10, paO2 = 290 ± 50 mmHg). Rats were extubated after reperfusion and reintubated after 24 hours for final examinations. Evans-Blue was injected after reocclusion of the LCA to determine the area at risk followed by a vital staining with tetrazoliumhydrochloride (TTC). The left ventricle (LV), the area at risk (AR), and the zone of myocardial infarction (MI) were determined through planimetry using a computer-based software system. Examinations of myocardial wall motion were performed at a 1.5-T Siemens Vision system using a small eye coil. The ECG-triggered spin-echo sequences (TR/TE = 600 ms/14ms, FOV 85mm, MA = 192 × 256, slice thickness 2mm) had an in-plane resolution of 0.33 × 0.33mm. Images were recorded at 20-ms increments following the R-wave of the ECG acquiring a basal and an apical slice. Maximum diastolic relaxation and systolic contraction were used for off-line analysis of regional wall thickening.

Results: Area at risk was similar in both groups (normoxia: AR/LV 32 ± 3%; hyperoxia: AR/LV 39 ± 4,5%). Hyperoxic reperfusion increased myocardial infarction in the area at risk significantly vs. normoxic reperfusion (hyperoxia: MI/AR 79 ± 4% vs. normoxia: MI/AR 39 ± 5%). Concerning myocardial function, the basal slice presented an impaired myocardial wall thickening of the left lateral wall after reperfusion with compensation of the nonischemic area without differences between normoxia and hyperoxia. Apical measurements showed a significant reduction of wall thickening of the left lateral wall in the hyperoxic group vs. the normoxic group. There is a close correlation between the size of myocardial infarction at the base and apex and impaired wall thickening.

Conclusions: Our study clearly presented the deleterious effects of hyperoxic ventilation during myocardial ischemia and reperfusion with increase of myocardial infarction. Using a conventional clinical 1.5-T Siemens Vision system, we acquired high-quality images for wall motion analysis presenting a significant reduction of wall thickening after hyperoxic reperfusion of the previously ischemic area.

48P. Value of magnetic resonance imaging (MRI) for the assessment of ventricular and anastomosis function in patients with extra- or intracardial total cavopulmonary connection (TCPC)—modified Fontan-operation

Matthias Gutberlet, MD, Norbert Hosten, MD, Hasim Abdul-Khaliq, MD, Simone Rechter, MD, Pavel Vojtovic, MD, Michael Vogel, MD, Christian Born, MD, Roland Hetzer, PhD, Peter Lange, PhD and Roland Felix, PhD

Aims: To evaluate different MR methods (ventricle and flow measurements) for the postoperative follow-up of hemodynamics in patients with extra- or intracardial TCPC.

Methods: Twenty-eight consecutive patients (14 female, 14 male) aged 2–38 years were examined using a 1.5-T Gyroscan ACS-NT scanner (Philips, Best, Netherlands). Seven patients had an extracardial (eTCPC), 21 an intracardial (iTCPC) tunnel. The calculation of the ventricular function and muscle mass was performed in "multislice-multiphase" technique by suming up the end-diastolic and end-systolic areas, the flow measurements by phase shift velocity mapping in the superior vena cava (SVC), interior vena cava (IVC), right (RPA), and left (LPA) pulmonary artery. Beside peak and mean velocity, the mean and maximal flow volume (ml/min) was calculated. For ventricle measurements a fast gradient echo sequence (TR = 14 ms, TE = 2.6ms, flip-angle = 20°, slice thickness = 3–6mm, FOV = 150–300mm, matrix = 128 × 256, retrospective gating), for flow measurements phase-shift velocity mapping was used (TR = 20ms, TE = 2.4ms, flip-angle = 30°, slice thickness = 3–6mm, FOV = 150–300mm, matrix = 96 × 128, retrospective gating).

Results: Ejection fraction (EF) of the functionally single ventricle was within the normal range (mean 57%) in 22/28 patients, mean muscle mass elevated in the group with eTCPC (mean 121 g/m^2). The mean flow volumes and the peak velocities were in all vessels higher in the group with iTCPC as compared to the one with eTCPC. Clinically relevant retrograde flow in the IVC was only found in the group with iTCPC (7/21), as well as a significant predominant flow distribution toward the RPA ($p < 0.05$; Wilcoxon-signed-rank-test); in the group with eTCPC toward the LPA (n.s.).

Conclusion: MRI is a useful method for the assessment of ventricular function and muscle mass in the follow-up after the modified Fontan operation. MRI flow measurements could additionally provide clinically relevant information about hemodynamics in Fontan patients.

49P. Characterization of right ventricular wall motion by cardiac MRI in normal individuals

T Bloomer, DJ Beacock, JP Ridgway, S Plein, UM Sivananthan. *MRI Unit, Leeds General Infirmary, Leeds, United Kingdom*

Purpose of the study: Right ventricular (RV) physiology is neglected in the investigation of heart disease due to the complex geometry. This

cardiac MRI study was undertaken to quantitate RV volumes and wall motion in normal individuals.

Methods: Forty normal volunteers underwent cardiac MRI on a Philips 1.5-T ACS NT MR system with a multielement surface coil. Gradient echo breathhold images were obtained in the axial plane from the diaphragm to the pulmonary artery. Four-chamber and short-axis views were also obtained. Volumetric analysis was performed with MASS software (MEDIS, Leiden). RV volumes were corrected for body surface area (BSA). Wall motion analysis was performed in the four chamber view and in two slices through the body of the RV at the level of the tricuspid annulus as follows

Motion of the tricuspid annulus (TA) at septal and free wall attachments toward the apex, motion of the mid-ventricular free wall toward the septum, and motion of the septum toward the left ventricular center line. The short-axis orientation was used to analyze the mid-inferior wall, mid free wall, and mid septal regions. Fractional area change was analyzed in an axial slice through the right ventricular outflow tract (RVOT).

Results:

RV volumes corrected for body surface area

	Mean Volume/BSA
RV diastolic volume	72.8 ± 17.5 ml/m^2
RV systolic volume	30.4 ± 9.4 ml/m^2
RV stroke volume	41.4 ± 10.9 ml/m^2
RV ejection fraction	59.4 ± 4.1%

The mean RV outflow tract area was 11.7 ± 3.0 cms_ in diastole with a fractional systolic change of 49.2 ± 6.9% in systole. In addition, there was translation of the outflow tract to the left during systole.

Right ventricular wall motion measurements

	Four Chamber	Higher Axial Slice	Lower Axial Slice
TA septal insertion	16.1 ± 4.4 mm	16.5 ± 3.6 mm	12.9 ± 3.9 mm
TA free wall insertion	24.5 ± 5.9 mm	24.9 ± 4.4 mm	21.4 ± 5.0 mm
Septal motion	3.0 ± 1.0 mm	3.4 ± 1.1 mm	3.8 ± 1.7 mm
RV free wall motion	5.8 ± 2.8 mm	5.2 ± 2.4 mm	4.7 ± 1.5 mm

Mean inferior wall motion was 6.6 ± 1.7 mm upward (measured on the axial slice).

Conclusion: The main component of RV systolic function is due to shortening of the RV free wall resulting in motion of the tricuspid annulus toward the apex. There is also significant contraction of the RV outflow tract. There is lesser motion of the RV free wall toward the septum and elevation of the RV inferior wall. The differences between the RV axial slices suggest that the four-chamber view may be superior for assessing the motion of the tricuspid annulus.

50P. Cardiac MRI is sensitive for the diagnosis and follow-up of right ventricular extension of inferior myocardial infarction

T Bloomer, JP Ridgway, UM Sivanathan. *MRI Unit, Leeds General Infirmary, Leeds, United Kingdom*

Aims: Right ventricular (RV) extension worsens the prognosis of inferior myocardial infarction. The presence of ST elevation in leads V3R and V4R on electrocardiography (ECG) is accepted as the main criterion. Anatomical imaging of the right ventricular infarction is complicated, however, by the complex right ventricular geometry. Cardiac magnetic resonance imaging (CMRI) can assess left and right ventricular function noninvasively without geometric assumptions. This study aims to assess the sensitivity of CMRI to diagnose RV extension of inferior MI.

Method: Eleven patients with acute inferior MI on ECG were recruited from the Coronary Care Unit. All patients had standard 12-lead ECG with additional RV leads. CMRI was performed on day 3 after MI on a Philips 1.5-T ACS NT MRI scanner with a cardiac surface coil. Gradient echo sequences were acquired in the axial plane from the diaphragm to the pulmonary bifurcation and in the left ventricular short-axis plane from the apex to the atria. Volumetric analysis was performed using the MASS software (MEDIS, Leiden). Patients were rescanned after 8 weeks. Clinical follow-up is planned over a 12-month period.

Results: Four patients had ECG evidence of RV extension. All 11 patients had inferior left ventricular wall motion abnormalities on CMRI. Mean left ventricular ejection fraction was reduced at 54.7%. Eight patients also had inferior RV wall motion abnormalities by CMRI including all four with ECG evidence of RV extension. Six patients (including four with RV extension) underwent follow-up CMRI. Four showed recovery of LV wall motion, but two had progressed to full thickness LV infarcts (one posterior). Both these patients had significant LV dilatation at follow-up. All four with RV wall motion abnormalities on the initial MRI demonstrated improvement of the RV inferior wall motion at follow-up with three scored as normal. Overall there was an increase in left ventricular volumes postinfarction (p = ns) with a maintained stroke volume and ejection fraction. RV volumes and ejection fraction were unchanged postinfarction.

Conclusion: Cardiac MRI is more sensitive than electrocardiography in the diagnosis of right ventricular extension of inferior MI and can be used to assess left and right ventricular recovery and remodeling after MI. Long-term clinical follow-up of these patients will determine whether the presence of RV extension demonstrated by MRI but not apparent on ECG criteria results in significant additional morbidity.

51P. Evaluation of Ventricular Function with MRI Using the New Blood Pool: Contrast Agent CLARISCAN™ in Patients

WG van Dockum,[1] MBM Hofman,[1] A Lehning,[2] AC van Rossum.[1]
[1]*University Hospital Vrije Universiteit, Amsterdam, The Netherlands,*
[2]*Nycomed Amersham Imaging, Munich, Germany*

Background: CLARISCAN™ (NC100150, Nycomed Amersham Imaging, Oslo, Norway) is a new blood pool agent for potential use in MRI. This agent reduces the T1 of blood, thereby increasing the MR contrast of left ventricular cavity to myocardium, which is expected to improve the image quality. The aim of the study was to determine the improvement and the optimal dose of this contrast agent for the evaluation of ventricular function.

Methods: Imaging data were acquired in this phase II clinical trial from seven patients with a history of cardiac disease. The left ventricu-

lar ejection fraction (LVEF) as determined by echocardiography ranged from 13–60%. Imaging was performed at 1.5 T (Magnetom Vision, Siemens, Germany), using a phased-array RF receiver coil. The patients received three intravenous injections of CLARISCAN™ with a cumulative dose of 0.75, 2.0, and 5.0 mg Fe/kg body weight. This agent has a plasma half-time longer than 2 hours, and subsequent injections were given within 20 minutes.

Imaging was performed using a 2D gradient-echo cine technique, acquiring one slice per breath-hold period of 15 heartbeats. Two variants were used, one optimized precontrast (TR 10 ms, TE 4.8 ms, α 20°, temp. resolution 50 ms, receiver bandwidth 195 Hz/pixel) and the other optimized postcontrast (TR 7 ms, TE 3 ms, α 35°, temp. resolution 35 ms, receiver bandwidth 390 Hz/pixel). Precontrast and after each injection a four-chamber view, a two-chamber view, and two short-axis views were acquired.

The LVEF was calculated by the modified Simpson's rule (1). LVEFs measured by MRI were compared with the data from radionuclide ventriculography. Signal-to-noise ratios (SNR) of LV blood and contrast-to-noise ratios (CNR) of blood to myocardium were calculated.

Results: With use of the blood pool contrast agent, CNR of blood to myocardium improved threefold at a dose of 2 mg Fe/kg compared to nonenhanced imaging (Figure 1). The SNR of blood itself did not improve after contrast administration. Bland-Altman analysis of LVEF of MR versus radionuclide ventriculography revealed a mean difference and standard deviation of 3 ± 7% and 2 ± 7% for the pre- and postcontrast MR scan, respectively. This is no significant improvement. The time used for analyzing the LVEF was scored, and found to be not different pre- and postcontrast.

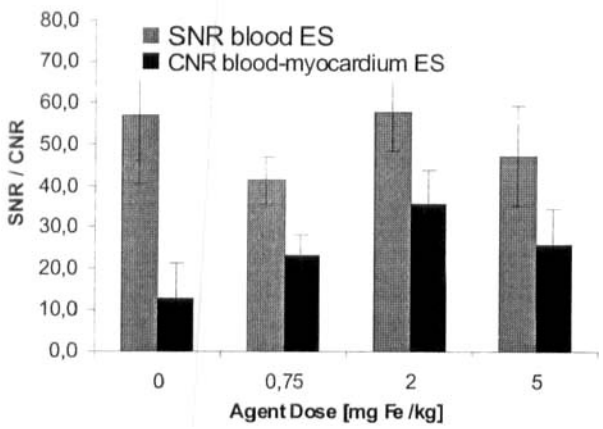

Figure 1. SNR of blood and CNR values of blood to myocardium at end systole as a function of blood pool agent dose.

Conclusion: Administration of the blood pool agent CLARISCAN™ resulted in a strong improvement of contrast in 2D cine images of the left ventricle, especially at end-systole and early diastole. This facilitates postprocessing, especially in patients with bad ventricular function. The SNR of blood did not improve which is caused by the high MR signal precontrast due to inflow refreshment and in part by the contrast agent induced reduction of the T2* value of blood.

No significant improvement in LVEF determination was found post contrast, maybe due to the small number of subjects and inaccuracy in the nuclear technique. Comparison with LVEF determined by the more accurate MR full coverage 2D cine is under analysis.

Reference

1. Dulce MC, Mostbeck GH, Friese KK, Caputo GR, Higgens CB. *Radiology* 1993; 188:371.

52P. First experiences with the blood pool contrast agent CLARISCAN™ for the analysis of LV function with cardiac MR in patients

I. Paetsch,[1] H. Thiele,[2] B. Schnackenburg,[3] A. Bornstedt,[1] V. Hoffmann,[4] A. Lehning,[4] E. Nagel,[1] E. Fleck.[1] *Clinic of Internal Medicine/Cardiology,[1] German Heart Institute & Charité Campus Virchow, Berlin, Germany; Clinic of Internal Medicine/Cardiology,[2] University of Leipzig, Heart Center Leipzig, Leipzig, Germany; Philips Medical Systems,[3] Hamburg, Germany; Nycomed Amersham Imaging,[4] Munich, Germany*

Functional cardiac magnetic resonance imaging with gradient echo techniques depends on contrast derived from the inflow of unsaturated blood. Especially in long-axis views this effect is less, which can make endocardial border delineation difficult. Improved contrast may be achieved by the use of strictly intravascular contrast agents (CA).

In 14 patients horizontal and vertical long-axis cine loops were imaged (turbo gradient echo technique; TE/TR/flip 1.9/5.0/35) prior to and after application of CA CLARISCAN™ (Nycomed, Norway), a pure intravascular contrast agent (half-life > 2 hours) based on a superparamagnetic iron oxide nanoparticle with an oxidized starch coating with both T1 and T2 shortening properties at 0.75, 2.0, and 5.0 mg Fe/kg BW using a 1.5-T MR tomograph (ACS NT, Philips, The Netherlands). Endocardial border delineation was assessed by a visual score (worst, 0 best, 6) for 12 myocardial segments at end-systole and -diastole (maximal score per patient: 144). Signal intensity (SI) was assessed in the mid-septal myocardium and within the left ventricular cavity (blood), signal-to-noise-ratio (SNR) was determined as SI blood or myocardium/SI air, contrast as SI blood/SI myocardium.

Blood pool-SNR significantly increased at all CA concentrations; however, the maximum effect was found at the lowest dose ($*p < 0.05$) probably mainly due to T2* effects; on the other hand myocardial SNR remained nearly constant at all concentration levels. Contrast between blood and myocardium was maximal at 2.0 mg Fe/kg with a tendency toward lower contrast at 0.75 and 5.0 mg Fe/kg. This increase was significant vs. noncontrast images at all levels. Endocardial border delineation score for standard TFE was 42 ± 14.4, for TFE with 0.75 mg/kg contrast agent 93 ± 15.8, with 2.0 mg/kg 104 ± 12.4, and with 5.0 mg/kg 110 ± 11.9 ($p < 0.01$ vs. TFE), respectively.

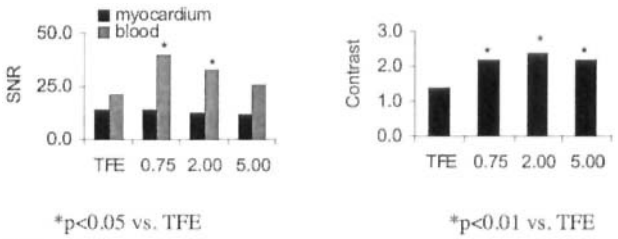

*p<0.05 vs. TFE *p<0.01 vs. TFE

Figure 1.

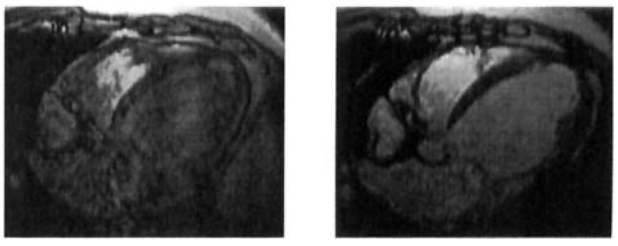

Figure 2. Patient with left ventricular ejection fraction < 20%.

CLARISCAN™ improves endocardial border delineation, SNR, and image contrast at all tested doses with an optimum at 2.0 mg Fe/kg. The higher visual score for endocardial border delineation at 5.0 mg Fe/kg is probably due to susceptibility artifacts between blood and myocardium. CLARISCAN™ will improve the determination of left cardiac volumes and the analysis of regional wall motion.

53P. Inflow independent functional MR imaging with true FISP significantly improves endocardial border delineation without contrast agents

H. Thiele,[1] I. Paetsch,[2] B. Schnackenburg,[3] A. Bornsted,[2] A. Wahl,[4] G. Schuler,[1] E. Nagel,[2] E. Fleck.[2] *Clinic of Internal Medicine/Cardiology,[1] University of Leipzig, Heart Center Leipzig, Leipzig, Germany; Clinic of Internal Medicine/Cardiology,[2] German Heart Institute & Charité Campus Virchow, Berlin, Germany; Philips Medical Systems,[3] Hamburg, Germany; Department of Cardiology,[4] Swiss Cardiovascular Center Bern, University Hospital, Bern, Switzerland*

For a reproducible and accurate assessment of cardiac regional wall motion, calculation of cardiac volumes and ejection fraction optimal image quality of the endocardial border is mandatory. Standard turbo gradient echo techniques depend on contrast from inflowing unsaturated blood, which is low in long axis views, especially in patients with impaired left ventricular function. True FISP is a new technique, which is independent from inflow contrast.

In 24 patients, functional images of the heart in two long-axis views (two- and four-chamber) were acquired during single breath hold of 6–16 heart beats using standard turbo gradient echo technique (TE 1.9 ms, TR 5.0 ms, flip angle 25°) compared with true FISP (TE 1.2 ms, TR 3.2 ms, flip-angle 60°) on a 1.5-T MR tomograph (ACS NT, Philips, The Netherlands). A five-element cardiac synergy coil was used for signal reception. Spatial resolution was 1.3 × 2.6 × 8 mm for standard turbo gradient echo technique and 2.6 × 2.6 × 8 mm for true FISP, temporal resolution was identical with 31 msec. A visual score for endocardial border delineation ranging from 0 (worst)–6 (best) for six myocardial segments in two long-axis projections during the systolic and end-diastolic phase (= 24 segments/patient) was assigned by two independent observers. Signal intensities for blood and myocardium were analyzed off-line, using a dedicated workstation (Easy Vision, Philips Medical Systems, The Netherlands).

Endocardial border delineation score for standard turbo-gradient echo technique was 44 ± 13.8 and 101 ± 14.8 ($p < 0.001$) for the true FISP sequence. Interobserver variability was low for standard turbo gradient echo technique ($r = 0.83$) and further improved with the true FISP sequence ($r = 0.90$). Contrast between blood and myocardium, defined as signal intensity blood/signal intensity myocardium, was 1.3 ± 0.4 during systolic and 1.4 ± 0.4 during diastolic phase for standard gradient echo technique and 4.4 ± 4.7 ($p < 0.01$ vs. TFE) in systole and 4.1 ± 3.7 ($p < 0.01$ vs. TFE) in diastole for true FISP, respectively. The determination of the contrast was highly reproducible ($r = 0.84$–0.94) between two independent observers.

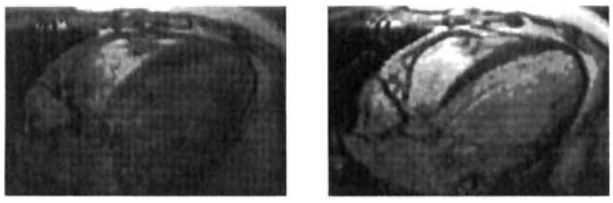

Figure 1. (a) Four-chamber-view in standard turbo-gradient echo technique (left ventricular ejection fraction of 18%). (b) Four-chamber-view in true FISP technique.

Contrast between blood and myocardium is increased by a factor of 3 using the true FISP sequence resulting in a better endocardial delineation. This is similar to the expected effects of intravascular contrast agents and may further improve diagnostic accuracy for stress MR imaging and reduce variability for the determination of cardiac volumes and ejection fraction.

54P. Quantification of Dysfunctional Myocardium by Wall Thickening or Strain Analysis: Correlation with Global Ventricular Function and Infarct Size

M.J.W. Götte, J.P.A. Kuijer, P.A.G. Vriend, J.T. Marcus, A.C. van Rossum. *University Hospital VU, Amsterdam, The Netherlands*

Background: The extent and degree of regional contractile dysfunction are both important factors determining long-term prognosis after myocardial infarction (MI). Systolic wall thickening (%WTh) is an established measure of contractile function but is dependent on accurate wall boundary delineation which is affected by the curvature and through-plane motion of the heart. Magnetic resonance (MR) tissue tagging in conjunction with strain analysis provides quantitative analysis of intramural function independent of wall boundary delineation. We quantified regional contractile dysfunction in patients with a MI by using MR imaging in conjunction with wall thickening analysis and two-dimensional (2D) strain analysis. Results were correlated to global ventricular function and enzymatic infarct size.

Methods Patients: Thirteen patients (12 male, aged 57 ± 11 years) were studied 103 ± 17 days after first anterior MI (peak ck-MB 238 ± 119 U/l). Thirteen-male volunteers (aged 53 ± 7 years) served as controls.

Imaging: Cardiac-triggered MR imaging was performed on a 1.5-T imaging system using a phased-array coil. Cine and tagged short-axis images at basal, mid, and apical level were acquired for measuring % WTh and 2D strain, respectively.

Imaging Parameters		Cine Gradient	Tissue Tagging
TR	(msec)	80	10
Flip Angle	(°)	25	15
Matrix size	(mm)	126 × 256	144 × 256
FOV	(mm)	219 × 250	250 × 250
Temp. resol.	(msec)	40	30

Analysis: In 12 circumferential segments per level, 36 in total, %WTh and 2D strain (radial stretch ε_r and circumferential shortening ε_c) were calculated. Segments with a value, which exceeded the mean value ± 2SD of the control group, were defined as abnormal. The extent of dysfunctional myocardium, represented by the number of segments with abnormal function, was correlated to ejection fraction (EF) and peak ck-MB.

Results:

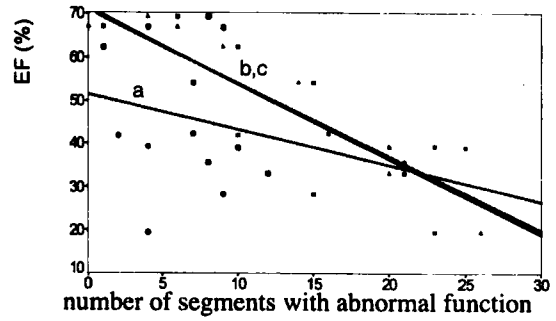

Correlation between EF and number of segments with abnormal regional function

	r	*p*-value
%WTh	−0.17	ns
ε_r	−0.83	<0.001
ε_c	−0.91	<0.001

Figure 1. Correlation between EF and %WTh (line a), radial stretch (ε_r, line b) and circumferential shortening (ε_c, line c).

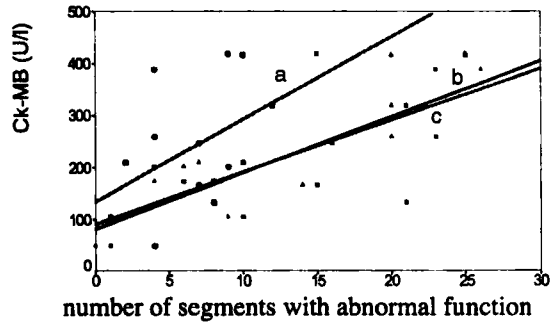

Correlation between ck-MB and number of segments with abnormal regional function

	r	*p*-value
%WTh	0.44	ns
ε_r	0.66	0.014
ε_c	0.77	0.002

Figure 2. Correlation between ck-MB and %WTh (line a), radial stretch (ϵ_r, line b) and circumferential shortening (ϵ_c, line c)

Conclusion: The extent of dysfunctional myocardium quantified by strain analysis is better correlated with global ventricular function and enzymatic infarct size, than the extent of dysfunction quantified by %WTh analysis. The strong correlation between regional and global ventricular function provided by 2D strain analysis may have implications for evaluation of ischemic heart disease and assessment of prognosis after infarction.

55P. Real-time MRI for qualitative and quantitative analysis of wall motion kinetics

S. Plein,[1] W.T.H. Smith,[1] T.N. Bloomer,[1] D.J. Beacock,[1] J.P. Ridgway,[2] A. Kassner,[3] U.M. Sivananthan.[1] [1]*Cardiac MRI Unit, Leeds General Infirmary, Leeds, UK,* [2]*Department of Medical Physics, University of Leeds, Leeds, UK,* [3]*Philips Medical Systems, Hammersmith, London, UK*

Aims: Qualitative and quantitative assessment of wall motion kinetics with MRI is accurate and reproducible and can be used for stress MRI studies. In the interest of patient safety, image acquisition in stress studies has to be fast. The conventionally used gradient echo sequences for wall motion studies require several minutes for image acquisition. Recently, ultrafast MRI sequences, which approach "real-time" acquisition, have been introduced. The purpose of this study was to evaluate a real-time MRI sequence in the assessment of wall motion kinetics in normal volunteers and patients in comparison with conventional gradient echo acquisition.

Methods: Twenty-one individuals (11 normal volunteers, 10 patients with wall motion abnormalities) were studied on a Philips 1.5-T Gyroscan NT ACS system using a five-element phased-array cardiac synergy coil. Short-axis slices of the left ventricle were acquired with a conventional TFE sequence (TR 8.8 ms, TE 5.2 ms, flip angle 35, matrix 56 × 119mm) and a TFE-EPI sequence (11 ms, TE 3.4 ms, flip angle 20, matrix 128 × 95, 7 EPI-readouts, half-scan factor 0.71). Five to seven midventricular slices were analyzed for wall motion kinetics using MASS software (Medis, Leiden, Netherlands). Each slice was divided into four segments: septal, anterior, lateral, and posterior. The regional function of each segment was assessed qualitatively in the movie display and scored as 1 = normal, 2 = hypokinetic, 3 = akinetic, and 4 = dyskinetic. Endo- and epicardial contours were then drawn in end-diastole and end-systole and wall motion (WM) and wall thickening (WT) computed for each segment. Mean values and SD for measurements derived from each acquisition method and the mean differences between measurements were calculated. Pearson's correlation coefficients for WM and WT were computed.

Results: A total of 493 myocardial segments were analyzed. Qualitative scores agreed in 451 segments between the two methods and disagreed by one grade in 42 segments, with the real-time derived scores lower in 32 of these. Results for quantitative WM and WT analysis are given in Table 1. The mean difference between all measurements from both methods was 0.51 mm (±1.51) for WM and 0.58 mm (±1.67) for WT, with the real-time derived values being lower for both parameters. Correlation coefficients were $r = 0.814$ for WM and $r = 0.836$ for WT.

Conclusion: MR images acquired in real-time allow qualitative and quantitative analysis of normal and abnormal regional left ventricular wall motion kinetics. The real-time derived quantitative measurements were lower than the conventionally derived measurements in this study, but overall correlation was good between the two methods. Real-time acquisition promises to be useful for stress-MR imaging.

Table 1

Mean wall motion (WM) and wall thickening (WT) in volunteers and patients for conventional and real-time derived measurements

	Volunteers		Patients	
	WM	WT	WM	WT
Conventional	8.94 mm (±1.82)	6.40 mm (±1.92)	4.45 mm (±2.46)	2.86 mm (±2.49)
Real-time	8.39 mm (±1.63)	5.89 mm (±1.74)	3.84 mm (±2.09)	2.02 mm (±1.82)

56P. Relation Between Intramural Mechanics and Change of Ejection Fraction 3 Months After First Myocardial Infarction

M.J.W. Götte,[1] J.P.A. Kuijer,[2] J.T. Marcus,[2] P.A.G. Vriend,[1] A.C. van Rossume,[1] C.A. Visser[1] [1]*Dept. of Cardiology,* [2]*Dept. of Medical Physics and Informatics, University Hospital VU, Amsterdam, The Netherlands*

Background: Left ventricular (LV) remodeling after myocardial infarction (MI) is characterized by progressive LV dilatation and global dysfunction expressed by a deterioration of ejection fraction (EF). It has been suggested that regional differences in intramural deformation are associated with this process of remodeling. The aim of this study was to determine the relation between changes of global LV function and regional intramural function in the first 3 months after MI, using magnetic resonance (MR) cine gradient and tissue tagging in conjunction with strain analysis.

Methods

Subjects: Seventeen patients (12 male, aged 56 ± 10 years) with an anterior MI (peak ck-MB 222 ± 114 U/l) were studied. All patients received reperfusion therapy and all but one received β-blocker therapy.

Imaging method: MR imaging was applied 7 ± 3 (t_0) and 97 ± 10 (t_1) days postmyocardial infarction. Imaging was performed on a 1.0- and 1.5-T system using a phased-array body coil and prospective cardiac triggering. Breath-hold cine gradient short-axis images covering the whole LV were used for volume and EF calculation. SPAMM was applied to obtain tagged images with 7 mm tag-to-tag distance.

Imaging Parameters		Cine Gradient	Tissue Tagging
TR	(msec)	80	10
Flip angle	(°)	25	15
Matrix size	(mm)	126 × 256	144 × 256
FOV	(mm)	219 × 250	250 × 250
Temp. resol.	(msec)	40	30

Analysis: Calculation of volumes and EF was performed using the MASS© software package (University of Leiden, The Netherlands). Two-dimensional strain analysis was performed using the SPAMMVU© software package (University of Pennsylvania, USA). Groups of three tag intersection points defined triangular elements of myocardium. These elements were analyzed for components of deformation including the radially directed stretch (λ_r) and the circumferentially oriented shortening (λ_c). Results were averaged for six circumferential segments, anteroseptal (**as**), anterior (**an**), anterolateral (**al**), posterolateral (**pl**), inferior (**in**), and inferoseptal (**is**), number 1 through 6.

Intramural deformation at mid-ventricular level in patients with decreased EF (**EF−**) was compared to patients with improved or preserved EF (**EF+**) at follow-up.

Statistical analysis: A Student's *t*-test for unpaired comparison was used for comparison between both patient groups. $p < 0.05$ was considered to be significant.

Results:

Clinical Parameters	Improved EF	Declined EF	*p*-value
n	9	8	
Peak ck-mb (U/l)	155 ± 56	309 ± 110	0.003
EF t_0 (%)	55 ± 12	42 ± 9	0.025
EF t_1 (%)	63 ± 10	33 ± 7	0.001

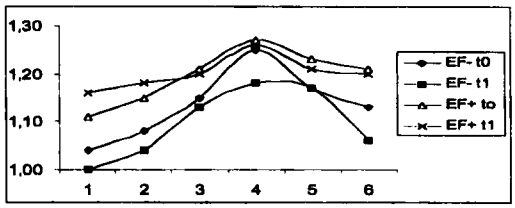

Figure 1. λ_r at mid-ventricular level.

Radial stretch (λ_r) at baseline (t0) and follow-up (t1).

	as	an	al	pl	in	is
EF− t0	1.04	1.08	1.15	1.25	1.17	1.13
EF+ t0	1.11	1.15	1.21	1.27	1.23	1.21
p-value	0.042	0.039	ns	ns	ns	ns
EF− t1	1.00	1.13	1.04	1.18	1.17	1.06
EF+ t1	1.16	1.20	1.18	1.26	1.21	1.20
p-value	0.004	ns	0.007	0.027	ns	0.005

Circumferential shortening (λ_c) at baseline (t0) and follow-up (t1).

	as	an	al	pl	in	is
EF− t0	0.98	0.92	0.83	0.81	0.89	0.97
EF+ t0	0.93	0.88	0.81	0.80	0.84	0.89
p-value	ns	ns	ns	ns	0.023	0.005
EF− t1	0.97	0.92	0.84	0.83	0.89	0.97
EF+ t1	0.87	0.81	0.80	0.80	0.85	0.87
p-value	0.005	0.001	0.007	ns	ns	0.001

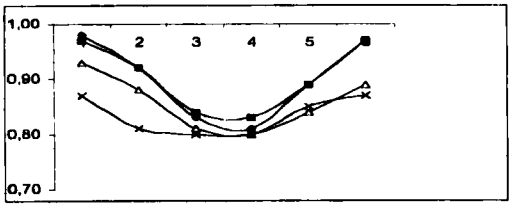

Figure 2. λ_c at mid-ventricular level.

Conclusion: At baseline, patients with deteriorated EF at 3 months follow-up after MI have reduced intramural myocardial function in the septum (infarcted area) compared to patients with improved EF at follow-up. At follow-up, patients with deteriorated EF have not only reduced function in the infarcted area but also in the lateral regions (remote area). Patients with improved EF showed increased function in the infarct area, and preserved function in the remote area. These findings reflect in a quantitative manner the mechanical consequences of infarction and may have predictive value for the occurrence of LV remodeling.

57P. Automatic observer-independent acquisition planning of cardiac MR short-axis images

B.P.F. Lelieveldt,[1] R.J. van der Geest,[1] H.J. Lamb,[2] J.H.C. Reiber[1] *Leiden University Medical Center, [1]Div. of Image Processing, [2]Dept. of Radiology, Leiden, The Netherlands*

Purpose: Multislice, multiphase short-axis (SA) cardiac MR imaging has proven to be highly suitable to assess left ventricular (LV) function and is now considered to be the gold standard for analysis of global and regional cardiac function. However, the acquisition planning of these scans is a timely process and requires substantial insight in cardiac anatomy. Planning of SA views in a reproducible manner has shown to be difficult in daily clinical practice. The purpose of this study was to develop and validate an automated observer-independent acquisition planning method for SA cardiac MR imaging studies.

Methods: Our approach is based on matching a 3D anatomical model of the thorax to a set of multistack scout views. This results in a set of geometric transformations, which can be applied to automatically calculate the position and orientation of the LV long axis for an individual patient. This method was retrospectively validated on routinely acquired examinations of 20 patients suffering from various cardiac pathologies. As a gold standard for the short-axis orientation in these patient studies, the orientation of the LV long-axis at end-diastole (ED) was assessed by manually drawing the ED endocardial contours and fitting a straight line through the contour centroids. To evaluate the automatically estimated LV axis against the reference LV long axis, the angle ϕ_{auto} was calculated between the reference LV axis and the automatically estimated LV long axis. In addition, five normal subjects were scanned in two examinations by acquiring a manually and an automatically planned SA image set and repeating this procedure after repositioning the subjects in the scanner bore, resulting in 20 SA volumes in total. A comparison between a manually and an automatically scanned SA set is given in Figure 1. To compare global functional measurements in both scan types, the endo- and epicardial contours were drawn by an expert in all 20-image sets, and the LV masses and ejection fractions (EF) were assessed.

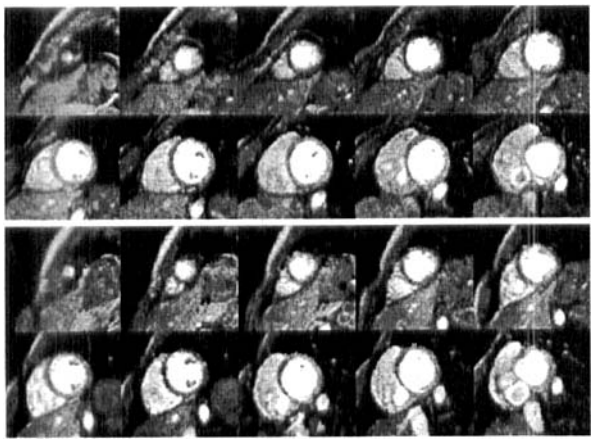

Figure 1. Comparison between a manually planned (top two rows) and an automatically planned (bottom two rows) SA set

Results: The results of the validation study can be summarized as follows:

1. In the 20 patient studies, the manual variation, ϕ_{man}, was on average 9.7 ± 5.8 degrees, while the angular offset in the automatic planning procedure, ϕ_{auto}, amounted on average to 12.2 ± 6.8 degrees. The paired differences between ϕ_{man} and ϕ_{auto} were found to be not statistically significant (p = 0.23). Moreover, the standard deviations in ϕ_{man} and ϕ_{auto} did not differ statistically significant (5.8 vs. 6.8 degrees, respectively, p = 0.49),
2. The EFs calculated from both scan types corresponded very well, with an average paired difference between the EFs of 1 ± 5.7%,
3. The end-diastolic LV mass calculated from both scan types corresponded well, with an average paired difference of −3 ± 8.5 g.
4. Both methods showed good correlation between repeated studies, both in image content, in EF (avg. paired diff.: automatic: 3 ± 3%, manual −2 ± 4%), and in LV mass (automatic: 3 ± 10g, manual: 0 ± 8.4g).
5. Differences in EF and LV mass as measured in both scan types were not statistically significant and were well within the best accuracy ranges reported in the literature.

Conclusions: In contrast to manual (real-time) planning protocols, the automated SA scan planning presented here requires no user interaction and expert knowledge. The method provides a uniform observer independent planning approach, yielding images of equal diagnostic quality as manually planned images. The manually and automatically planned SA scans showed to be equally suitable to quantitate global LV function.

58P. Three-Dimensional Myocardial Strain Analysis with MRI Tagging, Using a One-Dimensional Displacement Field

Joost P.A. Kuijer, J. Tim Marcus, Marco J.W. Götte, Albert C. van Rossum, Robert M. Heethaar. *Institute for Cardiovascular Research ICaR-VU, Vrije Universiteit, Amsterdam, The Netherlands*

This study concerns a method to calculate three-dimensional (3D) myocardial strains from a set of magnetic resonance (MR) tagged images. The method was validated using an analytical test case, and the feasibility was shown with data sets of four healthy volunteers. MR tagging offers the possibility to quantify the motion of the heart wall noninvasively with intramyocardial markers (tags). 3D strains have previously been computed with displacement fields fitted to the measured data for all three (x,y,z) motion components. Specific for our method is that the application of fitting and regularisation (or "smoothing") was kept to a minimum, preserving the true spatial resolution of the data. A displacement field was fitted only to the longitudinal (z) displacement, which was measured in long-axis tagged images. The x- and y-displacements of the tracked material points were obtained directly from short-axis images. Next, a mesh of tetrahedrons connecting the tracked points was used to compute 3D strains using homogeneous strain analysis. The strains were expressed as relative stretch and shear angle. The

Table 1

Mean Strains of Volunteers and Results of Analytical Test Case

	ε_r	ε_c	ε_l	α_{rc}[°]	α_{rl}[°]	α_{cl}[°]
Volunteers						
Mean (n = 4)	0.32	−0.21	−0.16	1.5	−0.2	7.8
SD	0.04	0.01	0.01	1.5	1.7	1.1
Analytical test						
Mean (n = 766)	0.36	−0.05	−0.19	4.8	12.5	8.5
Paired diff.						
Mean	0.001	−0.005*	−0.0004*	0.5*	0.3*	0.0
SD	0.06	0.04	0.005	2.4	1.5	1.4

*$p < 0.05$ in paired t-test over n = 766 tetrahedrons

method was tested with an analytical strain field of an incompressible cylinder; the strain of each tetrahedron was compared with the analytical strain. The results are presented Table 1. Little or no bias was introduced. The SD of the difference was substantial due to the exaggerated strains near the inner boundary of the cylinder. For the healthy volunteer data, the fitting procedure was stable with a minimum of global smoothing. The method proved to be feasible and accurate.

59P. Increased Brain and Atrial Natriuretic Peptides for early Diagnosis of Asymptomatic Right Ventricular Dysfunction in Patients with Chronic Right Ventricular Pressure Overload

Igor I. Tulevski MD,[1] Maarten Groenink MD,[1] Ernst E. van der Wall MD, PhD,[2] Dirk J. van Veldhuisen MD, PhD,[3] Frans Boomsma PhD,[4] Jaap Stoker MD PhD,[5] Barbara J.M. Mulder MD PhD[1] *From the Departments of Cardiology[1] and Radiology[5], Academic Medical Center Amsterdam, Department of Cardiology Leiden University Medical Center,[2] Department of Cardiology University Hospital Groningen,[3] Department of Internal Medicine, Erasmus University Medical Center, Rotterdam[4]*

Background: Early diagnosis of right ventricular (RV) dysfunction is difficult in clinical circumstances. The purpose of this study was to evaluate the role of plasma neurohormones in early diagnosis of asymptomatic RV dysfunction.

Methods and Results: Plasma brain natriuretic peptide (BNP) and atrial natriuretic peptide (ANP) levels were measured in 21 asymptomatic patients with chronic RV pressure overload and in 7 healthy volunteers. RV ejection fraction (EF) was determined using magnetic resonance imaging (MRI). RVEF of the volunteers was significantly higher than RVEF of the patients (69.0 ± 8.2% versus 58.0 ± 12.0%, respectively, $P = 0.006$). Left ventricular (LV) EF in volunteers and patients was 72.3 ± 7.8% versus 68.1 ± 11.0%, respectively, p = NS. Between patients and volunteers there was a significant difference in the plasma concentrations of BNP (5.3 ± 3.5 versus 2.3 ± 1.7 pmol/L, respectively, $p = 0.009$) and ANP (7.3 ± 4.5 versus 3.6 ± 1.4 pmol/L, respectively, $p = 0.05$). Both in patients and volunteers mean ANP plasma concentrations were higher than mean BNP plasma concentrations. RVEF was inversely correlated with BNP and ANP: $r = 0.65$; $p = 0.0002$ and $r = 0.61$; $P = 0.0012$, respectively. No correlations were found between LVEF and BNP ($r = 0.2$; P = NS) and LVEF and ANP ($r = 0.52$; P = NS).

Conclusion: Our study shows a significant inverse correlation between MRI-determined RVEF and the plasma neurohormones BNP and ANP in asymptomatic patients with RV pressure overload. Monitoring of changes in BNP and ANP levels might serve to predict early deterioration of RV function to anticipate adequate treatment.

60P. Dobutamine-induced increase of right ventricular contractility without increased stroke volume in asymptomatic patients with chronic right ventricular pressure overload

Igor I. Tulevski,[1] Peter L. Lee,[1] Maarten Groenink,[1] Ernst E. van der Wall,[3] Jaap Stoker,[2] P.G. Pieper,[4] Hans Romkes,[1] Barbara J.M. Mulder[1] *From the Departments of Cardiology[1] and Radiology[2], Academic Medical Center Amsterdam, Departments of Cardiology, Leiden University Medical Center[3] and Academic Hospital Groningen[4]*

Objective: In patients with chronic right ventricular (RV) pressure overload, RV adaptation remains a subject of major concern. We examined the role of dobutamine stress in the early detection of RV dysfunction in asymptomatic patients with chronic RV pressure overload using magnetic resonance imaging (MRI).

Design and patients: Sixteen asymptomatic patients with chronic RV pressure overload (aged 25.8(5.5) years; NYHA class I/II) and eight age- and sex-matched healthy volunteers (aged 26.3(3.8) years) were included. MRI was applied both at baseline and during dobutamine stress (start dose 5 μg/kg/min to maximum dose 15μg/kg/min) to determine RV and left ventricular (LV) stroke volumes and ejection fraction (EF).

Results: At baseline there were no significant differences in RV function between patients and controls: RVEF (61(12)% v 69(8)%, p = NS), RV stroke volume (78(28)ml v 87(22)ml, p = NS), RV end-diastolic volume (EDV)(125(33) ml v 128(36)ml, p = NS), and heart rate (66(14)bpm v 63(10)bpm, p = NS), respectively. During dobutamine stress RVEF increased significantly both in patients and controls (68(10)% and 84(3)%, $p < 0.01$ and $p < 0.001$ v rest, respectively), but absolute stress RVEF was significantly less in patients than in controls ($p < 0.0002$). RV stroke volume increased significantly in controls (26(17)%, $p < 0.01$), but the patients did not show a significant change in RV stroke volume (−9(20)%, p = NS). The controls showed no change in RVEDV (4(18)%, p = NS), but in patients a significant decrease in RVEDV was observed (−20(12)%, $p < 0.0001$). Maximal heart rate was similar in both groups 111(18)bpm in patients, 101(15)bpm in controls (p = NS).

Conclusion: In asymptomatic patients with RV pressure overload, dobutamine had a positive inotropic effect on RV_E but the increased contractility was not accompanied by an appropriate increase in stroke volume. Our data suggest abnormal RV filling due to early diastolic RV dysfunction in this category of patients.

59. Assessment of Coronary Artery Bypass Graft Flow Reserve using Magnetic Resonance Imaging and the Doppler Flow Wire

S.E. Langerak,[1] P. Kunz,[3] J.W. Jukema,[2] H.W. Vliegen,[2] P. Steendijk,[2] A. de Roos,[3] E.E. van der Wall,[2] *The Interuniversity Cardiology Institute of the Netherlands (ICIN),[1] Utrecht, Department of Cardiology[2] and Radiology[3] of the Leiden University Medical Center, Leiden, the Netherlands*

Introduction: Coronary flow velocity reserve measurement using the Doppler flow wire is considered an established diagnostic tool in detecting significant coronary artery stenosis. Recent advances in magnetic resonance (MR) flow mapping allow the noninvasive assessment of coronary artery bypass graft flow. However, previous MR flow sequences were either nonrespiratory compensated and took a few minutes, which does not allow application during adenosine infusion, or used breath holding with low temporal resolution.

The purpose of this study was twofold: to assess the feasibility of breath-hold high-resolution MR flow measurements in coronary artery bypass grafts during adenosine stress and to determine the correlation of this MR flow sequence with results obtained by the intravascular Doppler flow wire.

Methods: Twenty-one patients (63 ± 9 years) with 23 angiographically normal coronary artery bypass grafts were studied. During x-ray angiography proximal bypass graft flow velocity was measured before and after an adenosine bolus injection (18_g) using the intracoronary Doppler flow wire. MR flow mapping at the same level in the coronary artery bypass grafts was performed at rest and during a 6-minute intravenous adenosine infusion (140_g/kg/min). A 1.5-T MR scanner (max. slew rate 100T/m/s) and a phased array cardiac coil was used for flow mapping. Flow measurements were performed using turbo-field-echo-planar-imaging (TFEPI) which allows breath-hold flow mapping with a high temporal resolution (23 ms). This sequence involved two excitations within one heart phase interval, which are each followed by three EPI readouts, resulting in a shot length of 6 k-lines and scan duration of 20 heart beats. Other scan parameters included a spatial resolution of 0.8 × 0.8 × 6 mm, flip angle of 20°, TR of 11 ms, TE of 4.6 ms, and velocity encoding of 75 cm/s.

Results: The typical biphasic flow pattern in coronary artery bypass grafts was demonstrated at rest and during adenosine infusion using the Doppler flow wire (Figure 1) and MR flow mapping (Figure 2). A good correlation was found between MR and intravascular Doppler flow velocity ($r = 0.67$) and flow reserve values ($r = 0.66$). Flow velocities were lower by TFEPI MR flow mapping in comparison to Doppler flow measurements (baseline: 8.9 ± 4.3 vs. 16.9 ± 10.9 cm/s, $p < 0.05$; adenosine: 19.7 ± 7.4 vs. 38.6 ± 15.0 cm/s, $p < 0.05$), but a similar flow reserve was found (2.4 ± 0.8 vs. 2.6 ± 1.0, p = ns).

Conclusion: Breath-hold TFEPI proved to be a fast MR sequence, which enables sequential flow mapping in coronary artery bypass grafts during a 6-minute adenosine infusion. Flow velocities correlated well with the intravascular Doppler flow wire, but lower flow velocities were found. This can be explained by the fact that the Doppler flow wire samples flow velocities in the center of the vessel. On the contrary, MR flow is measured over the entire vessel area and thus includes pixels with slower flow velocities near the vessel boundary.

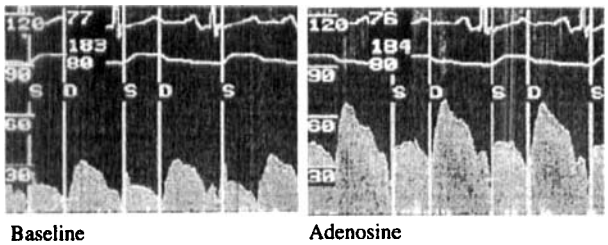

Figure 1. Doppler flow mapping in a coronary bypass graft.

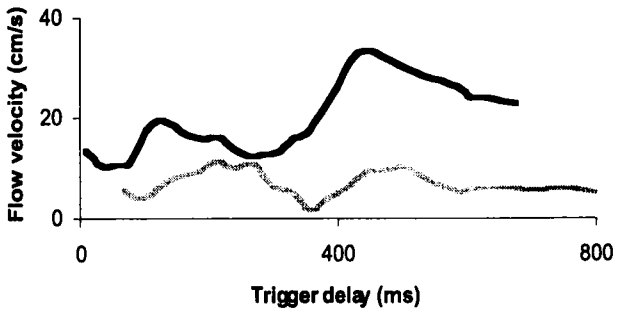

Figure 2. MR flow scan in a coronary bypass graft at rest (gray line) and during adenosine stress (black line).

60. Flow measurements in coronary arteries for the detection of significant coronary arteries stenoses

Th. Wittlinger,[1] T. Voigtlnder,[1] K.F. Kreitner,[2] S. Petersen,[1] P. Kalden,[2] M. Thelen,[2] J. Meyer[1] *2nd Medical Clinic[1] and Department of Radiology,[2] University Hospital Mainz, Germany*

Flow measurements in coronary arteries by magnetic resonance imaging (MRI) is a noninvasive technique. It was the aim of this study to find a correlation between a reduced coronary flow and the diagnosis of a significant coronary stenosis.

Methods: We investigated 30 patients and 10 healthy volunteers (men:34, women:6, age: 62.4) with in total 45 vessels (LAD: 30, RCA: 15). Twenty severe (>70%) stenoses of the left anterior descending artery (LAD) and 10 stenoses of the right coronary artery (RCA) were detected by x-ray angiography. All investigations were performed using an 1.5-T Magnetom Vision device (Siemens AG, Erlangen). For planning the flow measurements a T2-weighted, ECG-gated, breath-hold, turbo-spin-echo-sequence was used (Haste). Flow measurements was performed using a 3D-angiographic sequence with the phase constrast method. The final evaluation was done applying a multiplanar reconstruction procedure (MPR). Coronary flow was calculated in ml/RR-interval.

Results:

	Stenoses		Healthy Volunteers	
	Mean Flow/ RR	Flow [%] Aorta	Mean Flow/ RR	Flow [%] Aorta
LAD	0.286 ml	0.66%	0.82 ml	1.54%
RCA	0.369 ml	0.85%	0.58 ml	1.09%

Conclusions: The LAD of the healthy volunteers showed a predominantly diastolic flow, the flow in the RCA is equal in systole and diastole. There is a significant correlation ($p > 0.001$) between a reduced coronary flow und the presence of a significant stenosis. The stenotic LAD showed a predominantly systolic flow pattern.

61. Contrast-enhanced 3D breath-hold magnetic resonance coronary angiography in oblique planes for detection of coronary artery stenosis

Matthias Regenfus, Dieter Ropers, Stephen Achenbach, Winfried Kessler, Werner G. Daniel, Gerhard Laub,* Werner Moshage
*Department of Cardiology, University of Erlangen-Nürnberg, *Siemens Medical Engineering Group, Erlangen, Germany*

Aims: Recently, magnetic resonance (MR) coronary angiography made feasible the visualization of coronary arteries by means of the application of T1-shortening contrast agents and ultrashort gradient-echo sequences. The aim of this study was to evaluate a new ultrafast gadolinium-enhanced 3D breath-hold MR technique for detection of coronary artery stenoses in oblique projection angiograms.

Methods: MR investigation was performed in 61 patients with suspected coronary artery disease on a 1.5-T scanner (Vision, Siemens). After visualization of the course of the main coronary arteries using contiguous cross-axial spin-echo images, MR coronary angiography was performed within one single breath-hold using an ultrafast contrast-enhanced 3D gradient-echo sequence (TR/TE 4.2/1.6, spatial resolution 1.25 × 1.25 × 1.5 mm_). In successive studies the imaging volume which consisted of 32 contiguous parallel sections was positioned along the course of right (RCA) and left circumflex (LCX) and along left main (LM) and left anterior descending (LAD) coronary arteries, respectively. During each measurement 20 ml gadolinium-DPTA (Magnevist, Schering) was injected intravenously according to the individually determined contrast transit time. Image data were evaluated by two independent observers. The results were compared with conventional contrast angiography in a blinded manner.

Results: A total of 328 of 427 coronary segments (LM, proximal and mid-segments of RIVA, RCX, and RCA) could be visualized (76.8%). In these, 58 of 68 significantly stenotic (≥50%) and 235 of 261 nonstenotic coronary segments could be exactly classified. Thus, the overall sensitivity and specifity for stenosis detection resulted in 85.3% and 90.0%, respectively. Using ultrafast gadolinium-enhanced 3D breath-hold imaging oblique projection MR coronary angiograms can be successfully performed in the majority of cases. However, sensitivity for detecting coronary stenoses does not yet seem to be sufficient and further techniqual improvements are mandatory to introduce this technique as a reliable diagnostic tool in clinical setting.

62. Improvement of Magnetic Resonance Coronary Angiography Using the New Blood Pool Contrast Agent CLARISCAN™ in Patients

WLF Bedaux,[1] MBM Hofman,[1] CC de Cock,[1] PA Wielopolski,[2] A Lehning,[3] M Oudkerk,[2] PJ de Feyter,[2] CA Visser,[1] AC van Rossum.[1]
[1]*University Hospital Vrije Universiteit, Amsterdam and* [2]*University Hospital Rotterdam, The Netherlands,* [3]*Nycomed Amersham Imaging, Munich, Germany*

Background: CLARISCAN™ (NC100150, Nycomed Amersham Imaging, Oslo, Norway) is a new blood pool agent for potential use in magnetic resonance coronary angiography (MRCA) (1). The aim of the study was to assess the improvement of the quality of 3 dimensional (3D) breath-hold (BH) MRCA using this contrast agent in patients.

Methods: Imaging data were acquired in this phase II clinical trial from eight patients referred for diagnostic coronary angiography in the evaluation of chest pain. The images were acquired using a phased-array radio frequency receiver coil at 1.5-T (Vision, Siemens, Germany) before and after intravenous administration of CLARISCAN™ (2.5 mg Fe/kilogram body weight). This agent results in a reduction of blood T1 and T2* (85 and 7 ms, respectively) with a plasma half-time longer than 2 hours. Imaging was performed using a 3D BH volume coronary artery targeted scan (VCATS) with a TR of 4.8 ms, a TE of 2.0 ms, a slab thickness of 24 mm, and 21-segments per cardiac cycle (2). The postcontrast sequences had adapted flip angle sequencing and used an inversion prepulse to suppress myocardial signal, whereas precontrast magnetization transfer suppression was applied. From the postcontrast MRCA data the visualized length of the coronary arteries was determined. The presence and grading of stenoses (no stenose, <50%, 50–75%, 75–99% and occlusion) of the MR data were compared with the data from coronary angiography. The signal- and contrast-to-noise ratios to myocardium and fat (SNRs, CNRs) were measured before and after contrast administration.

Results: In total 32 segments (13 stenosis) were evaluated and compared with the data from coronary angiography. The visualized lengths of the left main (LM), left anterior descending (LAD), circumflex, and right coronary artery (RCA) were 1.1 ± 0.4, 3.9 ± 1.2, 2.6 ± 0.6, and 7.3 ± 1.8 cm, respectively. Overall agreement of visually assessed stenosis severity was 78%. In four segments the stenosis was missed; in three segments the degree of stenosis did not agree with the data from coronary angiography. The mean SNR post- and precontrast was 13 ± 3 and 11 ± 2, respectively, the mean ratio per subject was 1.2 ± 0.4 ($p = 0.1$). The mean CNR to myocardium post- and precontrast was 10 ± 2 and 4 ± 3, respectively; the mean ratio per subject was 4 ± 3 ($p = 0.02$). However, CNR to epicardial fat did not change after contrast administration. Finally, the vessel delineation was improved postcontrast, probably due to a more flow independent signal behavior

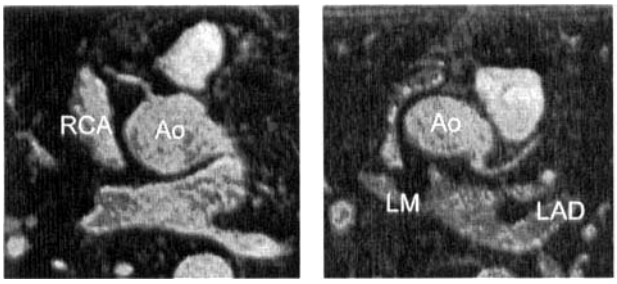

Figure 1. A 3D MRCA of the origin of the RCA (arrow in left panel) and the LM and LAD (arrows in right panel) in a transverse view with VCATS

Conclusion: CLARISCAN™ injection in combination with a BH VCATS allows rapid localization and coverage of the coronary arteries with improved myocardial suppression and better vessel delineation.

References

1. Nolte-Ernsting C, Adam G, Bucker A, Berges S, Bjornerud A, Gunther RW. *Am J Radial* 171:107; 1998.
2. Wielopolski PA, Van Geuns RJM, De Feyter PJ, Oudkerk M. *Radiology* 209:209–219; 1998.

63. Intravascular Contrast Agents (Clariscan™; NC100150 Injection) for Magnetic Resonance Coronary Imaging in Patients with Coronary Artery Disease

[1]C. Klein, [1]E. Nagel, [2]B. Schnackenburg, [1]A. Bornstedt, [1]S. Schalla, [3]V. Hoffmann, [3]A. Lehning, [1]E. Fleck [1]*Internal Medicine/ Cardiology, Charité, Campus Virchow, HU & German Heart Institute Berlin, Germany;* [2]*Philips Medical Systems, Hamburg, Germany;* [3]*Nycomed Amersham Imaging, Munich, Germany*

Introduction: 3D magnetic resonance coronary angiography (MRCA) of the proximal segments is possible; however, signal and contrast to noise ratio are low as they depend on the inflow of unsaturated blood into the vessels. Thus, the signal in peripheral coronary arteries and distal to a severe stenoses (reduced flow) and when acquiring large 3D volumes is particularly low. MRCA would benefit from a T1 shortening contrast agent to achieve high spatial resolution navigator techniques with free patient breathing have shown promising results. These techniques, however, cannot be used in combination with gadolinium-DPTA contrast enhancement, as this agent rapidly leaves the intravascular space. The aim of the present study was to test the feasibility of Clariscan™ (CS), an intravascular contrast agent to visualize the coronary arteries in patients with suspected or known coronary artery disease.

Method: CS is a superparamagnetic iron oxide nanoparticle with an oxidized starch coating. It is a pure intravascular (blood pool) agent with both T1 and T2 shortening properties (half-life > 2h). Twelve patients were examined with a 1.5-T scanner (ACS NT, Philips, The Netherlands,) in supine position using a 3D turbo gradient echo technique (TE/TR 2.3/8.0 ms, flip angle 50, spatial resolution 0.7 × 0.9 × 1.5 mm, matrix 512 × 512, fat suppression). To suppress breathing motion artifacts a prospective navigator technique with real-time slice correction was used. Myocardial signal in the contrast-enhanced images was suppressed with an inversion prepulse, in the unenhanced images a T2-preparation prepulse was used. Images were obtained at various doses of CS (range from 1 to 5 Fe mg/kg body weight). To evaluate image quality signal to noise ratio of the coronaries (SNR), contrast to noise between coronaries and fat (CNR_{fat}), between coronaries and myocardium (CNR_{myo}), the length and width of the visualized coronaries and the diagnostic value were calculated before and after CS administration.

Results: Image quality was nondiagnostic in one patient due to technical problems. Nineteen LAD, 7 RCA, 6 RCX, and 1 ACVB were evaluated. In all patients, the use of Clariscan™ lead to an improvement of image quality (Fig. 1). CNR_{fat} improved up to a dose of 2 mg Fe/kg BW, SNR up to a dose of 3 mg Fe/kg BW and CNR_{myo} up to a dose of 4 mg Fe/kg BW ($p < 0.05$) (Fig. 2). A reduction of signal was observed with 1 mg Fe/kg BW probably due to the inversion prepulse and submaximal T1 shortening. With higher doses a reduction of signal in comparison to lower doses was found, probably due to the T2*-shortening effect and susceptibility artifacts occurring with concentrations of more than 3 mg Fe/kg BW. More distal segments profited significantly more than proximal parts and the visual length of the coronary arteries increased by 21.8 ± 23.1 mm. The sensitivity and specificity for the detection of significant stenoses (> 50%) improved with CS from 58% to 75% and from 81% to 97%, respectively, in those segments which could be adequately visualized without contrast agent ($n = 43$). The visual width of the proximal coronaries decreased significantly ($p > 0.05$) with CS compared to the unenhanced images probably due to suppression of the vessel wall by the inversion prepulse (Fig. 3).

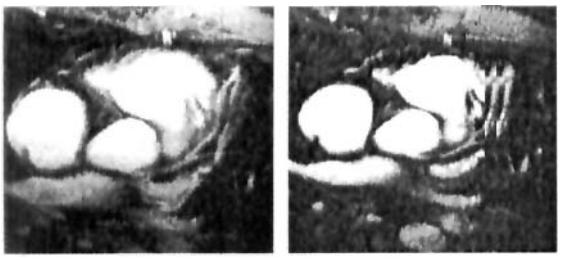

Figure 1.

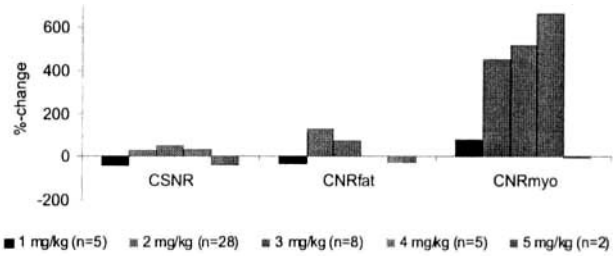

Figure 2. Percental change after different doses of Clariscan™

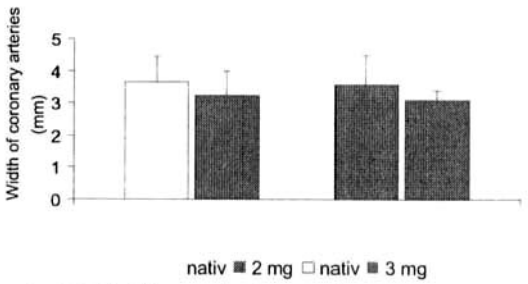

Figure 3. Width of the proximal coronaries.

Conclusion: In our experience Clariscan™ improves image quality and increases the length of the visualized coronary arteries by increasing the signal and contrast to noise ratio. The diagnostic accuracy of 3D MRCA for the diagnosis of coronary artery disease is improved.

64. Effects of a Clinically Available SPIO Contrast Agent on Magnetic Resonance Coronary Angiography

R.J.M. van Geuns,* P.A. Wielopolski,* H.G. de Bruin,* P.M.A. van Ooijen,* M. Oudkerk,* P.J. de Feyter* *Thorax Center and *Dept. of Radiology, Daniel den Hoed klinick, University Hospital Rotterdam, The Netherlands*

Introduction: A multitude of magnetic resonance coronary angiography (MRCA) techniques have been developed. Most of them depend on the inflow of blood from the aortic root or left ventricle between successive heartbeats. Consequently, 2D or relative small 3D volumes have been used to minimize blood saturation effects. To reduce the dependency on inflow effects and to enable larger image volumes, T1 shortening contrast agents can be used. Presently, available contrast media diffuse rapidly through out the extracellular space, which limits their use in the long acquisition schemes of respiratory gated MRCA. Super paramagnetic iron oxide (SPIO) contrast agents accumulate largely in the liver and spleen, but 10 to 20% behaves like a intravascular contrast agent with a longer blood half-life time of between 2.4 and 3.6 hours (1). This may be used to improve the signal-to-noise ratio in respiratory gated MRCA.

Materials and methods: Five patients underwent MRCA before and after intravenous administration of AMI-25 (Endorem, Guerbet, Aulnay-sous-Bois, France). AMI-25 is a SPIO contrast agent coated with dextran with a particle diameter of approximately 35 nm (2). AMI-25 was drip infused at a dose of 10–15 μmol Fe/kg body weight as a suspension in 100 ml isotonic glucose over 30 minutes. To estimate the T1 relaxation time of blood, a series of inversion recovery gradient echo images was acquired before and after administration of the contrast agent. Inversion time varied from 100 to 1400 ms. MRCA was performed with a three-dimensional gradient echo sequence with retrospective respiratory gating by a navigator signal from the dome of the right hemidiaphragm. The matrix size was 128 × 256 with a field of view of 240 × 320 and a slab thickness of 120 mm. TR and TR were 2.6/1.3 ms, respectively.

Figure 1. Oblique coronal reconstruction. (A) Precontrast the signal intensity is lower in the compared to the right ventricle. (B) Postcontrast the signal intensity in all cardiac structures is comparable.

Results: The T1 relaxation time of blood was reduced from 1562 ± 130 to 642 ± 244 ms ($p < 0.01$), while the T1 relaxation time of myocardium did not change significantly (T1 before: 1058 ± 30 ms, T1 post: 1001 ± 138 ms, $p = 0.48$). Precontrast the SNR in the aortic root was significantly less compared to the right atrium (Figure 1). Postcontrast the signal-to-noise ratio (SNR) of blood in the right atrium improved with 60.8%; the SNR in the aortic root improved with 90.5% and was equal to the SNR in the right atrium. The blood to myocardium contrast-to-noise ratio improved with 60.8%.

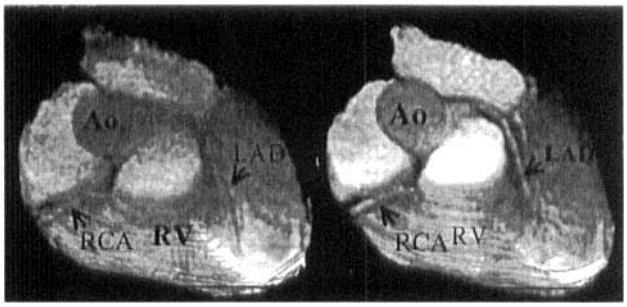

Figure 2. Volume rendering of 3D retrospective respiratory gated MRCA. Before administration of the contrast agent (A), the blood in the coronary arteries and aortic root is partly saturated, with the contrast agent the coronary arteries are depicted more clearly.

Conclusion: SNR and CNR of MRCA can be importantly improved with clinically approved SPIO contrast agents with a partially intravascular behavior.

References:

1. Hamm B, Staks T, Taupitz M, et al. Contrast-enhanced MR imaging of liver and spleen: first experience in humans with a new superparamagnetic iron oxide. *J Magn Reson Imaging* 1994;4(5):659–68.
2. Jung CW, Jacobs P. Physical and chemical properties of superparamagnetic iron oxide MR contrast agents: ferumoxides, ferumoxtran, ferumoxsil. *Magn Reson Imaging* 1995; 13(5):661–74.